A rem(a)inder on Ideal Fluid - Boundary Layer decomposition

P.-Y. Lagrée
CNRS & UPMC Univ Paris 06, UMR 7190,
Institut Jean Le Rond ∂'Alembert, Boîte 162, F-75005 Paris, France
pierre-yves.lagree@upmc.fr ; www.lmm.jussieu.fr/∼lagree

October 28, 2022

Abstract

In this chapter first we recall simple solutions of slightly disturbed Euler equations (small disturbance theory). The main thing is that we will write the perturbation of the flow proportional to the small angle of a bump placed on a flat plate. Then classical Boundary Layer Theory ([22], [21]) is presented. We introduce the fundamental $L/\sqrt{Re}$ scaling. We introduce the integral method and define the boundary layer displacement thickness. The problem of boundary layer separation is quickly presented (Goldstein 1948 problem). Finally we present briefly the second order boundary layer theory. The unsteady boundary layer is introduced as well.

1 Incompressible Navier Stokes equations

The problem that we have to solve is the problem of the solution of Navier Stokes equations around a given body at large Reynolds number. The Reynolds number Re is constructed with a velocity (U_0) and a typical length (L). We use very restrictive hypothesis: we suppose that we are always in a laminar flow even if the Reynolds number is very very large. The flow is supposed to remain laminar. In fact, this is not an issue, the ideas developed may be applied, to some extend, in the turbulent case. We will describe 2D or axi flows. The flow is supposed steady and incompressible (even we present some compressible results).

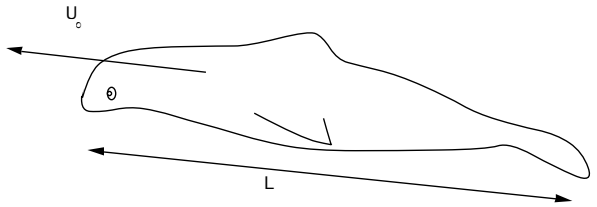

Figure 1: A typical problem a body of length L in a uniform velocity U_0; the Reynolds number is large $Re = U_0 L/\nu >> 1$. The body of this image is 3D, or may be approximated by a axi geometry, but **all the chapter deals with 2D equations** x, y **and** u, v.

1.1 Small Reynolds flows

We first non-dimensionalise the equations with L (the typical length of the body) and U_0 (the typical velocity) in all directions of space and velocity (with "bars" over the variables *i.e.* $\bar{x} = x/L$, $\bar{y} = y/L$, $\bar{u} = u/U_0$, $\bar{v} = v/U_0$ and $\bar{p} = p/(\rho U_0^2/Re)$, the reference pressure is here taken to be 0. The pressure scales by dominant balance with $\rho U_0^2/Re$ which is $\mu U_0/L$. Small Reynolds flows will be presented in a special chapter dedicated to these flows, see:

`http://www.lmm.jussieu.fr/~lagree/COURS/M2MHP/petitRe.pdf` so that the Stokes problem is obtained in taking the limit of the following problem for $Re \to 0$:

$$\left\{\begin{array}{l} \dfrac{\partial \bar{u}}{\partial \bar{x}} + \dfrac{\partial \bar{v}}{\partial \bar{y}} = 0, \\ Re(\bar{u}\dfrac{\partial \bar{u}}{\partial \bar{x}} + \bar{v}\dfrac{\partial \bar{u}}{\partial \bar{y}}) = -\dfrac{\partial \bar{p}}{\partial \bar{x}} + (\dfrac{\partial^2 \bar{u}}{\partial \bar{x}^2} + \dfrac{\partial^2 \bar{u}}{\partial \bar{y}^2}), \\ Re(\bar{u}\dfrac{\partial \bar{v}}{\partial \bar{x}} + \bar{v}\dfrac{\partial \bar{v}}{\partial \bar{y}}) = -\dfrac{\partial \bar{p}}{\partial \bar{y}} + (\dfrac{\partial^2 \bar{v}}{\partial \bar{x}^2} + \dfrac{\partial^2 \bar{v}}{\partial \bar{y}^2}). \end{array}\right. \tag{1}$$

which is

$$\left\{\begin{array}{l} \dfrac{\partial \bar{u}}{\partial \bar{x}} + \dfrac{\partial \bar{v}}{\partial \bar{y}} = 0, \\ 0 = -\dfrac{\partial \bar{p}}{\partial \bar{x}} + (\dfrac{\partial^2 \bar{u}}{\partial \bar{x}^2} + \dfrac{\partial^2 \bar{u}}{\partial \bar{y}^2}), \\ 0 = -\dfrac{\partial \bar{p}}{\partial \bar{y}} + (\dfrac{\partial^2 \bar{v}}{\partial \bar{x}^2} + \dfrac{\partial^2 \bar{v}}{\partial \bar{y}^2}). \end{array}\right. \tag{2}$$

some results like the drag force may be scaled in 3D were the drag is scaled by $(\mu U_0/L)L^2 = \mu U_0 L$, so that for a sphere with $L = R$ the radius of a sphere

$$D = 6\pi\mu R U_0.$$

The "prefactor" 6π is not so easy to compute, but it is tractable.
The drag force may be scaled in 2 D by $(\mu U_0/L)L = \mu U_0$, for example, on a cylinder of radius L:

$$D = \frac{4\pi\mu U_0}{1/2 - \gamma - log(\frac{U_0 L}{4\nu})} \text{ or } D = \frac{\frac{4\pi L}{Re}\rho U_0^2}{\log(\frac{1}{Re}) + \frac{1}{2} - \gamma + 2\log 2} \quad \text{with } \gamma \simeq 0.5772$$

the "prefactor" is here far more complicated, it involves the logarithm of the Reynolds. As says Keith Moffat in the "cours des Houches" 1973 "The complexity of the formula is indicative of the complexity of the underlying analysis" that we will see in the above mentioned chapter.

1.2 Large Reynolds flows

So, come back to large Reynolds flows, Re is large. We first non-dimensionalise the equations with L (the typical length of the body) and U_0 (the typical velocity) in all directions of space and velocity (with "bars" over the variables *i.e.* $\bar{x} = x/L$, $\bar{y} = y/L$, $\bar{u} = u/U_0$, $\bar{v} = v/U_0$ and $\bar{p} = p/(\rho U_0^2)$, the reference pressure is here taken to be 0, this must be changed in compressible flows. We can anyway say that there is a reference pressure p_0, and then $\bar{p} = (p - p_0)/(\rho U_0^2)$. Incompressible steady adimensionalised Navier Stokes equations are:

$$\left\{\begin{array}{l} \dfrac{\partial \bar{u}}{\partial \bar{x}} + \dfrac{\partial \bar{v}}{\partial \bar{y}} = 0, \\ \bar{u}\dfrac{\partial \bar{u}}{\partial \bar{x}} + \bar{v}\dfrac{\partial \bar{u}}{\partial \bar{y}} = -\dfrac{\partial \bar{p}}{\partial \bar{x}} + \dfrac{1}{Re}(\dfrac{\partial^2 \bar{u}}{\partial \bar{x}^2} + \dfrac{\partial^2 \bar{u}}{\partial \bar{y}^2}), \\ \bar{u}\dfrac{\partial \bar{v}}{\partial \bar{x}} + \bar{v}\dfrac{\partial \bar{v}}{\partial \bar{y}} = -\dfrac{\partial \bar{p}}{\partial \bar{y}} + \dfrac{1}{Re}(\dfrac{\partial^2 \bar{v}}{\partial \bar{x}^2} + \dfrac{\partial^2 \bar{v}}{\partial \bar{y}^2}). \end{array}\right. \tag{3}$$

Boundary conditions are no slip at the wall (defined by a function $\bar{y}_w(\bar{x})$ for simplicity as in practice it is an implicit surface) :

if $\bar{y} = \bar{y}_w(\bar{x})$ the wall: $\bar{u}(\bar{x}, \bar{y}_w(\bar{x})) = 0$, $\bar{v}(\bar{x}, \bar{y}_w(\bar{x})) = 0$ and $u = 1$ far away from the body.

Note that those boundary conditions are vague, see annex for an example with `freefem` and *Gerris*, in practice for sure, we impose $\bar{u} = 0$, $\bar{v} = 0$ on the body, $\bar{u} = 1$, $\bar{v} = 0$ at the entrance, and $\bar{p} = 0$ at the output. Then, $\partial\bar{p}/\partial\bar{n} = 0$ at the entrance, the algorithms impose the hidden BC: it is $\partial\bar{p}/\partial\bar{n} = 0$ on the body, Far from the body, Neumann B.C.

We can stop the story here. The problem is just to solve those equations. Our point of view is to examine those equations as a singular perturbation problem, as we saw in the chapter devoted on matched asymptotic expansions: `http://www.lmm.jussieu.fr/~lagree/COURS/M2MHP/MAE.pdf`.

Hence we identify the Navier Stokes equations to be a singular problem. When the small parameter Re^{-1} is small, we look at the Euler equations. Then we do a change of scale and look at the boundary layer problem. We will follow the Friedrichs problem procedure presented in that chapter, find the "outer solution", see that the problem is singular as there are too many boundary conditions. Then find by change of scale and "dominant balance" the new scale of the "inner problem", and find the solution by "asymptotic matching".

2 Some Euler simple solutions on a nearly flat plate: "small disturbance theory"

2.1 Euler equations

As the Reynolds number is large, a first idea is to put $1/Re = 0$. We obtain Euler equations (with "bars" over the variables *i.e.* $\bar{x} = x/L$, $\bar{u} = u/U_0$ etc for y and v):

$$\begin{cases} \dfrac{\partial \bar{u}}{\partial \bar{x}} + \dfrac{\partial \bar{v}}{\partial \bar{y}} = 0, \\ \bar{u}\dfrac{\partial \bar{u}}{\partial \bar{x}} + \bar{v}\dfrac{\partial \bar{u}}{\partial \bar{y}} = -\dfrac{\partial \bar{p}}{\partial \bar{x}}, \\ \bar{u}\dfrac{\partial \bar{v}}{\partial \bar{x}} + \bar{v}\dfrac{\partial \bar{v}}{\partial \bar{y}} = -\dfrac{\partial \bar{p}}{\partial \bar{y}}. \end{cases} \tag{4}$$

Boundary conditions are now slip at the wall: if $\bar{y} = \bar{y}_w(\bar{x})$ the wall:
$-\bar{u}(\bar{x}, \bar{y}_w(\bar{x}))\frac{d}{d\bar{x}}\bar{y}_w(\bar{x}) + \bar{v}(\bar{x}, \bar{y}_w(\bar{x})) = 0$: normal velocity equals to zero
and $\bar{u} = 1$ far away from the body.

From now, we prefer to restrain to the simple case of a nearly flat plate in an uniform stream. **Our aim is to compute the slip velocity, i.e. the tangential ideal fluid velocity on the wall**

The most simple case is the flat plate case, $\bar{y}_w(\bar{x}) = 0$. In this simple case the velocity remains everywhere 1; $(\bar{u}, \bar{v}) = (1, 0)$. So the velocity at the wall, "slip velocity" is $\bar{u}_e = 1$. All this chapter we use this hypothesis.

We will show that this problem is a regular perturbation of the flat plate case.

2.2 Historical note

Computing solution is the system is a great task since Euler first attempts "Principes généraux du mouvement des fluides" 1757 published in Mémoires de l'Académie des Sciences de Berlin. Do note that in "Essai d'une nouvelle théorie de la résistance des fluides" , ∂'Alembert in 1752 wrote equations more close to the decomposition in stream-function and potential as the main feature of the flow are incompressibility and irrotational flow. In 2D incompressibility gives $\overrightarrow{u} = \overrightarrow{\nabla} \times (\psi \overrightarrow{e}_z)$ and irrotational flow $\overrightarrow{\nabla}^2\psi = 0$. Or irrotational flow gives $\overrightarrow{u} = \overrightarrow{\nabla}\phi$ and incompressibility gives $\overrightarrow{\nabla}^2\phi = 0$. We prefer not to use so much ϕ and ψ, nevertheless for transonic flows, the expansion with ϕ is the most simple.

2.3 Linearized Euler boundary conditions

We then put a small bump or relative height α,

$$\bar{y}_w(\bar{x}) = \alpha \bar{f}(\bar{x}) \quad \text{with} \ \ \alpha \ll 1$$

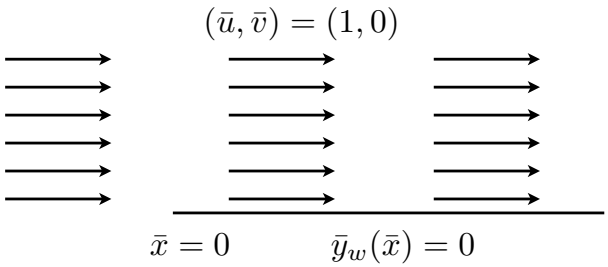

Figure 2: The basic flow is the constant flow over a semi infinite flat plate, $(\bar{u}, \bar{v}) = (1, 0)$, valid in any régime. We will consider next a regular perturbation of this uniform free stream

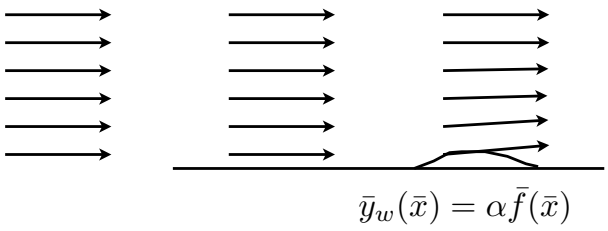

Figure 3: We deal with the most simple problem, a flat plate in a stream with a small bump of typical size $\alpha \ll 1$. We construct the solution as a regular perturbation of the uniform free stream

then we investigate a disturbance field as an asymptotic approximation (of course we hope it is a regular problem)

$$\bar{u} = 1 + \alpha \bar{u}_1 + \alpha^2 \bar{u}_2 + ...$$

$$\bar{v} = 0 + \alpha \bar{v}_1 + \alpha^2 \bar{v}_2 + ...$$

$$\bar{p} = 0 + \alpha \bar{p}_1 + \alpha^2 \bar{p}_2 + ...$$

This is called "small disturbance theory", as the wall disturbance is very small $\alpha \ll 1$. Depending of the various régimes various sets of equations may be obtained.

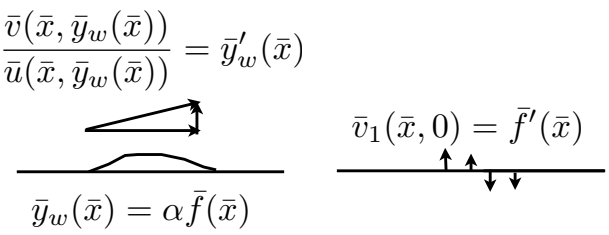

Figure 4: Left slip on a bump: it means that the slope of bump is v/u. Right: by "Transfer of Boundary Condition" the boundary boundary condition for the velocity is imposed at the flat wall, no more on the bump, it is called the "transpiration velocity".

At first, the boundary condition of no slip velocity reads:

$$\frac{\bar{v}(\bar{x}, \bar{y}_w(\bar{x}))}{\bar{u}(\bar{x}, \bar{y}_w(\bar{x}))} = \bar{y}'_w(\bar{x})$$

so that after taking the Taylor expansion of the velocity *i.e.*:

$$\bar{v}(\bar{x}, \bar{y}_w(\bar{x}) = \alpha \bar{v}_1(\bar{x}, \bar{y}_w(\bar{x}) + O(\alpha^2) = \alpha(\bar{v}_1(\bar{x}, 0) + \alpha \bar{f} \partial(\bar{v}_1(\bar{x}, 0)/\partial \bar{y} + ...$$

at leading order we obtain the value of the transverse velocity in $\bar{y} = 0$ as:

$$\frac{\bar{v}_1(\bar{x}, 0) + ...}{1 + ...} = \bar{f}'(\bar{x})$$

This boundary condition justifies the development for the transverse velocity.

The boundary boundary condition for the velocity is imposed at the flat wall, no more on the bump, it is called the "transpiration velocity". This change in boundary conditions is called "Transfer of Boundary Condition" (see Van Dyke [26]).

Now, we will write the linearized Euler equation, the gam consists in finding $\bar{u}_1$, $\bar{v}_1$ and $\bar{p}_1$ in a lot of flows. We will try to evaluate these quantities as a function of $\bar{f}$ in incompressible flow, in compressible flow, in shallow water flow...

These evaluation will be useful for the boundary layer theory.

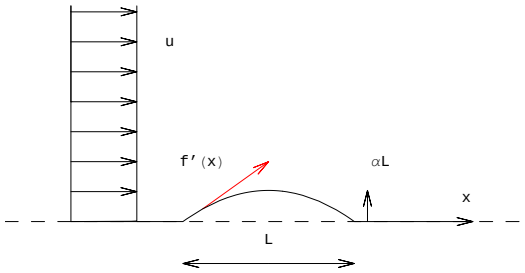

Figure 5: A plane plate with a small bump in a subsonic or incompressible flow

2.4 Linearized Euler incompressible flow

• We can imagine a non flat plate in a incompressible flow, we linearize the Euler equations as :

$$\begin{cases} \dfrac{\partial \bar{u}_1}{\partial \bar{x}} + \dfrac{\partial \bar{v}_1}{\partial \bar{y}} = 0, \\ \dfrac{\partial \bar{u}_1}{\partial \bar{x}} = -\dfrac{\partial \bar{p}_1}{\partial \bar{x}}, \\ \dfrac{\partial \bar{v}_1}{\partial \bar{x}} = -\dfrac{\partial \bar{p}_1}{\partial \bar{y}}. \end{cases} \tag{5}$$

Eliminating the velocity gives a Laplace equation for the pressure:

$$\frac{\partial^2 \bar{p}_1}{\partial \bar{x}^2} + \frac{\partial^2 \bar{p}_1}{\partial \bar{y}^2} = 0,$$

with $\bar{p}_1 = 0$ far away from the plate and the no slip condition is rewritten with the transpiration velocity as

$$-\frac{\partial \bar{p}_1}{\partial \bar{y}} = \bar{f}''(\bar{x}) \text{ in } \bar{y} = 0.$$

The pressure at the wall is obtained by classical Hilbert formula:

$$\bar{p}_1(\bar{x}, 0) = \frac{-1}{\pi} \fint \frac{\frac{d\bar{f}}{d\bar{x}}}{\bar{x} - \xi} d\xi$$

• Demonstration 1: to find this, we use Fourier Transform, so the wall is a superposition of modes e^{ikx}, the Laplacian is $-k^2 + \frac{\partial^2}{\partial \bar{y}^2} = 0$ and obtain the pressure as

$$A_- e^{ikx - |k|y} + A_+ e^{ikx + |k|y},$$

with $A_+ = 0$ as disturbances are zero far away, and the condition at the wall is $|k|A_- = ik((\hat{f}'))$, or $A_- = isign(k)((\hat{f}'))$, where $(\hat{f}')$ is the Fourier transform of f' and as the function "sign", which is $sign(k) = |k|/k$. The Heaviside or unit step distribution is H, with $H(x < 0) = 0$ and $H(x > 0) = 1$. They are linked by $sign(x)/2 + 1/2 = H(x)$. The derivative of H is δ the Dirac distribution. In Fourier space $ikTF(sign) = 2TF(\delta)$, so $TF(sign(x)) = 2/(ik)$ so that (2π from inverse transform and -1 due to ∂_x and ∂_k)

$$TF[sign(k)] = +\frac{i}{\pi} vp(\frac{1}{x}).$$

"Principal value", means that there is no problem in 0, This comes from the derivation in Fourier, and from the integration $1/(ik)$ $sign(k)$ has the same derivative than Heaviside function. So, the pressure is the convolution of f' and $\frac{1}{x}$:

$$p_1 = -\frac{1}{\pi} vp(\frac{1}{x}) * f'.$$

This is

$$\bar{p}_1 = \frac{-1}{\pi} \fint \frac{\frac{d\bar{f}}{d\bar{x}}}{\bar{x}-\xi} d\xi$$

We have by the definition of an integral in principal value:

$$\fint \phi(\xi) d\xi = \lim_{\varepsilon \to 0} \big(\int_{-\infty}^{-\varepsilon} \phi(\xi) d\xi + \int_{\varepsilon}^{\infty} \phi(\xi) d\xi \big)$$

We find that the solution is a convolution of $1/x$ and f' as proposed.

• Demonstration 2: to find this an alternate technique is the use of the Green function of the Laplacian which is a logarithm. the solution of Laplacian with a Dirac in source:

$$\frac{\partial^2 G}{\partial x^2} + \frac{\partial^2 G}{\partial y^2} = \delta(x,y)$$

written in r, θ, δ is function of r:

$$\frac{1}{r}(\frac{\partial}{\partial r} r \frac{\partial G}{\partial r}) + \frac{1}{r^2}\frac{\partial^2 G}{\partial \theta^2} = \delta$$

with the Dirac

$$\int\int \delta(x,y) dx dy = 1, \quad \text{or} \int_0^{\infty} \int_0^{2\pi} \delta(r,\theta) r d\theta dr = 1,$$

integrating the equation up to r and try a radial function $G(r)$ (by symmetry): $2\pi r \frac{\partial G}{\partial r} = 1$ so the Green function is

$$G = \frac{\ln(r)}{2\pi}.$$

This is a well know result in electrostatics, magnetostatics, fluid mechanics...

Consider now a problem with diracs only on $y = 0$ of weight say $\sigma(x)$, we have to solve with as a source a distribution $\sigma(x)\delta(y)$, such as

$$\partial_x^2 \Phi + \partial_y^2 \Phi = \sigma(x)\delta(y)$$

by integration across $y = 0$ from $y = 0^-$ to $y = 0^+$ the first term is 0, the second is the change of slope gives

$$\partial_y \Phi(x,0^+) - \partial_y \Phi(x,0^-)) = \sigma(x), \quad \text{so that} \quad 2\partial_y \Phi(x,0^+) = \sigma(x)$$

because by symmetry $\partial_y \Phi(x,0^-) = -\partial_y \Phi(x,0^+)$. We can now write Φ as a function of σ such that,

$$\Phi = \int \sigma(\xi) \frac{\ln(\sqrt{(x-\xi)^2 + y^2})}{2\pi} d\xi \quad \text{so} \quad \Phi = \int 2\partial_y \Phi(\xi,0) \frac{\ln(\sqrt{(x-\xi)^2 + y^2})}{2\pi} d\xi.$$

Hence the pressure in the plane is obtained (Φ is our pressure):

$$\bar{p}_1 = \frac{1}{\pi} \int (-f''(\xi)) \ln(\sqrt{(\bar{x}-\xi)^2 + \bar{y}^2}) d\xi$$

integrating by parts (at infinity, 0)

$$\bar{p}_1 = \frac{1}{\pi} \int f'(\xi) \frac{1}{(\sqrt{(\bar{x}-\xi)^2 + \bar{y}^2})} d\xi.$$

The pressure at the wall is then obtained with $\bar{y} = 0$. But the value on the wall is a problem (it involves $\sqrt{(\bar{x}-\xi)^2}$, so we cut the previous integral at the position $\bar{x}$ (i.e. $\bar{x} > \xi$ and $\bar{x} < \xi$)

$$\bar{p}_1 = \frac{1}{\pi} \int (-f''(\xi)) \ln(|\bar{x}-\xi|) d\xi = \frac{1}{\pi} \int_{-\infty}^{\bar{x}-\varepsilon} (-f''(\xi)) \ln(\bar{x}-\xi) d\xi + \frac{1}{\pi} \int_{\bar{x}+\varepsilon}^{\infty} (-f''(\xi)) \ln(-\bar{x}+\xi) d\xi$$

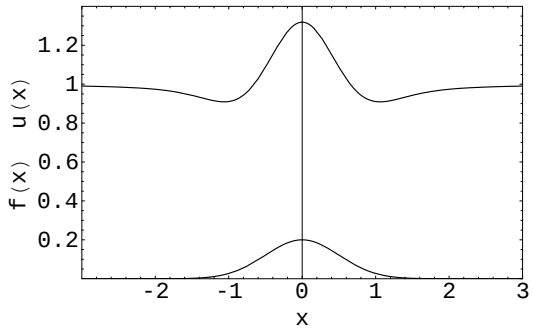

Figure 6: The bump $\bar{f}$ and the perturbed velocitywith the Hilbert integral subsonic flow. Note that the flow is perturbed before the bump (the Laplacian acts every were in the flow).

we integrate it by parts

$$\bar{p}_1 = \frac{1}{\pi}\int_{-\infty}^{\bar{x}-\varepsilon} f'(\xi)\frac{-1}{(\bar{x}-\xi)}d\xi + [(-f'(\xi))\ln(|\bar{x}-\xi|)]_{-\infty}^{\bar{x}-\varepsilon} +$$

$$+\frac{1}{\pi}\int_{\bar{x}+\varepsilon}^{\infty} f'(\xi)\frac{1}{(-\bar{x}+\xi)}d\xi + [(-f'(\xi))\ln(|\bar{x}-\xi|)]_{\bar{x}+\varepsilon}^{\infty}$$

but as

$$[(-f'(\xi))\ln(|\bar{x}-\xi|)]_{-\infty}^{\bar{x}-\varepsilon} + [(-f'(\xi))\ln(|\bar{x}-\xi|)]_{\bar{x}+\varepsilon}^{\infty} = -f'(\bar{x}-\varepsilon)\ln(|\varepsilon|) + f'(\bar{x}+\varepsilon)\ln(|\varepsilon|)$$

if we suppose that f' is enough small at infinity, this is zero for small ε and we have by the definition of an integral in principal value:

$$\bar{p}_1 = \lim_{\varepsilon\to 0}\Big(\frac{-1}{\pi}\int_{-\infty}^{\bar{x}-\varepsilon}\frac{f'(\xi)}{(\bar{x}-\xi)}d\xi + \frac{-1}{\pi}\int_{\bar{x}+\varepsilon}^{\infty}\frac{f'(\xi)}{(\bar{x}-\xi)}d\xi\Big) = \frac{-1}{\pi}⨍_{-\infty}^{\infty}\frac{f'(\xi)}{\bar{x}-\xi}d\xi.$$

• Final value of the pressure at the wall

$$\bar{p}_1(\bar{x},0) = \frac{-1}{\pi}⨍_{-\infty}^{\infty}\frac{f'(\xi)}{(\bar{x}-\xi)}d\xi.$$

The velocity at the wall is then:

$$\bar{u}_e(\bar{x}) = 1 + \alpha\frac{1}{\pi}⨍_{-\infty}^{\infty}\frac{\frac{d\bar{f}}{d\bar{x}}}{\bar{x}-\xi}d\xi$$

this is the "slip velocity" (it will be the velocity at the "edge" of the boundary layer).

The most important thing to have in mind, is that the Laplacian has an action far from the perturbation (log terms). On the wall, this long range interaction is this integral from $-\infty$ to ∞. So boundary conditions are important at the boundaries of the problem (for example if ψ is not zero at the wall, there are extra terms in $\psi\nabla G$.

We will see that other régimes give different behaviors, The next case for example has no influence of what happens downstream.

Note 0:
This problem is a regular perturbation of the flat plate case.

Note 1:
As an exercise, we should compare with `freefem++` (either with a domain with a bump or a flat bottom

with a Neuman BC.

Note 2:
This is called the thickness problem, the curvature problem gives the lift, but this is another story... To make a long story short, let us consider a wing of length L, inclined by an angle α_i compared to the free stream, the curvature induces a velocity field in terms of vorticies,

$$v = U_0\alpha_i - \frac{1}{2\pi}\int_0^L \frac{\gamma(\xi)}{x-\xi}d\xi$$

as this this flow is tangential to the airfoil,

$$U_0(\alpha_i - \frac{dy}{dx}) = \frac{1}{(2\pi)}\int_0^c \frac{\gamma(\xi)}{(x-\xi}d\xi$$

The problem is that the distribution $\gamma(x)$ is unknown, we have to reverse the problem. The trick introduced by Glauert consists in changing the variable: $x = c(1-\cos(\theta))/2$ and to decompose it in a Fourier series :

$$\frac{\gamma(\theta)}{(2U_0)} = A_0\frac{(1+\cos(\theta))}{\sin(\theta)} + \sum A_n\ \sin(n\theta))$$

As the following identities may be demonstrated

$$\int_0^\pi \frac{\cos n\vartheta}{\cos\theta - \cos\vartheta}d\vartheta = -\frac{\pi\sin n\theta}{\sin\theta},\ \text{and}\ \int_0^\pi \frac{C+\cos\vartheta}{\cos\theta-\cos\vartheta}d\vartheta = -\pi$$

and applying Kutta condition at the trailing edge allows to reconstruct the γ.

Note 3:
There are other methods with complex analysis to do that...

Note 4:
There is no note 4.

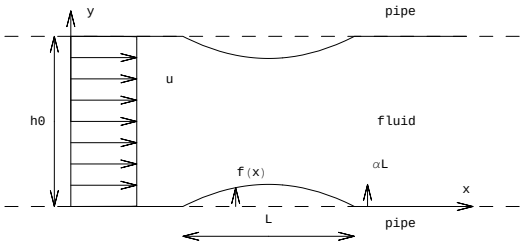

Figure 7: A channel with a small bump (here symmetrical) in a an incompressible flow

2.5 Linearized Euler confined incompressible flow

• We can imagine a flow in a long channel $x = L\bar{x}$ using the height as scale thus $y = h_0\bar{y}$, by mass conservation

$$\frac{\partial \bar{u}_1}{\partial \bar{x}} + \frac{\partial \bar{v}_1}{\partial \bar{y}} = 0 \tag{6}$$

we have that the scale associated to $\bar{v}$ is $U_0 h_0/L$. It is straightforward to see that the longitudinal velocity and pressure are linked as previously:

$$\frac{\partial \bar{u}_1}{\partial \bar{x}} = -\frac{\partial \bar{p}_1}{\partial \bar{x}},$$

but now, we have for the transverse velocity

$$(h_0/L)^2 \frac{\partial \bar{v}_1}{\partial \bar{x}} = -\frac{\partial \bar{p}_1}{\partial \bar{y}}.$$

so that $-\frac{\partial \bar{p}_1}{\partial \bar{y}} = 0$ so we deduce that $\bar{p}_1$ is a function $\bar{x}$ only; and so is $\bar{u}_1$. The flow will look like a "plug flow".

The slip boundary conditions on the wall are $\bar{v}_1(\bar{x}, 0) = \bar{f}'$ and $\bar{v}_1(\bar{x}, 1) = -\bar{f}'$ (note the sign!).. Hence, integrated over the pipe ($\int_0^1 d\bar{y}$), the mas conservation gives, as $\bar{u}_1$ is not a function of $\bar{y}$:

$$\frac{\partial}{\partial \bar{x}} \bar{u}_1 - 2\bar{f}' = 0,$$

so, as perturbation are zero far upstream

$$\bar{u}_1 = 2\bar{f}, \qquad \bar{p}_1 = -2\bar{f}'.$$

The velocity at the wall is then:

$$\bar{u}_e = 1 + 2\alpha \bar{f}.$$

Note that in a pipe, the velocity is in phase with the bump shape.

• This solution may be obtained in an alternative way. We may start from a flow like in the previous sub-section "linearized Euler incompressible flow". From the previous case

$$\frac{\partial \bar{u}_1}{\partial \bar{x}} = -\frac{\partial \bar{p}_1}{\partial \bar{x}},$$

the $\bar{v}_1$ was present as the scales in x and y are L.

$$\frac{\partial \bar{v}_1}{\partial \bar{x}} = -\frac{\partial \bar{p}_1}{\partial \bar{y}}.$$

with $\bar{v}_1(0) = \bar{f}_1'$. But now the height is $\bar{h}_0 = h_0/L$ and thus $\bar{v}_1(\bar{h}_0) = -\bar{f}_1'$. Previously in the sub-section "linearized Euler incompressible flow", this velocity was zero as previously $\bar{h}_0 = \infty$.

Tehn, Laplace equation may be obtained for every field

$$\frac{\partial^2 \bar{p}_1}{\partial \bar{x}^2} + \frac{\partial^2 \bar{p}_1}{\partial \bar{y}^2} = 0, \quad \frac{\partial^2 \bar{v}_1}{\partial \bar{x}^2} + \frac{\partial^2 \bar{v}_1}{\partial \bar{y}^2} = 0,$$

taking into account the boundary condition for the upper plate allows to obtain exactly the solution, so that in Fourier space solutions are:

$$A_+ e^{k\bar{y}} + A_- e^{-k\bar{y}}$$

it then then easy to show that in Fourier space:

$$\bar{v}_1 = (ik\bar{f}_1)\frac{\sinh(k(\bar{h}_0/2 - y))}{\sinh(k\bar{h}_0/2)}$$

$$\bar{u}_1 = (k\bar{f}_1)\frac{\cosh(k(\bar{h}_0/2 - y))}{\sinh(k\bar{h}_0/2)}$$

- then if $k\bar{h}_0 \to \infty$, which corresponds to an infinite domain

$$\bar{v}_1 = (ik\bar{f}_1)$$

$$\bar{u}_1 = (k\bar{f}_1)$$

which is the previous one leading to the Hilbert integral of the sub-section "linearized Euler incompressible flow",
- then as $k\bar{h}_0 \to 0$, which corresponds to this section of a thin channel, the expansion

$$\bar{v}_1 = (ik\bar{f}_1)\frac{\sinh(k(\bar{h}_0/2 - \bar{y}))}{\sinh(k\bar{h}_0/2)} \to (ik\bar{f}_1)(1 - 2\bar{y}/\bar{h}_0)$$

in real space:

$$\bar{v}_1 \to (\bar{f}_1')(1 - 2\bar{y}/\bar{h}_0)$$

then velocity is

$$\bar{u}_1 = (k\bar{f}_1)\frac{1}{(k\bar{h}_0/2)} = (2\bar{f}_1)/(\bar{h}_0)$$

which indeed tells that f must be measured by h_0 as done during the previous point.

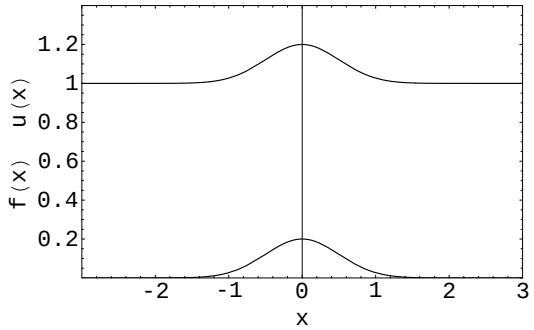

Figure 8: The bump and the perturbed longitudinal velocity, slender channel flow. Note that the flow is not perturbed before the bump.

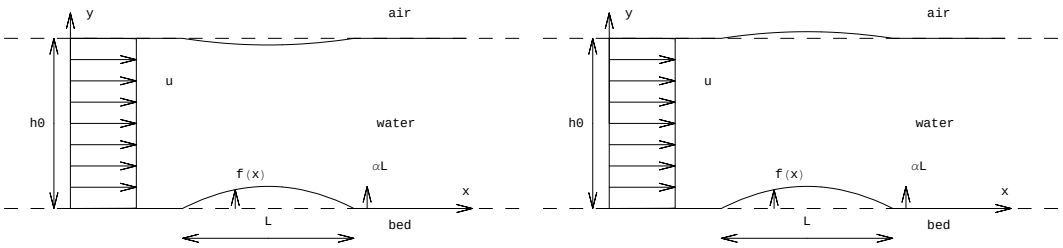

Figure 9: A liquid layer with a free surface with a small bump in subcritical régime and right supercritical régime

2.6 Linearized Euler with free surface (for shallow water flow)

• But we can imagine a thin liquid layer in the gravity field g with an interface η flowing on plate with a long bump of length L, using h_0 as transversal scale $\eta = h_0\bar{\eta}$, $y = h_0\bar{y}$, and using the long size of the bump L for x: $x = L\bar{x}$, so $u = U_0\bar{u}$ and $v = U_0 h_0\bar{v}/L$ to ensure dominant balance in incompressibility $\frac{U_0}{L}\frac{\partial\bar{u}}{\partial\bar{x}} + \frac{U_0(h_0/L)}{h_0}\frac{\partial\bar{v}}{\partial\bar{y}} = 0$: For pressure let us take $p = \rho U_0^2\bar{p}$ (note that we can take $p = gh_0\bar{p}$, the final result will be the same.

$$\begin{cases} \dfrac{\partial\bar{u}}{\partial\bar{x}} + \dfrac{\partial\bar{v}}{\partial\bar{y}} = 0, \\ \bar{u}\dfrac{\partial\bar{u}}{\partial\bar{x}} + \bar{v}\dfrac{\partial\bar{u}}{\partial\bar{y}} = -\dfrac{\partial\bar{p}}{\partial\bar{x}}, \\ \dfrac{h_0^2}{L^2}(\bar{u}\dfrac{\partial\bar{v}}{\partial\bar{x}} + \bar{v}\dfrac{\partial\bar{v}}{\partial\bar{y}}) = -\dfrac{\partial\bar{p}}{\partial\bar{y}} - \dfrac{gh_0}{U_0^2}. \end{cases} \tag{7}$$

For Shallow water flow $\frac{h_0^2}{L^2} \to 0$,

$$\begin{cases} \dfrac{\partial\bar{u}}{\partial\bar{x}} + \dfrac{\partial\bar{v}}{\partial\bar{y}} = 0, \\ \bar{u}\dfrac{\partial\bar{u}}{\partial\bar{x}} + \bar{v}\dfrac{\partial\bar{v}}{\partial\bar{y}} = -\dfrac{\partial\bar{p}}{\partial\bar{x}}, \\ 0 = -\dfrac{\partial\bar{p}}{\partial\bar{y}} - \dfrac{1}{F^2} \end{cases} \tag{8}$$

We take a small bump: $\bar{y}_w(\bar{x}) = \alpha\bar{f}(\bar{x})$ with $\alpha << 1$ in the gravity field with a Froude number ($F^2 = U_0^2/(gh_0)$). We obtain the almost the Shallow Water equation (or Saint Venant) $\bar{u} = 1+\alpha\bar{u}_1+...$, $\bar{v} = \alpha\bar{v}_1+...$ interface is $\bar{y} = 1 + \alpha\eta_1 + ...$ at the surface $p = 0$ pressure is zero at the interface (atmospheric pressure is the reference) $\bar{p} = (\bar{\eta} - \bar{y})/F^2$, so as we will expand $\bar{p} = \bar{p}_0 + \alpha\bar{p}_1 + ...$, we guess :

$$\bar{p} = (1 - \bar{y})/F^2 + \alpha\bar{\eta}_1/F^2 + ... \text{ so } \ \bar{p}_0 = (1 - \bar{y})/F^2 \text{ and } \ \bar{p}_1 = \bar{\eta}_1/F^2$$

the system reads

$$\begin{cases} \dfrac{\partial\bar{u}_1}{\partial\bar{x}} + \dfrac{\partial\bar{v}_1}{\partial\bar{y}} = 0, \\ \dfrac{\partial\bar{u}_1}{\partial\bar{x}} = -\dfrac{\partial\bar{p}_1}{\partial\bar{x}}, \\ 0 = -\dfrac{\partial\bar{p}_1}{\partial\bar{y}} \end{cases} \tag{9}$$

so the momentum gives $\bar{u}_1 = -\bar{\eta}/F^2$. Integrating over the depth the continuity equation gives

$$1\frac{\partial\bar{u}_1}{\partial\bar{x}} + [\bar{v}_1]_0^1 = 0$$

but on the wall $\bar{v}_1(\bar{x}, 0) = \frac{d\bar{f}}{d\bar{x}}$ and on the surface, the same slip $\bar{v}_1(\bar{x}, 1) = \frac{d\bar{\eta}_1}{d\bar{x}}$, by integration,

$$\bar{u}_1 = -\bar{\eta} + \bar{f}$$

This gives an other expression for $\bar{u}_1$, by substitution, the perturbation of the free surface is

$$\bar{\eta_1} = F^2 \frac{\bar{f}}{F^2 - 1}$$

whereas the slip velocity is

$$\bar{u}_e = 1 + \frac{\alpha \bar{f}}{1 - F^2} + ...$$

For a fluvial flow $F < 1$, the interface is deviated to the bottom, the velocity increases over a positive bump. For a torrential flow $F > 1$, the disturbance of the free surface is positive, and the velocity decreases on the bump. Note that the flow is not perturbed before the bump. There is no upstream influence of the downstream.

2.7 Compressible Euler equations

2.7.1 Full Compressible Navier Stokes equations

In this section we deal with compressible flow. We recall first the equations and write them with potential. it will be useful for transonic flows. After having presented this, we write the compressible small disturbance theory (completely similar to the incompressible one présented before). See annex 6 for introduction to acoustics.
The complete NS equations for a compressible Newtonian fluid:
mass conservation:

$$\frac{d\rho}{dt} + \rho \underline{\nabla} \cdot \underline{u} = 0.$$

momentum conservation:

$$\rho \frac{d\underline{u}}{dt} = \underline{\nabla} \cdot \underline{\underline{\sigma}} + \underline{f}.$$

Energy conservation:

$$\rho \frac{de}{dt} = \underline{\underline{\sigma}} : \underline{\underline{D}} - \underline{\nabla} \cdot \underline{q} + r.$$

constitutive relations:

$$\underline{\underline{\sigma}} = -p\underline{\underline{I}} + \lambda \underline{\nabla} \cdot \underline{u}\underline{\underline{I}} + 2\mu \underline{\underline{D}}, \qquad \underline{q} = -k\underline{\nabla} T.$$

law of state:

$$p(\rho, T)$$

coefficients:

$$c_v(T), \quad c_p(T), \quad \lambda(T), \quad \mu(T), \quad k(T)...$$

boundary conditions T_w **OR** q_w imposed, non slip conditions at the wall.

Note that we define as well enthalpy

$$h = e + p/\rho$$

and entropy

$$ds = \frac{de}{T} + (\frac{p}{T}) d(\frac{1}{\rho}).$$

So the terms with λ and μ and with k will be of order $1/Re$. They will disappear from the equations, so that we can write the Euler system. We have $\underline{\underline{\sigma}} = -p\underline{\underline{I}}$, and $\underline{q} = 0$ and $r = 0$.

2.7.2 Compressible Euler equations

Sowe obtain the compressible Euler equations which are : ($\frac{d}{dt} = \frac{\partial}{\partial t} + \overrightarrow{u} \cdot \overrightarrow{\nabla}$):

$$\begin{cases} \dfrac{\partial \rho}{\partial t} + \overrightarrow{\nabla} \cdot (\rho \overrightarrow{u}) = 0, \\ \dfrac{\partial \overrightarrow{u}}{\partial t} + \overrightarrow{u} \cdot \overrightarrow{\nabla} \overrightarrow{u} = -\dfrac{\overrightarrow{\nabla} p}{\rho}, \\ \dfrac{\partial h}{\partial t} + \overrightarrow{u} \cdot \overrightarrow{\nabla} h = \dfrac{1}{\rho}(\dfrac{\partial p}{\partial t} + \overrightarrow{u} \cdot \overrightarrow{\nabla} p). \end{cases} \tag{10}$$

The last one (10) is the enthalpy equation, it comes from energy equation which is here $\rho de/dt = -p\overrightarrow{\nabla} \cdot \overrightarrow{u}$ using mass $\overrightarrow{\nabla} \cdot \overrightarrow{u} = -(\frac{1}{\rho})\frac{d\rho}{dt}$ it transforms in $\rho \frac{de}{dt} = \frac{p}{\rho} \frac{d\rho}{dt}$. As definition of entropy is $Tds = de + pd(\frac{1}{\rho})$ we have $ds = \frac{p}{\rho^2} d\rho + pd(\frac{1}{\rho}) = 0$ as expected.

By definition of enthalpy $h = e + p/\rho$, the obtained energy equation $\rho \frac{de}{dt} = \frac{p}{\rho} \frac{d\rho}{dt}$ becomes as written above:

$$\rho(\frac{dh}{dt} - \frac{1}{\rho}\frac{dp}{dt}) = 0$$

2.7.3 Potential flow

We are looking at isentropic flows, so that $ds = 0$ remember:

$$ds = \frac{de}{T} + (\frac{p}{T})d(\frac{1}{\rho}) \text{ and as } h = e + p/\rho, \;\; dh = Tds + \rho^{-1}dp,$$

by definition of c_p, c_v, r we have $dh = c_p dT$ and $de = c_v dT$ and $p/\rho = rT$, this gives the Mayer relation $c_p = c_v + r$, but we define the index $\gamma = c_p/c_v$. We then have $c_p = r/(\gamma - 1)$ so that $dh = \gamma r/(\gamma - 1)dT = \gamma/(\gamma - 1)d(p/\rho)$, and

$$dh = Tds + \rho^{-1}dp \text{ becomes } \gamma/(\gamma - 1)d(p/\rho) = Tds + dp/\rho$$

or

$$(\gamma - 1)Tds = dp/\rho - p\gamma d\rho/\rho^2$$

giving the final expected:

$$ds = c_v(dp/p - \gamma d\rho/\rho)$$

so when $ds = 0$ we have $\gamma d\rho/\rho = dp/p$ (latter we will write $c^2 = \gamma p/\rho$ so that $dp = c^2\rho$, see appendix 6). This gives then the famous relation (Laplace law PV^γ=cste):

$$p \propto \rho^\gamma.$$

In the second equation (momentum), it is classical that

$$\overrightarrow{u} \cdot \overrightarrow{\nabla}\overrightarrow{u} = \overrightarrow{\nabla}\frac{\overrightarrow{u}^2}{2} + (\overrightarrow{\nabla} \times \overrightarrow{u}) \times \overrightarrow{u}.$$

Then with the third (energy):

$$\overrightarrow{\nabla}(\frac{\overrightarrow{u}^2}{2} + h) - T\overrightarrow{\nabla}s + (\overrightarrow{\nabla} \times \overrightarrow{u}) \times \overrightarrow{u} = 0.$$

If we multiply it by $\overrightarrow{u}$ we have the "compressible Bernoulli" equation along a stream line (remember $ds/dt = 0$):

$$\overrightarrow{u} \cdot \overrightarrow{\nabla}(\frac{u^2}{2} + h) = 0$$

If $ds/dt \neq 0$ and if the flow is iso energetic (i.e. $(\frac{u^2}{2} + h) = cst$), then the creation of entropy is linked to the rotational of the flow by the Crocco theorem:

$$T\overrightarrow{\nabla}s = (\overrightarrow{\nabla} \times \overrightarrow{u}) \times \overrightarrow{u}.$$

As $h = c_pT = \frac{\gamma}{\gamma-1}\frac{p}{\rho}$, the enthalpy may be expressed with the local speed of sound $h = \frac{c^2}{\gamma-1}$. So that we obtain the relation between the speed of sound and the velocity:

$$\frac{u^2 + v^2}{2} + \frac{c^2}{\gamma - 1} = \frac{U_0^2}{2} + \frac{c_0^2}{\gamma - 1}.$$

It is here important to remind the definition of the Mach number:

$$M_0^2 = \frac{U_0^2}{c_0^2}, \;\; \text{with} \;\; c_0^2 = \frac{\gamma p_0}{\rho_0}.$$

Sometimes one uses the symbol a_0 instead of c_0. Another useful equation may be found, let us multiply the second by $\overrightarrow{u}$

$$\overrightarrow{u} \cdot (\overrightarrow{u} \cdot \overrightarrow{\nabla}\overrightarrow{u}) = -\frac{\overrightarrow{u} \cdot \overrightarrow{\nabla}p}{\rho} \text{ or, this is } c^2\frac{\overrightarrow{u} \cdot \overrightarrow{\nabla}\rho}{\rho}$$

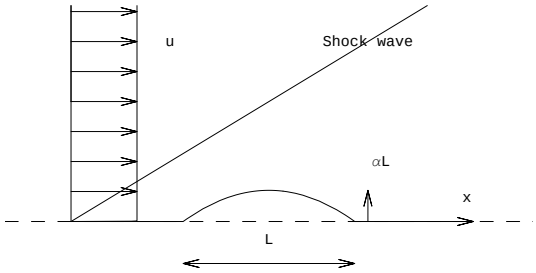

Figure 10: A plane plate with a small bump in a supersonic flow.

this is due to $ds = 0$ so that $p \propto \rho^{-\gamma}$ and $dp = (d\rho)c^2$. Eliminating the density from the continuity equation gives:

$$\overrightarrow{u} \cdot (\overrightarrow{u} \cdot \overrightarrow{\nabla}\overrightarrow{u}) = c^2 \overrightarrow{\nabla} \cdot \overrightarrow{u}.$$

We may develop it as:

$$(c^2 - u^2)\frac{\partial u}{\partial x} - uv(\frac{\partial u}{\partial y} + \frac{\partial v}{\partial x}) + (c^2 - v^2)\frac{\partial v}{\partial y} = 0.$$

So that if we look at potential flows (cf Crocco theorem) we define a potential of velocities $u = \partial_x \phi$ and $v = \partial_y \phi$. the previous equation reads

$$(\phi_x^2 - c^2)\phi_{xx} + 2\phi_x\phi_y\phi_{xy} + (\phi_y^2 - c^2)\phi_{yy} = 0.$$

This equation is powerful, we will use it for transonic flow. Before this we come back to simple disturbance theory without the potential function.

2.8 Linearized Euler compressible supersonic flow

• We can imagine a compressible flow on flat plate: $\bar{y}_w(\bar{x}) = \alpha \bar{f}(\bar{x})$ with $\alpha << 1$, compressible steady linearized Euler, mass, momentum and energy (adiabatic) are after non dimensionalizing by ρ_0, p_0, U_0, L just as we did for incompressible flows:

$$u = U_0(1 + \alpha\bar{u}_1 + ...);\ v = U_0(\alpha\bar{v}_1 + ...);\ p = p_0(1 + \alpha\bar{p}_1 + ...);\ \rho = \rho_0(1 + \alpha\bar{\rho}_1 + ...)$$

so that :

$$\begin{cases} \dfrac{\partial\bar{\rho}_1}{\partial\bar{x}} + \dfrac{\partial\bar{u}_1}{\partial\bar{x}} + \dfrac{\partial\bar{v}_1}{\partial\bar{y}} = 0, \\ \dfrac{\partial\bar{u}_1}{\partial\bar{x}} = -\dfrac{1}{\gamma M_0^2}\dfrac{\partial\bar{p}_1}{\partial\bar{x}}, \\ \dfrac{\partial\bar{v}_1}{\partial\bar{x}} = -\dfrac{1}{\gamma M_0^2}\dfrac{\partial\bar{p}_1}{\partial\bar{y}}, \\ \bar{p}_1 = \gamma\bar{\rho}_1. \end{cases} \tag{11}$$

Note that at some point we had to estimate $p_0/(\rho U_0^2)$ which is $(\gamma p_0/\rho)/(\gamma U_0^2) = (c_0^2/U_0^2)/\gamma$, that is the $\frac{1}{\gamma M_0^2}$ term in the above equations. The definition of c_0 is presented in annex 6 were the expansion around the steady equilibrium is presented. Eliminating the velocity and the density gives a Heat/Wave (depending on the Mach number) equation for the pressure:

$$(1 - M_0^2)\frac{\partial^2\bar{p}_1}{\partial\bar{x}^2} + \frac{\partial^2\bar{p}_1}{\partial\bar{y}^2} = 0,$$

with the BC:

$$\frac{df'}{d\bar{x}} = -\frac{1}{\gamma M_0^2}\frac{\partial\bar{p}_1}{\partial\bar{y}}|_0$$

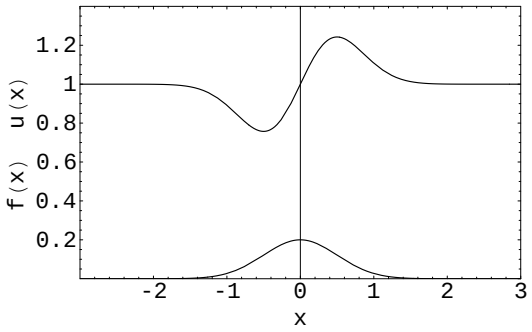

Figure 11: Supersonic flow on a small bump , bump and velocity

• The subsonic case $M_0 < 1$ gives again the same result than previously with a coefficient in $\sqrt{1-M_0^2}$, which can be removed in changing the scale of say $\sqrt{1-M_0^2}\bar{y} = \bar{Y}$ so that

$$\frac{\partial^2 \bar{p}_1}{\partial \bar{x}^2} + \frac{\partial^2 \bar{p}_1}{\partial \bar{Y}^2} = 0,$$

which is the Laplace equation, with B.C.:

$$\frac{\partial \bar{p}_1}{\partial \bar{Y}}|_0 = -\frac{\gamma M_0^2}{\sqrt{1-M_0^2}} \frac{df'}{d\bar{x}}$$

etc, this is the Prandtl Glauert similarity:

$$\bar{p}_1 = \quad \frac{-1}{\pi} \frac{\gamma M_0^2}{\sqrt{1-M_0^2}} \fint \frac{f'(\xi)}{(\bar{x}-\xi)} d\xi$$

note that for small M_0 and after rescaling with $\rho_0 U_0^2$ instead of p_0 we reobtain the incompressible case $\frac{-1}{\pi} \fint \frac{f'(\xi)}{(\bar{x}-\xi)} d\xi$

• the supersonic case ($M_0 > 1$) gives the ∂'Alembert equation, the solution for pressure is :

$$\bar{p}_1 = F(\bar{x} - \sqrt{M_0^2 - 1}\bar{y}) + G(\bar{x} + \sqrt{M_0^2 - 1}\bar{y})$$

the pressure is contant along the characteristic lines $\bar{y} = \pm \bar{x}/\sqrt{M_0^2 - 1} + cst$, clearly the bump creates the perturbation, and there is no perturbation upstream, so that $G = 0$. hence, using the B.C. at the wall:

$$\partial_{\bar{y}} p_1(\bar{x}, 0) = -\gamma M_0^2 \partial_{\bar{x}} v_1(\bar{x}, 0) \text{ so } \sqrt{M_0^2 - 1} F'(\bar{x}) = -\gamma M_0^2 f''(\bar{x})$$

the final expression or the perturbation of pressure:

$$\bar{p}_1 = \frac{\gamma M_0^2}{\sqrt{M_0^2 - 1}} \frac{d\bar{f}}{d\bar{x}} + ...$$

which is the "Ackeret formula" and the velocity is then

$$\bar{u}_e = 1 - \frac{1}{\sqrt{M_0^2 - 1}} \frac{\alpha d\bar{f}}{d\bar{x}} + ...$$

2.9 Low Mach approximation

We have seen that the system (10) is the system of Euler compressible equations. With $\overrightarrow{u} = U_0 \overrightarrow{\bar{u}}$, $p = p_0 \bar{p}$, $\rho = \rho_0 \bar{\rho}$, then as $M_0^2 = U_0^2/(\gamma p_0/\rho_0)$, as $dh = c_p dT$, we have $dh = \gamma r/(\gamma - 1) d\bar{T}$ so the system (10) is

$$\left\{ \begin{array}{l} \dfrac{\partial \bar{\rho}}{\partial \bar{t}} + \overrightarrow{\bar{\nabla}} \cdot (\bar{\rho} \overrightarrow{\bar{u}}) = 0, \\ \dfrac{\partial \overrightarrow{\bar{u}}}{\partial \bar{t}} + \overrightarrow{\bar{u}} \cdot \overrightarrow{\bar{\nabla}} \overrightarrow{\bar{u}} = -\dfrac{\overrightarrow{\bar{\nabla}} \bar{p}}{\gamma M_0^2 \bar{\rho}}, \\ \dfrac{\partial \bar{h}}{\partial \bar{t}} + \overrightarrow{\bar{u}} \cdot \overrightarrow{\bar{\nabla}} \bar{h} = \dfrac{\gamma - 1}{(\gamma)\bar{\rho}} (\dfrac{\partial \bar{p}}{\partial \bar{t}} + \overrightarrow{\bar{u}} \cdot \overrightarrow{\bar{\nabla}} \bar{p}). \end{array} \right. \tag{12}$$

This system may be linearised at a given Mach number M_0 and we obtain the previous linearised system (11).

Now we look to what happens when $M_0 \to 0$. We see that the problem (12) is singular (because we loose $d\overrightarrow{u}/dt$ in momentum!)

To solve it, we have to do a low Mach expansion (Paolucci 1982 and 1994):

$$\overrightarrow{\bar{u}} = \overrightarrow{\bar{u}}_0 + M_0 \overrightarrow{\bar{u}}_1 + ...$$

$$\bar{\rho} = \bar{\rho}_0 + M_0 \bar{\rho}_1 + M_0^2 \bar{\rho}_2 ...$$
$$\bar{T} = \bar{T}_0 + M_0 \bar{T}_1 + M_0^2 \bar{T}_2 + ...$$
$$\bar{p} = \bar{p}_0 + M_0 \bar{p}_1 + M_0^2 \gamma \bar{p}_2 ..$$

(mind the γ which is for aestetics) which gives

$$\left\{ \begin{array}{ll} \text{at order } 0 & \dfrac{\partial \bar{\rho}_0}{\partial \bar{t}} + \overrightarrow{\bar{\nabla}} \cdot (\bar{\rho}_0 \overrightarrow{\bar{u}}_0) = 0, \\ \text{at order } M_0^{-2} & 0 = -\dfrac{\overrightarrow{\bar{\nabla}} \bar{p}_0}{\gamma \bar{\rho}_0}, \\ \text{at order } M_0^{-1} & 0 = -\dfrac{\overrightarrow{\bar{\nabla}} \bar{p}_1}{\gamma \bar{\rho}_0}, \\ \text{at order } 0 & \dfrac{\partial \overrightarrow{\bar{u}_0}}{\partial \bar{t}} + \overrightarrow{\bar{u}}_0 \cdot \overrightarrow{\bar{\nabla}} \overrightarrow{\bar{u}}_0 = -\dfrac{\overrightarrow{\bar{\nabla}} \bar{p}_2}{\bar{\rho}_0}, \\ \text{at order } 0 & \dfrac{\partial \bar{h}_0}{\partial \bar{t}} + \overrightarrow{\bar{u}}_0 \cdot \overrightarrow{\bar{\nabla}} \bar{h}_0 = \dfrac{\gamma - 1}{\gamma \bar{\rho}_0} (\dfrac{\partial \bar{p}_0}{\partial \bar{t}} + \overrightarrow{\bar{u}}_0 \cdot \overrightarrow{\bar{\nabla}} \bar{p}_0). \end{array} \right. \tag{13}$$

and : $\bar{p}_0 = \bar{\rho}_0 \bar{T}_0$. The second and the third show that $\bar{p}_0$ and $\bar{p}_1$ are function of $\bar{t}$ uniquely, not of space, so the last one is with time only:

$$\frac{dp_0(\bar{t})}{d\bar{t}} = \frac{\gamma \bar{\rho}_0}{\gamma - 1} \left(\frac{\partial \bar{T}_0}{\partial \bar{t}} + \overrightarrow{\bar{u}}_0 \cdot \overrightarrow{\bar{\nabla}} \bar{T}_0 \right).$$

If we impose at entrance temperature, we see that the global pressure increases in time.

If we heat the flow at the boundaries, by conservation of mass

$$\frac{d}{d\bar{t}} \int_V \rho_0 dv = 0$$

but as $p_0(\bar{t}) = \rho_0(\bar{x}, \bar{y}, \bar{z}, \bar{t}) T_0(\bar{x}, \bar{y}, \bar{z}, \bar{t})$:

$$p_0(\bar{t}) = \frac{1}{\int_V \frac{1}{T_0} dv}$$

If we do not input heat, $\bar{T}_0$ is constant, and then $\bar{p}_0$ as well, and so is $\bar{\rho}_0$, hence

$$\begin{cases} \overrightarrow{\nabla} \cdot (\overrightarrow{u}_0) = 0, \\ \dfrac{\partial \overrightarrow{u_0}}{\partial \bar{t}} + \overrightarrow{u}_0 \cdot \overrightarrow{\nabla} \overrightarrow{u}_0 = -\dfrac{\overrightarrow{\nabla} \bar{p}_2}{\bar{\rho}_0}, \end{cases} \tag{14}$$

this is as expected the incompressible standard Euler system were variations of pressure are not the thermodynamical ones but the $O(M_0^2)$ ones. Variations of pressure are $O(\rho_0 U_0^2)$ as expected because variations of pressure around the reference state p_0 are

$$p_0 \gamma M_0^2 \bar{p}_2 = \rho_0 U_0^2 \bar{p}_2$$

the total pression being

$$p = p_0 + \rho_0 U_0^2 \bar{p}_2 + O(M_0^4)$$

We have shown that the compressible Euler equations are the incompressible ones at low Mach number.

2.10 Linearized Euler compressible supersonic flow with potential

We have considered the equation with u, v, we can write it with ϕ. Of course if we take back the full potential equation

$$(\phi_x^2 - c^2)\phi_{xx} + 2\phi_x \phi_y \phi_{xy} + (\phi_y^2 - c^2)\phi_{yy} = 0,$$

and linearize it

$$(\phi_x^2 - c^2)\phi_{xx} = (u^2 - c_0^2)\phi_{xx} + ...2\phi_x \phi_y \phi_{xy} + ...$$

and

$$(\phi_y^2 - c^2)\phi_{yy} = (v^2 - c_0^2)\phi_{yy} + ... = (... - c_0^2)\phi_{yy} + ...$$

which is the expected wave equation for the potential

$$(1 - M_0^2)\phi_{xx} + \phi_{yy} = 0$$

This point of view is useful is the transonic case that we will see next.

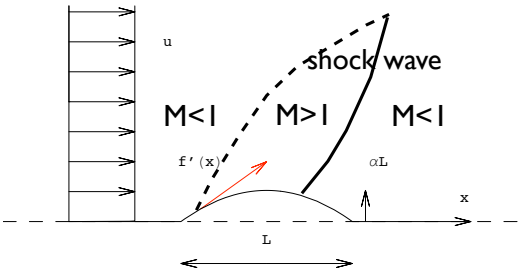

Figure 12: A plane plate with a small bump in a transonic flow. A region of supersonic flow appears.

2.11 Linearized Euler trans sonic flow

• As just seen the value $M_0^2 - 1$ appears in the equations. It is clear that the previous analysis was dealing with $0 \leq M_0 < 1$ and $1 \leq M_0$ with $M_0^2 - 1$ not too small. If this arrives, the flow is transonic, and the wave equation

$$(1 - M_0^2)\frac{\partial^2 \bar{p}_1}{\partial \bar{x}^2} + \frac{\partial^2 \bar{p}_1}{\partial \bar{y}^2} = 0,$$

degenerates for the pressure:

$$0 + \frac{\partial^2 \bar{p}_1}{\partial \bar{y}^2} = 0,$$

and as $\bar{p}_1 \propto \frac{1}{\sqrt{1-M_0^2}}$...tends to infinity. It is then clear than one has to take a new scale $\lambda\hat{y} = \bar{y}$ so that $|M^2 - 1|$ balances λ^{-2}. We will use $\varepsilon = |M^2 - 1|$ as a small parameter in the expansion, we have to compare it with α the small slope of the wall. To do that come back to equation of potential:

$$(c^2 - u^2)\frac{\partial u}{\partial x} - uv(\frac{\partial u}{\partial y} + \frac{\partial v}{\partial x}) + (c^2 - v^2)\frac{\partial v}{\partial y} = 0.$$

So that if we look at potential flows (cf Crocco theorem) we define a potential of velocities $u = \partial_x \phi$ and $v = \partial_y \phi$. the previous equation reads

$$(\phi_x^2 - c^2)\phi_{xx} + 2\phi_x\phi_y\phi_{xy} + (\phi_y^2 - c^2)\phi_{yy} = 0.$$

Now let us look at perturbation at unknown level ε of the potential, bearing in mind that $x = L\bar{x}$ and $y = \lambda L\hat{y}$ with $\lambda >> 1$ (to be determined):

$$\phi = U_0 L(\bar{x} + \varepsilon\hat{\phi} + ...)$$

so that $u = U_0(1 + \varepsilon\hat{u}_1 + ...$ and $v = \frac{U_0}{\lambda}\varepsilon\hat{v}_1$ The local speed of sound

$$c^2 = c_0^2(1 - \frac{\gamma - 1}{2}\frac{(u^2 + v^2)}{c_0^2}) \text{ becomes } c^2 = c_0^2(1 - (\gamma - 1)M_0^2\varepsilon\hat{\phi}_{\bar{x}} + ...)$$

The dangerous term $(u^2 - c^2)$ is rewritten using this expression:

$$(c^2 - u^2) = c_0^2(1 - (\gamma - 1)M_0^2\varepsilon\hat{\phi}_{\bar{x}} - M_0^2(1 + 2\varepsilon\hat{\phi}_{\bar{x}}) + ...) = c_0^2(1 - M_0^2 - (\gamma + 1)M_0^2\varepsilon\hat{\phi}_{\bar{x}} + ...)$$

this gives the order of magnitude of ε as we want it to come back when $M_0 \sim 1$ so $\varepsilon = O(|1 - M_0^2|)$. The second term $2\phi_x\phi_y\phi_{xy}$ remains negligible, but the third $(\phi_y^2 - c^2)\phi_{yy}$ is now (remember $\hat{y}\lambda = \bar{y}$): $(\phi_y^2 - c^2)\phi_{yy} = -\varepsilon\frac{c_0^2 U_0}{L^2\lambda^2}\hat{\phi}_{\hat{y}\hat{y}}$. The equation is then:

$$((1 - M_0^2 - (\gamma + 1)M_0^2\varepsilon\hat{\phi}_{\bar{x}})\hat{\phi}_{\bar{x}\bar{x}} + \frac{1}{\lambda^2}\bar{\phi}_{\hat{y}\hat{y}} = 0.$$

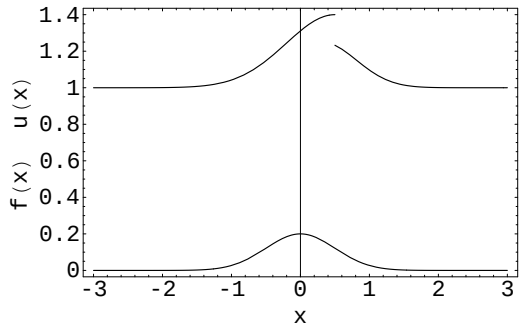

Figure 13: The bump and the perturbed velocity, transsonic flow, there is a shock.

with as claimed at the beginning $\varepsilon = O(\lambda^{-2})$ but furthermore the choice $\varepsilon = (|1 - M_0^2|)$ is such that we indeed have the non linear term.

But remember as well that the boundary condition of transpiration velocity $\hat{v} = \varepsilon\lambda^{-1}\partial_{\hat{y}}\hat{\phi}$ same as $\alpha\bar{f}'$ this gives : $\varepsilon\lambda^{-1} = \alpha$. We have $\varepsilon = O(\lambda^{-2})$ and the last one $\varepsilon\lambda^{-1} = \alpha$, this gives that $\alpha = \lambda^{-3}$ and $\varepsilon = \alpha^{2/3}$.

Let us define the "transonic parameter":

$$K = \frac{M_0^2 - 1}{(\gamma + 1)M_0^2\alpha^{2/3}}$$

then the equation is called the "Euler Tricomi" equation (Landau [14], Germain [10], Ashley Landhal [2], Kevorkian and Cole [13])

$$-(K + \hat{\phi}_{\bar{x}})\hat{\phi}_{\bar{x}\bar{x}} + \hat{\phi}_{\hat{y}\hat{y}} = 0.$$

in front of the derivative is $K + \hat{\phi}_{\bar{x}}$ which may again change of sign. The pressure is of order of magnitude

$$\rho U_0^2\varepsilon \sim \gamma p_0 M_0^2\alpha^{2/3},$$

it is no more singular... Solving the equation is another story, but here we wanted to focus on the singularities.

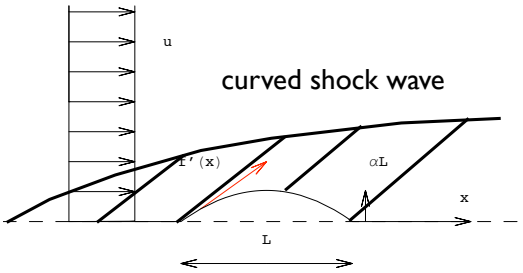

Figure 14: A plane plate with a small bump in a hypersonic flow.

2.12 Linearized Euler hypersonic flow

• We may now look at the other limit $M_0 >> 1$. This is the hypersonic flow régime. The wave equation

$$\frac{\partial^2 \bar{p}_1}{\partial \bar{x}^2} - (M_0^2 - 1)^{-1} \frac{\partial^2 \bar{p}_1}{\partial \bar{y}^2} = 0,$$

is again singular for large Mach numbers,

$$\frac{\partial^2 \bar{p}_1}{\partial \bar{x}^2} = 0$$

The flow is so fast that it does not see the body. Hence, again we have to look carefully at the equations. A good idea, is to rescale $\bar{Y} = \frac{1}{M_0}\bar{y}$ to reobtain the lost term by dominant balance.

As $1/M_0$ is very small, it can interfere with the small slope of the body. If we define from the Mach Number M_0 and from the local angle of the shock σ and from the slope of the body τ the parameters:

$$K_s = M_0\sigma, \quad K = M_0\tau$$

they define self similar parameters in the Hypersonic Small Disturbance Theory (Chernyi [4]). Either $K > O(1)$ or $K \ll 1$.

First we look at the shock wave:

The oblique shock wave relation (Germain [10])

$$\frac{\tan(\sigma - \tau)}{\tan \tau} = 1 - \frac{2}{\gamma + 1}(1 - \frac{1}{M_0^2 \sin^2 \sigma})$$

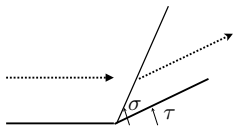

gives for small angles τ and σ :

$$\frac{M_0\sigma}{M_0\tau} = \frac{\gamma + 1}{4} + \sqrt{(\frac{\gamma + 1}{4})^2 + \frac{1}{(M_0\tau)^2}}$$

the pressure is then

$$\frac{p}{p_0} = \frac{2\gamma}{\gamma + 1} K_s^2 - \frac{\gamma - 1}{\gamma + 1} \tag{15}$$

$$= 1 + \gamma \frac{\gamma + 1}{4} K^2 + \gamma K \sqrt{(\frac{\gamma + 1}{4} K)^2 + 1}. \tag{16}$$

then for moderate Mach number, we recover that the angle of the shock is a Mach Wave $(1/M_0)$ and the pressure is:

$$\frac{p - p_0}{\rho_0 U_0^2} \simeq 1 + K_s$$

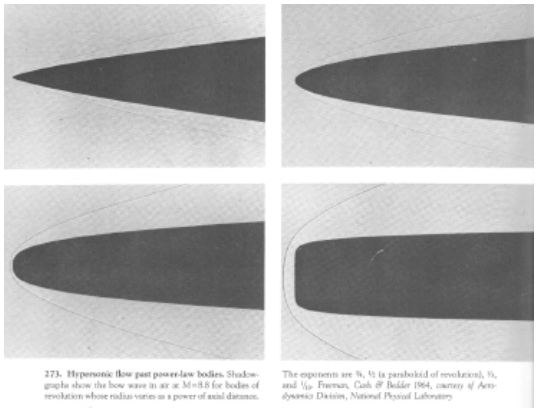

273. Hypersonic flow past power-law bodies. Shadowgraphs show the bow wave in air at $M=8.8$ for bodies of revolution whose radius varies as a power of axial distance. The exponents are $\frac{3}{4}$, $\frac{1}{2}$ (a paraboloid of revolution), $\frac{1}{3}$, and $\frac{1}{10}$. Freeman, Cash & Bedder 1964, courtesy of Aerodynamics Division, National Physical Laboratory.

Figure 15: A self similar flows over self similar shapes in a hypersonic flow (Van Dyke 82 book).

this is the "weak hypersonic" regime. It is just the usual case with $\sqrt{M_0^2-1}$ replaced by M_0!.

For a large Mach number and large K the body and the shock are proportional, this is called the tangent wedge approximation:

$$\frac{M_0\sigma}{M_0\tau} = \frac{\gamma+1}{2},$$

and the pressure:

$$\frac{p-p_0}{\rho_0 U_0^2} \simeq K_s^2.$$

this is the "strong hypersonic regime" This gives the idea of expansion with $M^2\tau^2$ for the pressure, so that for a weak case $M^2\tau^2 \leq O(1)$ we can expand

$$\bar{u} = 1 + \tau^2 \bar{u}_1 + ...$$

$$\bar{v} = \tau \bar{v}_1 + ...$$

$$\bar{p} = 1 + M^2\tau^2 \bar{p}_1 + ...$$

We have the so called "piston analogy" as the equations are the same with x changed in time thann the equation of the flow induced by a piston moving in y with time.

$\frac{\partial}{\partial \bar{x}}\bar{U} + \frac{\partial}{\partial \bar{y}}F(\bar{U}) = 0$ with $\bar{U} = \begin{pmatrix} \bar{\rho} \\ \bar{\rho}\bar{v}_1 \\ \bar{\rho}(\bar{e} + \frac{\bar{v}_1^2}{2}) \end{pmatrix}$ and $F(\bar{U}) = \begin{pmatrix} \bar{\rho}\bar{v} \\ \bar{\rho}\bar{v}^2 + \bar{p} \\ \bar{\rho}(\bar{e} + \frac{\bar{v}^2}{2}) + \bar{p} \end{pmatrix}$ Selfsimilar solution may be then obtained for bodies with an $\bar{x}^n$ shape.

2.13 Conclusion of the Ideal fluid section

At the end of this section, we have for several flows the solution of the pressure distribution over a small bump on a a flat plate in an inviscid Euler description.

We turn now to the wall in order to insure the no slip boundary condition.

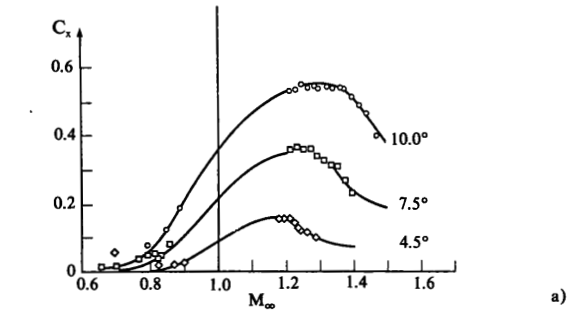

Figure 32.
Trainée d'un obstacle semi-infini (écoulement plan) en fonction du nombre de Mach. Théorie H.P.P. et résultats expérimentaux.
La figure b) fait apparaître de façon saisissante l'intérêt du paramètre de similitude et des grandeurs réduites.

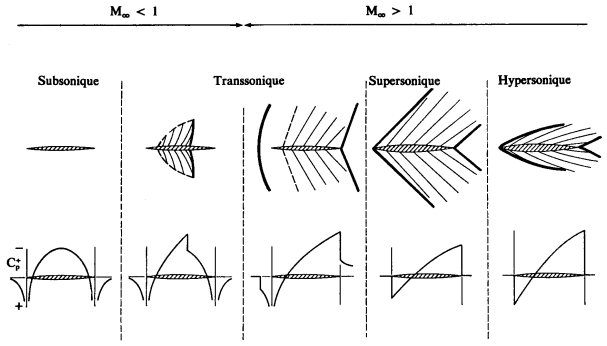

Figure 31.

Evolution schématique de l'écoulement avec M_∞.

Au-dessus : allure de l'écoulement ; les régions supersoniques sont indiquées par les caractéristiques de l'onde simple dominante. En traits forts : ondes de choc.
Au-dessous : variations de C_p^*, cœfficient de pression sur l'extrados ($x_3 = +0$).

Figure 16: Experimental C_x of a cone, From Germain. Sketch of pressure coefficient (up side down: positive values are toward the bottom) from Germain from Spreiter 62

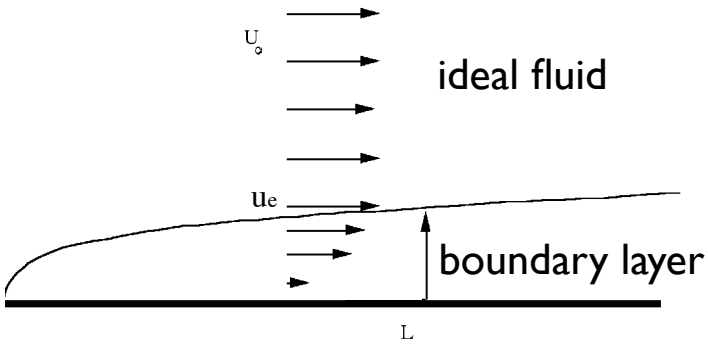

Figure 17: The typical problem a plane plate (neglect curvature).

3 Classical Boundary Layer on a flat plate

We have looked at solutions of ideal fluid which correspond to Navier Stokes equations for $Re^{-1} = 0$. We obtained the Euler equations. The problem is that with $Re^{-1} = 0$ we can no more write the no slip boundary condition at the wall. That is the signature of the singularity of the problem. To solve the equation we had to impose a slip boundary condition. This slip boundary condition is in fact the matching condition between the outer and inner problem. Hence now we look at the inner problem and do a change of scale to focus on the thin boundary layer. We begin by the simple flat plate case. We then see the influence of pressure gradient and discuss separation.

3.1 Blasius solution on a flat plate

Ideal fluid
So we have now some examples of ideal fluid flows with a basic flow mainly in the $\bar{x}$ direction. Let us look at what happens when the body is a simple semi infinite flat plate. First, we compute the ideal fluid solution, here a uniform flow. We obtain the "slip velocity" written $\bar{u}_e$ the value of the ideal fluid velocity at the wall

Boundary layer
Near the wall the ideal fluid solution is no more valid as the velocity is zero at a wall. We have to introduce a "Boundary layer". To obtain this we use the "least degeneracy principle" (Van Dyke [26], Darrozès & François [9]): we want the convective terms and at least re hook one diffusive term (as $\bar{y} = \tilde{y}\delta/L$):

$$\tilde{u}\frac{\partial \tilde{u}}{\partial \bar{x}} \propto \frac{1}{Re(\delta/L)^2}\frac{\partial^2 \tilde{u}}{\partial \tilde{y}^2},$$

we then say that the boundary layer is of relative order $Re^{-1/2}$.

Dynamical equations
in these new scales, the Navier Stokes equation are the Prandtl equations:

$$\frac{\partial \tilde{u}}{\partial \bar{x}} + \frac{\partial \tilde{v}}{\partial \tilde{y}} = 0,$$

$$\tilde{u}\frac{\partial \tilde{u}}{\partial \bar{x}} + \tilde{v}\frac{\partial \tilde{u}}{\partial \tilde{y}} = \frac{\partial^2 \tilde{u}}{\partial \tilde{y}^2}.$$

With boundary conditions $\tilde{u}(\bar{x}, 0) = 0$, $\tilde{u}(\bar{x}, \infty) = 1$. this latter coming from the asymptotic matching

$$\tilde{u}(\bar{x}, \tilde{y} \to \infty) \to \bar{u}(\bar{x}, \bar{y} \to 0).$$

(we call $\bar{u}_e(\bar{x}) = \bar{u}(\bar{x}, \bar{y} \to 0)$, the velocity at the "edge" of the boundary layer). An initial boundary condition at the leading edge is

$$\tilde{u}(\bar{x} = 0, \tilde{y}) = 1.$$

Self similarity

We can observe that they have a special invariance (see thereafter the Falkner Skan solution, see chapter on Self Sim `http://www.lmm.jussieu.fr/~lagree/COURS/M2MHP/SSS.pdf`), this gives the selfsimilar variables

$$\psi = \xi^{1/2} f(\eta), \quad \xi = \bar{x}, \quad \eta = \tilde{y}/\sqrt{\bar{x}}.$$

with

$$\frac{\partial}{\partial \bar{x}} = \frac{\partial}{\partial \xi} - \frac{\eta}{2\xi}\frac{\partial}{\partial \eta}, \quad \text{and} \quad \frac{\partial}{\partial \tilde{y}} = \frac{1}{\sqrt{\xi}}\frac{\partial}{\partial \eta}$$

the velocities are;

$$\tilde{u} = f'(\eta), \quad \tilde{v} = \frac{1}{2\sqrt{\xi}}(\eta f' - f)$$

so that (note the 2 in front of the higher order derivative, it is removed in Falkner Skan)

$$2f''' + ff'' = 0 \quad \text{with} \quad f(0) = f'(0) = 0 \quad \text{et} \quad f'(\infty) = 1.$$

Numerical resolution by an *ad hoc* method gives $f''(0) = 0.332$, and the velocity profiles are on figure 18. On figure 19, we present a Navier Stokes computation which shows the selfsimilarity of various profiles.

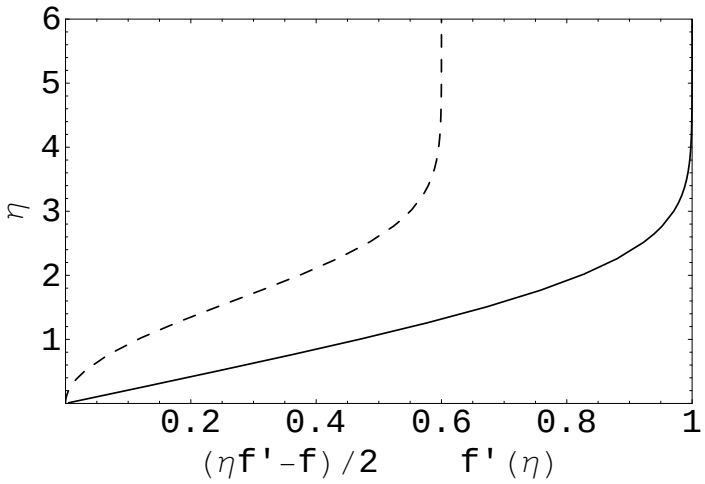

Figure 18: $f'(\eta)$ Selfsimilar longitudinal velocity profile : f' in abscissa, η in ordinate (plain line). Selfsimilar transversal velocity profile : $(\eta f' - f)/2$ in abscissa, η (dashing).

We observe that the velocity at infinity is not zero. Note that $\eta f' - f = \eta(f' - 1) + \int_0^\eta (1 - f')d\eta$, then as $1 - f'$ goes to zero faster enough

$$\lim_{\eta\to\infty}(\frac{1}{2}(\eta f' - f)) = \frac{1}{2}\int_0^\infty (1 - f')d\eta = \frac{1.7208}{2} = .8604. \tag{17}$$

We introduce a quantity called "displacement thickness" δ_1, and define the skin friction

$$\tilde{\tau} = \frac{\partial \tilde{u}}{\partial \tilde{y}}, \qquad \tilde{\delta_1} = \int_0^\infty (1 - \frac{\tilde{u}}{\bar{u}_e})d\tilde{y},$$

that we write here with dimensions:

$$\delta_1 = 1.7208\frac{L}{\sqrt{Re}}\bar{x}^{1/2}, \text{ and } \tau = 0.332\ \rho U_0^2 \frac{1}{\sqrt{Re}}\bar{x}^{-1/2},$$

Furthermore, far away $v \to 0.8604\ U_0 \frac{1}{\sqrt{Re}}\bar{x}^{-1/2}$.

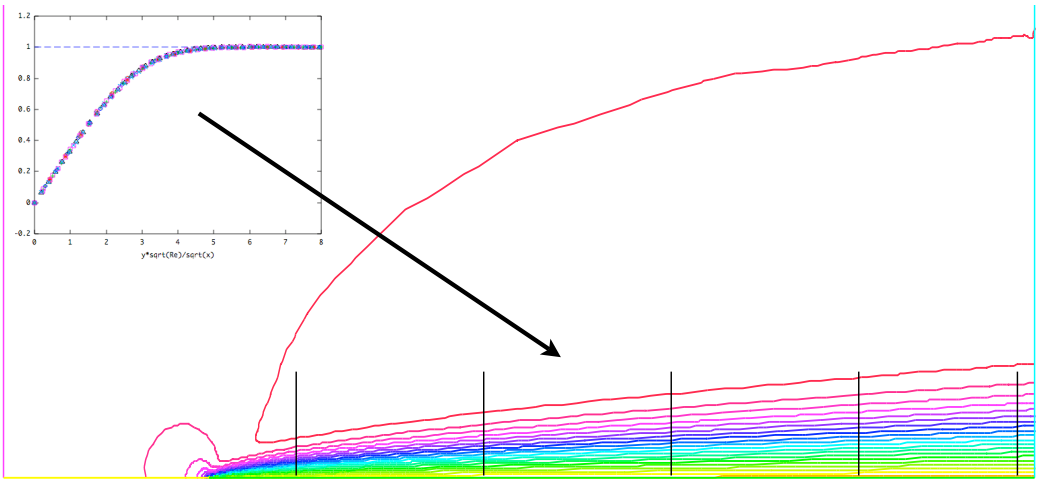

Figure 19: The flow over a flat plate computed with `Freefem++` at $Re = 500$ is Self Similar: at the five vertical cuts indicated we plot and superpose the profiles of the numerical solution written in boundary layer scale: $\bar{u}(\bar{x}, \bar{y}\sqrt{Re/\bar{x}})$, indeed all profiles collapse on the same curve.

3.2 Approximations of Blasius profile

3.2.1 Blasius solution

We have just exactly solved Blasius. So the problem is solved. But historically, approximate solutions were found. And those approximate solutions are useful to understand Shallow Water flows as well.

We can here test some approximations and show that they are close to Blasius. We found the shear $f_0'' = 0.332$ the "displacement thickness" is 1.72.

There is another integral which will be usefull, the "energy displacement thickness", by definition it is:

$$\tilde{\delta}_2 = \int_0^\infty (\frac{\tilde{u}}{\bar{u}_e})(1 - \frac{\tilde{u}}{\bar{u}_e}) d\tilde{y},$$

which value is, in the case of Blasius solution

$$\int_0^\infty f'(\eta)(1 - f'(\eta)) d\eta = 0.664$$

so that the ratio H is

$$H = \frac{\int_0^\infty (1 - f'(\eta)) d\eta}{\int_0^\infty f'(\eta)(1 - f'(\eta)) d\eta} = 2.591$$

H is called the "shape factor".

To see the link between all those quantities, we have to write again the Prandtl equation and to notice that

$$\tilde{u}\frac{\partial \tilde{u}}{\partial \bar{x}} + \tilde{v}\frac{\partial \tilde{u}}{\partial \tilde{y}} = \frac{\partial^2 \tilde{u}}{\partial \tilde{y}^2}.$$

may be rewritten if we collect the velocities before the derivatives using the incompressibility as

$$\frac{\partial \tilde{u}\tilde{u}}{\partial \bar{x}} + \frac{\partial \tilde{v}\tilde{u}}{\partial \tilde{y}} = \frac{\partial^2 \tilde{u}}{\partial \tilde{y}^2}. \text{ or even } \frac{\partial \tilde{u}\tilde{u}}{\partial \bar{x}} - \frac{\partial \tilde{u}}{\partial \bar{x}} + \frac{\partial \tilde{v}\tilde{u}}{\partial \tilde{y}} - \frac{\partial \tilde{v}}{\partial \tilde{y}} = \frac{\partial^2 \tilde{u}}{\partial \tilde{y}^2},$$

after using the incompressibility again. Changing the sign, and collecting, this is

$$\frac{\partial}{\partial \bar{x}}\tilde{u}(1 - \tilde{u}) + \frac{\partial}{\partial \tilde{y}}\tilde{v}(1 - \tilde{u}) = -\frac{\partial^2 \tilde{u}}{\partial \tilde{y}^2}.$$

integrating from $\tilde{y}=0$ to ∞, and thanks to Boundary conditions (the part with $\frac{\partial}{\partial\tilde{y}}$ is zero), and this gives the Von Kármán equation with no pressure gradient :

$$\frac{\partial}{\partial\bar{x}}\int_0^\infty \tilde{u}(1-\tilde{u})d\tilde{y} = \frac{\partial\tilde{u}}{\partial\tilde{y}}_0 .$$

We can check that the derivative of the energy thickness $\int_0^\infty \tilde{u}(1-\tilde{u})d\tilde{y} = 0.664\sqrt{\bar{x}}$ is $\frac{\partial\tilde{u}}{\partial\tilde{y}}_0 = 0.332/\sqrt{\bar{x}}$ which is the shear at the wall as expected.

We now test simple profile shapes and see wether they are good approximation of this Blasius solution. We will look at the expression of δ_1, δ_2, H and $\frac{\partial\tilde{u}}{\partial\tilde{y}}$. Note that in the integral method, we will use f_2 linked to the skin friction as: $\frac{\partial\tilde{u}}{\partial\tilde{y}} = f_2\frac{\bar{u}_e}{\delta_2} = f_2\frac{H\bar{u}_e}{\delta_1}$. For Blasius $f_2 = 0.218$ We have as well $f'(4.906) = 0.99$

The global shape starts from 0 and goes to one at infinity. In the next sub-sub sections we test given shapes that start from 0 and goes to one, like exponential or error function. And we compare all.

This is a classical text book exercise for polynomial profiles. In the books, δ is defined to be the value of the boundary layer thickness, where the velocity is exactly one. This is an approximation as the velocity is never one (except at infinity). So we can exhibit a thickness δ_∞ (because δ is for us the scaling of the boundary layer, not a value of the boundary layer itself) of finite value.

It should not be confused with the effective δ_{99}. This thickness is such that $\tilde{u}(\delta_{99}) = 0.99$, here say $\tilde{u}(\delta_\infty) = 1$. So that for $\tilde{y} < \delta_\infty$, the velocity goes from zero to one. For $\tilde{y} > \delta_\infty$ the velocity is one.

3.2.2 Linear profile

We first test the simple linear profile

$$\tilde{u}(\tilde{y}) = \tilde{y}/\delta_\infty \text{ for } \tilde{y} < \delta_\infty \text{ and else } \tilde{u}(\tilde{y}) = 1$$

this seems to be a crude approximation. The chosen δ_∞ is a unknown function which represents the "size" of the boundary layer (it has a finite value, as we will see). Let us compute the integrals

$$\int_0^\infty (1-\tilde{u})d\tilde{y} = \int_0^{\delta_\infty}(1-\tilde{y}/\delta_\infty)d\tilde{y} = \delta_\infty\int_0^1(1-y')dy' = \delta_\infty/2$$

$$\int_0^\infty \tilde{u}(1-\tilde{u})d\tilde{y} = \int_0^{\delta_\infty}(\tilde{y}/\delta_\infty)(1-\tilde{y}/\delta_\infty)d\tilde{y} = \delta_\infty\int_0^1 y'(1-y')dy' = \delta_\infty/6$$

and $\partial\tilde{u}(\tilde{y})/\partial\tilde{y} = 1/\delta_\infty$ in 0, so

$$\delta_1 = \delta/2,\ \ \delta_2 = \delta_\infty/6,\ \ \frac{\partial\tilde{u}}{\partial\tilde{y}}_0 = \frac{1}{\delta_\infty}$$

we put that in the Von Kármán equation with no pressure gradient :

$$\frac{\partial}{\partial\bar{x}}\int_0^\infty \tilde{u}(1-\tilde{u})d\tilde{y} = \frac{\partial\tilde{u}}{\partial\tilde{y}}_0 .$$

This gives us the evolution of the "thickness" δ_∞ because the previous equation is :

$$\frac{\partial}{\partial\bar{x}}\frac{\delta_\infty}{6} = \frac{1}{\delta_\infty} \text{ hence } \frac{\partial}{\partial\bar{x}}\frac{\delta_\infty}{6} = \frac{1}{\delta_\infty} \text{ hence } \frac{\partial}{\partial\bar{x}}\frac{\delta_\infty^2}{12} = 1 \text{ so that } \delta_\infty = \sqrt{12}\sqrt{\bar{x}}$$

from this

$$\delta_1 = \sqrt{3}\sqrt{\bar{x}},\ \ \delta_2 = \sqrt{1/3}\sqrt{\bar{x}},\ \ H = \frac{\delta_1}{\delta_2} = 3 \ \text{ and } \frac{\partial\tilde{u}}{\partial\tilde{y}}_0 = \frac{1}{\sqrt{12}\sqrt{\bar{x}}}$$

the numerical values

$$\delta_1 = 1.732\sqrt{\bar{x}},\ \ \delta_2 = 0.57\sqrt{\bar{x}},\ \ H = 3. \text{ and } \frac{\partial\tilde{u}}{\partial\tilde{y}}_0 = 0.288\sqrt{\bar{x}}$$

are not so far from the Blasius solution which are respectively 1.7 0.66 2.59 and 0.33.

3.2.3 Sinusoidal profile

We test the simple sinusoidal profile now

$$\tilde{u}(\tilde{y}) = \sin(\frac{\pi\tilde{y}}{2\delta_\infty}) \text{ for } \tilde{y} < \delta_\infty \text{ and else } \tilde{u}(\tilde{y}) = 1$$

again the "thickness" δ_∞ is artificial. Let us compute the integrals

$$\int_0^\infty (1-\tilde{u})d\tilde{y} = \int_0^{\delta_\infty} (1-\sin(\frac{\pi\tilde{y}}{2\delta_\infty}))d\tilde{y} = \delta_\infty \int_0^1 (1-\sin(\frac{\pi y'}{2}))dy' = \delta_\infty(1-2/\pi)$$

$$\int_0^\infty (1-\tilde{u})d\tilde{y} = \delta_\infty(2/\pi - 1/2)$$

so that after substitution in the Von Kármán equation with no pressure gradient :

$$\delta_1 = \sqrt{\frac{2}{4-\pi}}(\pi-2)\sqrt{\bar{x}},\ H = -\frac{2(\pi-2)}{\pi-4},\ \frac{\partial\tilde{u}}{\partial\tilde{y}}_0 = \frac{\sqrt{2-\frac{\pi}{2}}}{2}\bar{x}^{-1/2}$$

which gives

$$\delta = 4.79\sqrt{\bar{x}},\ \delta_1 = 1.742\sqrt{\bar{x}},\ \delta_2 = 0.655\sqrt{\bar{x}},\ H = 2.66,\ \frac{\partial\tilde{u}}{\partial\tilde{y}}_0 = 0.32\bar{x}^{-1/2}$$

(Blasius solution respectively ∞ 1.7 0.66 2.59 and 0.33)

3.2.4 Exponential

We test the simple exponential profile

$$\tilde{u}(\tilde{y}) = 1 - e^{-\tilde{y}/\delta_\infty}$$

which gives (with integration to infinity, not to 1)

$$\delta_\infty = 2\sqrt{\bar{x}},\ \delta_1 = 2\sqrt{\bar{x}},\ \delta_2 = \sqrt{\bar{x}},\ H = 2,\ \frac{\partial\tilde{u}}{\partial\tilde{y}}_0 = 0.5\bar{x}^{-1/2}$$

3.2.5 Erf

We test the error function (see Stokes problem)

$$\tilde{u}(\tilde{y}) = erf(\frac{\tilde{y}}{2\delta_\infty})$$

which gives (with integration to infinity, not to 1)

$$\delta_1 = \frac{2x^{1/2}}{\sqrt{\pi}},\ \delta_2 = \frac{2(\sqrt{2}-1)x^{1/2}}{\sqrt{\pi}},\ H = 1+\sqrt{2},\ \frac{\partial\tilde{u}}{\partial\tilde{y}}|_0 = \frac{1}{\sqrt{\pi x}}.$$

which is numerically

$$\delta_1 = 1.753x^{1/2},\ \delta_2 = 0.726x^{1/2},\ H = 2.414,\ \frac{\partial\tilde{u}}{\partial\tilde{y}}|_0 = \frac{.36}{\sqrt{x}}.$$

so that

$$f_2 = \frac{\delta_1}{H}\frac{\partial\tilde{u}}{\partial\tilde{y}}|_0 \text{ is } f_2 = 0.215$$

3.2.6 Pohlhausen polynomial order one

We can imagine a polynomial expression:

$$\tilde{u}(\tilde{y}) = a_1\tilde{y}/\delta + a_2(\tilde{y}/\delta)^2 + a_3(\tilde{y}/\delta)^3 + a_4(\tilde{y}/\delta)^4 + ... \text{ for } \tilde{y} < \delta_\infty \text{ and else } \tilde{u}(\tilde{y}) = 1$$

the case $\tilde{u}(\tilde{y}) = a_1\tilde{y}/\delta_\infty$ has been seen right now.

3.2.7 Pohlhausen polynomial order two

The case $\tilde{u}(\tilde{y}) = a_1\tilde{y}/\delta_\infty + a_2(\tilde{y}/\delta_\infty)^2$ leads to

$$\tilde{u}(\tilde{y}) = 2\tilde{y}/\delta_\infty - (\tilde{y}/\delta\infty)^2 \text{ for } \tilde{y} < \delta_\infty \text{ and else } \tilde{u}(\tilde{y}) = 1$$

to fit the BC $\tilde{u}(\delta_\infty) = 1$ and $\tilde{u}'(\delta_\infty) = 0$. After substitution:

$$\delta_\infty = \sqrt{30}\sqrt{\bar{x}},\ \delta_1 = \sqrt{10/3}\sqrt{\bar{x}},\ \delta_2 = \sqrt{8/15}\sqrt{\bar{x}},\ H = 5/2,\ \left.\frac{\partial\tilde{u}}{\partial\tilde{y}}\right|_0 = \sqrt{2/15}\bar{x}^{-1/2}$$

numerical values

$$\delta_\infty = 5.47723\sqrt{\bar{x}},\ \delta_1 = 1.8\sqrt{\bar{x}},\ \delta_2 = 0.7\sqrt{\bar{x}},\ H = 2.5,\ \left.\frac{\partial\tilde{u}}{\partial\tilde{y}}\right|_0 = .36\bar{x}^{-1/2}$$

3.2.8 Pohlhausen polynomial order three

We continue

$$\tilde{u}(\tilde{y}) = a_1\tilde{y}/\delta_\infty + a_2(\tilde{y}/\delta_\infty)^2 + a_3(\tilde{y}/\delta_\infty) \text{ for } \tilde{y} < \delta_\infty \text{ and else } \tilde{u}(\tilde{y}) = 1$$

to fit the BC $\tilde{u}'(\delta_\infty) = 0$ we have $a_1 = (-2a_2 - 3a_3)$, and if we notice that

$$\tilde{u}\frac{\partial\tilde{u}}{\partial\bar{x}} + \tilde{v}\frac{\partial\tilde{u}}{\partial\tilde{y}} = \frac{\partial^2\tilde{u}}{\partial\tilde{y}^2} \text{ gives in 0: } 0 = \frac{\partial^2\tilde{u}}{\partial\tilde{y}^2}$$

so $a_2 = 0$ and $\tilde{u}(\delta_\infty) = 1$ gives

$$\tilde{u}(\tilde{y}) = (3/2)\tilde{y}/\delta_\infty - (\tilde{y}/\delta_\infty)^3/2 \text{ for } \tilde{y} < \delta_\infty \text{ and else } \tilde{u}(\tilde{y}) = 1$$

After substitution:

$$\delta_\infty = 4.64\sqrt{\bar{x}},\ \delta_1 = 1.7\sqrt{\bar{x}},\ \delta_2 = 0.65\sqrt{\bar{x}},\ H = 2.7,\ \left.\frac{\partial\tilde{u}}{\partial\tilde{y}}\right|_0 = .32\bar{x}^{-1/2}$$

of course we may continue... we will see the order 4 for Pohlhausen in the section of the resolution of boundary layer with a pressure gradient.

Schlichting says "it is seen the the approximate methods leads to satisfactory results in the case of a flat plate at zero incidence, and the extraordinary simplicity of the calculation is quite remarkable, compared to the complexity of the exact solution".

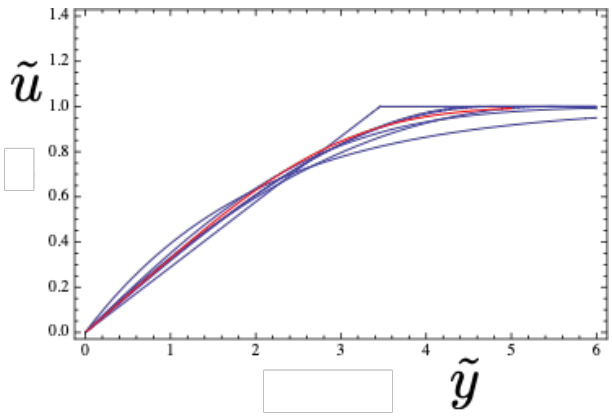

Figure 20: Various profiles: linear (with the angle), parabolic, cubic, sinus, exponential (the worst one, it is always lower than one), error function and Blasius in red.

3.3 Compressible boundary layer

Interestingly enough, the compressible counter part problem is very similar (Stewartson [20]). The constant velocity is the ideal fluid solution of a flat plat even in compressible flow (neglecting a weak shock at the nose). The dynamical equations are written with the same scales, the compressible Navier Stokes equation are the compressible Prandtl equations:

$$\frac{\partial \tilde{\rho}\tilde{u}}{\partial \bar{x}} + \frac{\partial \tilde{\rho}\tilde{v}}{\partial \tilde{y}} = 0, \quad \tilde{\rho}(\tilde{u}\frac{\partial \tilde{u}}{\partial \bar{x}} + \tilde{v}\frac{\partial \tilde{u}}{\partial \tilde{y}}) = \frac{\partial}{\partial \tilde{y}}\tilde{\mu}\frac{\partial \tilde{u}}{\partial \tilde{y}}$$

With boundary conditions $\tilde{u}(\bar{x}, 0) = 0$, $\tilde{u}(\bar{x}, \infty) = 1$. this latter comming from the matching

$$\tilde{u}(\bar{x}, \tilde{y} \to \infty) \to \bar{u}_e(\bar{x}, \bar{y} \to 0).$$

The Energy equation reads with the enthalpy:

$$\tilde{\rho}(\tilde{u}\frac{\partial \tilde{h}}{\partial \bar{x}} + \tilde{v}\frac{\partial \tilde{h}}{\partial \tilde{y}}) = \frac{\partial}{\partial \tilde{y}}(\frac{\tilde{\mu}}{Pr}\frac{\partial}{\partial \tilde{y}}(\tilde{h} + \frac{Pr-1}{2}\tilde{u}^2))$$

The transverse variable is rewritten with the Lees Dorodnitsyn Howarth Stewartson variable $dY = \tilde{\rho}d\tilde{y}$, and when the viscosity is approximated to be proportional to $\tilde{T}$ and when Prandt number Pr is one, then a selfsimilar solution may be found leading to $f''' + ff'' = 0$!

3.4 Classical Falkner Skan solutions of flow past wedges

3.4.1 Flow at wedges

This problem corresponds to the solution of the flow on a wedge, see figure 21. The flow comes from the left and there is a dividing stream line with a stagnation point between the intrados and extrados (symmetrical). The total angle of the wedge is $\beta\pi$.
The problem and approximate solutions were first given by V. M. Falkner (meet Paul Germain in NPL after the war) and Sylvia W. Skan in 1930. First computations after Blasius solution 1908 and Hiemenz 1911, were done by Hartree 1937 and latter Stewartson 1954. This very classical solution is necessary to find simple relationships between the pressure gradient and the boundary layer thickness.

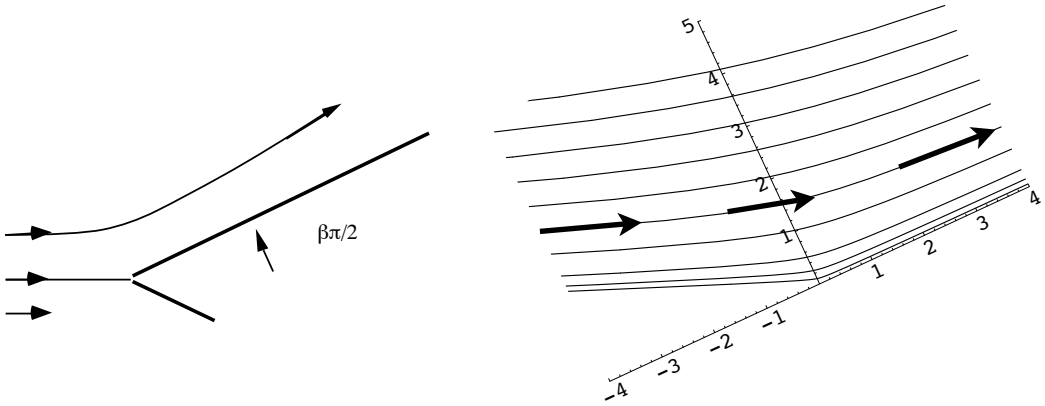

Figure 21: Symmetrical flow against a wedge shaped leading edge. Note that the x axis is along the body. so that tangential velocity is 0 in $\theta = 0$ and in $\theta = 2\pi - 2\beta\pi/2$. By symmetry, the transverse velocity is 0 along the dividing stream line $\theta = \pi - \beta\pi/2$

3.4.2 Ideal Fluid solution

The first move consists in solving the ideal fluid problem obtained from Navier Stokes after having defined a Reynolds number and having said that it is infinite. There is here no length scale, we take any, say L, there is in fact no velocity scale as well in this problem (we know why: because it is a second kind of self similarity). The choice of the velocity scale is that the ideal fluid velocity will be $\bar{u} = 1$ in $\bar{x} = 1$.
The Euler equations are not solved directly, we define from incompressibility a stream function ψ with $\bar{u} = \partial_{\bar{r}}\bar{\psi}$ and $\bar{v} = -\bar{r}^{-1}\partial_\theta\bar{\psi}$. Supposing a flow with no vorticity (as it is classical since ∂'Alembert [1]), we have to solve:

$$\frac{1}{\bar{r}}\frac{\partial}{\partial\bar{r}}(\bar{r}\frac{\partial}{\partial\bar{r}}\bar{\psi}) + \frac{1}{\bar{r}^2}\frac{\partial^2}{\partial\theta^2}\bar{\psi} = 0, \text{ with } \bar{\psi}(\bar{r}, \theta = 0) = 0, \;\; \bar{\psi}(\bar{r}, \pi - \beta\pi/2) = 0.$$

The boundary conditions correspond to give the symmetry line and the upper part of the wedge to be a stream line. The solution is straightforward (it is a special case of solution that we may write in the complex form $F(z) = z^m$, with $z = \bar{x} + i\bar{y}$):

$$\bar{\psi} = \psi_0\bar{r}^{\frac{2}{2-\beta}}\sin(\frac{2}{2-\beta}\theta).$$

The velocity at the wall "slip velocity" is as in $\theta = 0$, $\bar{r} = \bar{x}$, and as the velocity is 1 at the location $\bar{x} = 1$ by the choice of velocity unit:

$$\bar{u}_e = \bar{x}^n \;\text{ with }\; n = \frac{\beta}{2-\beta}, \quad \beta = \frac{2n}{n+1}$$

[Of course, one may look at solution of the Laplacian by separated variables, so that $\bar{\psi} = A\cos K\theta + B\sin K\theta$ and $\bar{r} = C\bar{r}^K + D\bar{r}^{-K}$, then form the boundary conditions, $A = 0$ and $K = \frac{2}{2-\beta}$, and $C = 0$ (condition at infinity)].

Writing the Euler equation at the wall leads to the important relation between the slip velocity and the value of the pressure at the wall $\bar{p}_e$:

$$\bar{u}_e \frac{d\bar{u}_e}{d\bar{x}} = -\frac{d\bar{p}_e}{d\bar{x}}$$

which is in fact the Bernoulli relation.

We note that there is no characteristic velocity "far away" the apex of the wedge, so the velocity scale depends on the chosen scale L by the power n. We note that this solution is an example of self similarity of second kind.

This problem is a kind of leading edge problem figure 21, for $\beta > 0$, we have a symmetrical flow between the dividing stream line (on figure 21 we have $0 < \beta < 1$, the flow is against a convex corner). The flow is accelerated, $n > 0$. A special case $\beta = 1$ is the flow against a wall (stagnation point solution). Larger values of β correspond to the flow against a concave corner.
$\beta = 0$ is the flow on a flat plate.
For negatives values of β there is no more corner, no symmetry is possible, it is the flow round a corner. The velocity is decelerated, $n < 0$.

3.5 Boundary layer solution

The second move consists is writing again the Navier Stokes equations and to introduce a stretched transverse variable by $1/\sqrt{Re}$ so that they become:

$$\begin{cases} \dfrac{\partial \tilde{u}}{\partial \bar{x}} + \dfrac{\partial \tilde{v}}{\partial \tilde{y}} = 0, \\ u\dfrac{\partial \tilde{u}}{\partial \bar{x}} + \tilde{v}\dfrac{\partial \tilde{u}}{\partial \tilde{y}} = -\dfrac{\partial \tilde{p}}{\partial \bar{x}} + \dfrac{\partial^2 \tilde{u}}{\partial \tilde{y}^2}, \\ 0 = -\dfrac{\partial \tilde{p}}{\partial \tilde{y}}. \end{cases} \tag{18}$$

boundary conditions are $\tilde{u} = \tilde{v} = 0$ on $\tilde{y} = 0$, $\tilde{u}(\bar{x}, +\infty) = \bar{u}_e$, $\tilde{p}(\bar{x}, +\infty) = \bar{p}_e$. As $\frac{\partial \tilde{p}}{\partial \tilde{y}} = 0$ the pressure in the boundary layer is exactly the pressure of the ideal fluid at the wall. And using the Bernouli relation we can eliminate the pressure and write as $\bar{u}_e \frac{d\bar{u}_e}{d\bar{x}} = n\bar{x}^{2n-1}$:

$$\frac{\partial \tilde{u}}{\partial \bar{x}} + \frac{\partial \tilde{v}}{\partial \tilde{y}} = 0, \;\; \tilde{u}\frac{\partial \tilde{u}}{\partial \bar{x}} + v\frac{\partial \tilde{u}}{\partial \tilde{y}} = n\bar{x}^{2n-1} + \frac{\partial^2 \tilde{u}}{\partial \tilde{y}^2}.$$

Often, it is written in stream function in a single equation of third order with three BC in $\tilde{y}$ as (the BC in $\bar{x} = 0$ is not important):

$$\frac{\partial \tilde{\psi}}{\partial \tilde{y}}\frac{\partial^2 \tilde{\psi}}{\partial \bar{x}\partial \tilde{y}} - \frac{\partial \tilde{\psi}}{\partial \bar{x}}\frac{\partial^2 \tilde{\psi}}{\partial \tilde{y}^2} = n\bar{x}^{2n-1} + \frac{\partial^3 \tilde{\psi}}{\partial \tilde{y}^3}.$$

$$\tilde{\psi}(\bar{x}, 0) = 0, \;\; \frac{\partial}{\partial \tilde{y}}\tilde{\psi}(\bar{x}, 0) = 0, \;\; \frac{\partial}{\partial \tilde{y}}\tilde{\psi}(\bar{x}, +\infty) = \bar{x}^n.$$

3.6 Self similarity

To solve this equation we try the selfsimilar technique:

$$\bar{x} \to Xx^*, \; \tilde{y} \to Yy^*, \; \tilde{u} \to Uu^*, \; \tilde{v} \to Vv^* \; ...$$

the boundary condition gives $U = X^n$, the continuity gives $V = YX^{n-1}$, the balance between inertia and viscosity gives $(X^n)(X^n)/X = (X^n)Y^{-2}$ so that $Y = X^{(1-n)/2}$, and then $V = X^{(n-1)/2}$, and as well we have

$\Psi = X^{(1+n)/2}$. The change of scale is then for any X:

$$\bar{x} \to Xx^*,\ \tilde{y} \to X^{(1-n)/2}y^*,\ \tilde{u} \to X^n u^*,\ \tilde{v} \to X^{(n-1)/2}v^*,\ \tilde{\psi} \to X^{(1+n)/2}\psi^*,$$

The formal implicit solution is invariant by this transform:

$$F(\bar{x}, \tilde{y}, \tilde{u}) = 0 \text{ gives } F(X\bar{x}, X^{(1-n)/2}\tilde{y}, X^n\tilde{u}) = 0$$

if we write it for ψ the formal implicit solution is invariant by the transform:

$$F(\bar{x}, \tilde{y}, \tilde{\psi}) = 0 \text{ gives } F(X\bar{x}, X^{(1-n)/2}\tilde{y}, X^{(n+1)/2}\tilde{\psi}) = 0$$

removing the X from the slots (divide by adequate powers of $X\bar{x}$) gives

$$F_2(X\bar{x}, \tilde{y}\bar{x}^{(n-1)/2}, \tilde{\psi}\bar{x}^{-(n+1)/2}) = 0, \forall X \text{ gives } F_3(\tilde{y}\bar{x}^{(n-1)/2}, \tilde{\psi}x^{-(n+1)/2}) = 0$$

hence $\tilde{\psi}x^{-(n+1)/2}$ is a function of $\tilde{y}\bar{x}^{(n-1)/2}$. So that the selfsimilar variable and the stream function are:

$$\xi = \bar{x},\ \ \eta = (\sqrt{\frac{n+1}{2}})\frac{\tilde{y}}{\bar{\xi}^{(1-n)/2}}\ \ \psi = (\sqrt{\frac{2}{n+1}})\bar{\xi}^{(n+1)/2}f(\eta)$$

the prefactors like $(\sqrt{\frac{n+1}{2}})$ are just historical and help to have a nice equation. As:

$$\frac{\partial}{\partial\bar{x}} = \frac{\partial}{\partial\xi} + \frac{n-1}{2}\frac{\eta}{\xi}\frac{\partial}{\partial\eta} \text{ and } \frac{\partial}{\partial\tilde{y}} = \sqrt{\frac{n+1}{2}}\xi^{(n-1)/2}\frac{\partial}{\partial\eta},$$

the velocities are obtained:

$$\tilde{u} = \xi^n f'(\eta),\ \ \tilde{v} = -\sqrt{\frac{n+1}{2}\xi^{n-1}}(f + \frac{n-1}{n+1}\eta f')$$

and after substitution, the stream function equation is :

$$f'''(\eta) + f(\eta)f''(\eta) + \beta(1 - f'(\eta)^2) = 0,\ \ f(0) = f'(0) = 0 \text{ and } f'(\infty) = 1.$$

Solutions of this equation are plotted on figure 23.

3.7 Numerical Tricks

3.7.1 Shooting method

In fact it is not so simple to solve this equation, the natural way consists in a shooting method: for a given set $f(0) = 0, f'(0) = 0, f''(0) = f_0''$ one solve up to a given η_m say 7, and try to obtain $f'(\eta_m) = 1$. In practice, we write $f''' + ff'' + \beta(1 - f'^2) = 0$ as a first order equation in matrix ($U' = F(U)$ with $U = (f, u, v)$) :

$$\left\{\begin{array}{ll} f' & = u \\ u' & = v \\ v' & = -vf - \beta(1 - u^2) \end{array}\right.$$

$f(0) = 0, u(0) = 0$, we guess $v(0) = f''(0)$ so that $u(\infty) = 1$. With this form it is clear that any Euler forward, or Runge Kutta Metho is suitable: sarting from $U(0)$ we compute:

$$U(\eta + \Delta\eta) = U(\eta) + \Delta\eta F(U(\eta))$$

from $\eta = 0$, where $U(0) = (f = 0, u = 0, v = f''(0))$ to η_m where the first component of U must be close to 1. We compute as well as a result $\int(1 - u)d\eta$.

Playing with this system, it works well for $\beta > 0$, but we observe that it is a very stiff problem for $\beta < 0$. It means that a very small change in $f''(0)$ can dramatically change the value of $u(\eta_m)$. So, the best way is to solve the equations in an "inverse way" with two variables: we have to find the given value of $u(\infty)$ and the given value of the displacement $I(\infty) = \int_0^\infty(1 - u)dy$. We add the integral to the previous one.

$$\left\{\begin{array}{ll} f' & = u \\ u' & = v \\ v' & = -vf - \beta(1 - u^2) \\ I' & = (1 - u) \end{array}\right.$$

$f(0)=0, u(0)=0, I(0)=0$ we guess $v(0)$ so that $u(\infty)=1.$ and $I(\infty)=D$, were say D is the given value. We shoot the condition $f'(\eta_m)=1$ and $\int_0^{\eta_m}(1-f'(\eta))d\eta=D$ to do this we try and guess the values of f_0'' and β. This procedure allows to obtain the reverse branch on figure 23 and the reverse profiles (where u is negative at first).

3.7.2 Unsteady method

Rewrite the Falkner Skan equation and ad an unsteady terl

$$\frac{\partial f'}{\partial \tau}=f'''+ff''+\beta(1-f'^2),\ \text{with}\ (f'=u)\ \text{it reads}\ \frac{\partial u}{\partial \tau}=u''+fu'+\beta(1-u^2)$$

at iteration n

$$\frac{(u^{n+1}-u^n)}{\Delta t}=u^{n+1\prime\prime}+f^n u^{n+1\prime\prime}+\beta(1-u^{n2})\ \text{and}\ f^{n+1\prime}=u^{n+1}$$

it is a two point BV problem $u^{n+1}(0)=0$ and $u^{n+1}(y_{max})=0$ the second order derivative is solved implicitly, the tridiagonal system is solved with Thomas algorithm.

3.7.3 alternate methods

http://basilisk.fr/sandbox/easystab/blasius.m
http://basilisk.fr/sandbox/easystab/hiemenz.m
http://basilisk.fr/sandbox/easystab/falkner-skan.m

3.8 Special cases

• for $\beta=0$ we obtain the Blasius solution:
$n=0$, $\tilde{u}=f'(\eta), \eta=\tilde{y}/\sqrt{2\bar{x}}$, $\tilde{v}=(1/(\sqrt{2\bar{x}}))(\eta f'-f)$.
the Blasius equation

$$f'''+ff''=0,\ \text{solution}\ f"_0=0.47\ \int_0^\infty(1-f')d\eta=1.2$$

then $f"_0/\sqrt{2}=0.332,\ \sqrt{2}\int_0^\infty(1-f')d\eta=1.72$
Of course the Blasius equation was writen $2f'''+ff''=0$ at the beginning of this chapter, the "2" is removed by the historical change of scale from Falkner Skan, that is the reason of the $\sqrt{2}$ in displacement and $1/\sqrt{2}$ in friction).

• for $\beta=1$ we obtain a stagnation point solution (Hiemenz) $n=1$:
$\tilde{u}=\bar{x}f'(\eta)$ $\tilde{v}=-f(\eta)$, $\eta=\tilde{y}$

$$f'''+ff''+(1-f'^2)=0,\ \ f_0''=1.23,\ \int_0^\infty(1-f')d\eta=0.6479,\ H=2.15$$

On figure 25 we compare the full Navier Stokes resolution, we clearly see the stream function in hyperbola (corresponding to $\psi=\bar{r}^2 sin(2\theta)$. On the right figure, the longitudinal velocity divided by x is plotted, we compare it to the selfsimilar solution (in fact it is an exact solution of Navier Stokes).

• For $\beta>2$ there is no physical solution but we may compute them with no problem. In fact we can even compute $\beta\to\infty$, Falkner Skan solution reduces $(1-f'^2)=0$, so that there is an external solution $f'=1$ every where. Near the wall, we introduce a "boundary layer"say $f'=F'(Y)$ and $\eta=\varepsilon Y$, so with $\varepsilon=\beta^{-1/2}$

we obtain $F''' + (1 - F'^2) = 0$, which is the self similar flow in a convergent $u_e = -x^{-1}$.
$\int_0^\infty (1 - F')dY = 0.779$, $F''(0) = 1.15$. There is even an exact solution:

$$F'(\eta) = \frac{3\left(1 - \frac{(-\sqrt{2}+\sqrt{3})e^{-\sqrt{2}\eta}}{\sqrt{2}+\sqrt{3}}\right)^2}{\left(1 + \frac{(-\sqrt{2}+\sqrt{3})e^{-\sqrt{2}\eta}}{\sqrt{2}+\sqrt{3}}\right)^2} - 2$$

The convergent $\beta = \infty$ and $n = -1$ $u = -x^{-1} f'(\eta)$, with $\eta = y$ $f''' + 1 - f'^2 = 0$. $f_0'' = 1.1547$, and $\int_0^\infty (1 - f')d\eta = 0.7783$ and $\int_0^\infty (1 - f')f'd\eta = 0.376$, so $H = 2.070$

• For $\beta < 0$ the flow is decelerated;

• For $\beta = -.1988$ it is the point of "incipient separation", the derivative of the velocity is always 0:
$f''(0) = 0$; $n = -0.091$ and $\int_0^\infty (1 - f')d\eta = 2.3$, $\delta_1 = 3.49$

• For $0 > \beta > -.1988$ there are in fact two solutions, one with $f''(0) > 0$ and another one with $f''(0) < 0$. The two solutions have different values of $\int (1 - f')d\eta$.
Other branches of solution exist.

• Falkner Skan solutions, small β
In Brown & Stewartson (On The Reversed Flow Solutions Of The Falkner-Skan Equation Mathematica 1966), they looked at the dependance in $f'"_0$ in β for small β (the returning curve). the obtained that :

$$f'"_0 \simeq 1.544(-\beta)^{3/4}$$

• Some triplet solution ($\int (1 - f')d\eta, f''(0), \beta$)= (0.649,1.23,1), (0.8,0.93,0.51), (1,0.669,0.18), (1.21,0.44,0), (1.5,0.29,-0.12), (2,0.09,-0.189), (2.5,-0.026,-0.198), (3,-0.09,-0.183), (4,-0.042,-0.196))

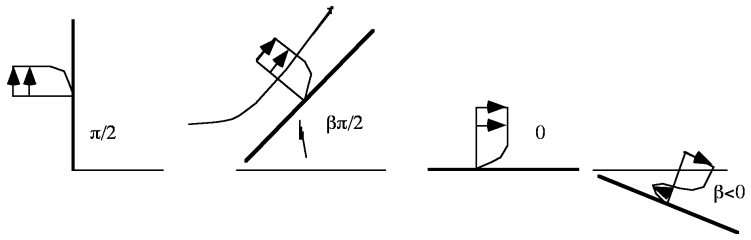

Figure 22: Some remarkable cases of Falkner Skan flow, for $\beta = 1$ to the negative β massively separated flow.

We seen on figure 23 that there is a non uniqueness in the solutions. Libby & Liu 1967computed far more branches of solution for $\beta < 0$. They correspond to oscillating f' (see Sobey's boook).

3.9 Non self similarity

A generalization of the FS equation may be obtained when the flow is non similar. If f^o is a short hand for $\partial_{\bar{x}} f$, we may write the Prandtl equations in introducing $n = \frac{\bar{x}}{\bar{u}_e}\frac{d\bar{u}_e}{d\bar{x}}$ then

$$f''' + ff'' + \beta(1 - f'^2) = x(f'f'^o - f^o f'').$$

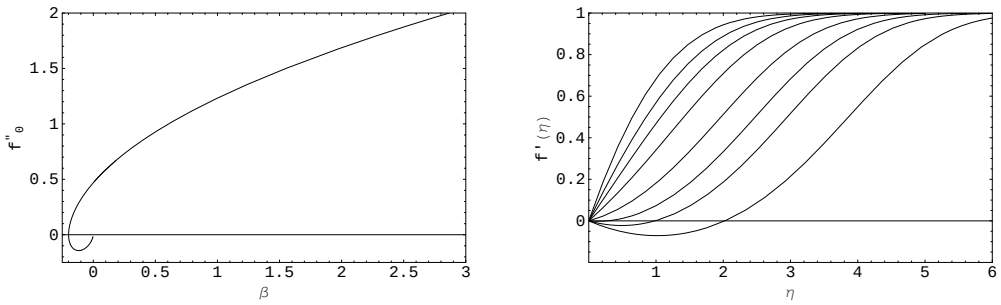

Figure 23: Left, dependence of the slope at the wall $f''(0)$ as a function of the acceleration parameter β. right some velocity profiles.

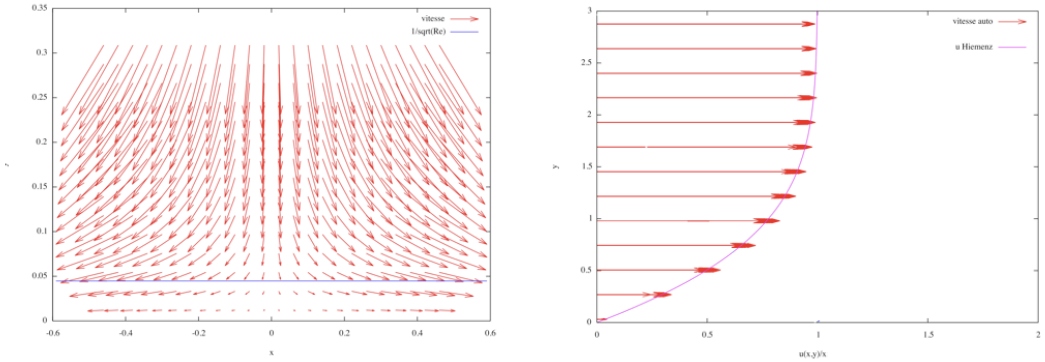

Figure 24: Navier Stokes computation with `freefem++` of the flow field and comparisons of the computed profiles $u/\bar{x}$ compared with the selfsimilar solution $f'(y)$ of Hiemenz.

3.10 Compressible Falkner Skan solutions

In the case with pressure gradients, in the case of model flows, a selfsimilar problem may be obtained:

$$f''' + ff'' + \beta(S - f'^2) = 0, \quad S'' + fS' = 0...$$

where S is the total enthalpy (see Stewartson 64).

4 Integral relations

4.1 Von Kármán equation integral relation

Boundary layer equations are a 2D PDE which is not so simple to solve. Nevertheless, we observed that the velocity profile is sometimes self similar. It means that there is a unique profile and that all the profiles are deduced by stretching it. The velocity of the ideal fluid at the wall and the thickness of the profile are two fundamental parameters which stretch the fundamental profile.

In this part we present the Von Kármán-Pohlhausen (1921) equation which consists in writing only the global dependance between $\bar{u}_e$ and the displacement thickness δ_1 supposing that in fact all the profiles are nearly similar.
An interpretation of δ_1 is that the flux of mass trough an enough large y say $\mathscr{H}$ (not to be confused by the shape factor H that we define just after) is the same than the flux of a constant velocity across a smaller section $\mathscr{H} - \delta_1$ so that (we are just in non dimensional variables, no tilde):

$$\psi = \int_0^{\mathscr{H}} u dy = (\mathscr{H} - \delta_1)u_e, \;\; i.e. \;\; \delta_1 u_e = \int_0^{\mathscr{H}} (u_e - u)dy$$

then, we suppose that $\mathscr{H}$ is large enough so it may be changed by ∞. This gives the physical definition of the displacement thickness, it is the distance by which the external stream lines are shifted due to the boundary layer development.

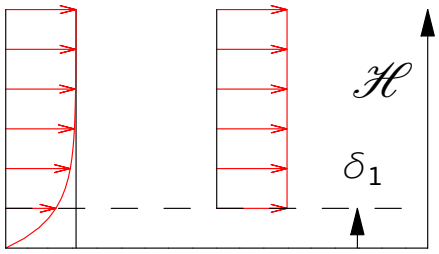

Figure 25: The flux of mass is the same in the boundary layer and in a equivalent layer of ideal fluid shifted by an amount of $\tilde{\delta}_1$.

Let us now look at Von Kármán equation, we write the total derivative $\tilde{u}\frac{\partial \tilde{u}}{\partial \tilde{x}} + \tilde{v}\frac{\partial \tilde{u}}{\partial \tilde{y}}$ in conservative form then adding $\partial_{\bar{x}}(\tilde{u}\bar{u}_e) = \tilde{u}\partial_{\bar{x}}(\bar{u}_e) - \bar{u}_e\partial_{\tilde{y}}\tilde{v}$ allows to write the momentum equation as:

$$\frac{\partial}{\partial \bar{x}}(\tilde{u}\bar{u}_e - \tilde{u}^2) + (\bar{u}_e - \tilde{u})\frac{\partial \bar{u}_e}{\partial \bar{x}} - \frac{\partial}{\partial \tilde{y}}(\tilde{v}(\tilde{u} - \bar{u}_e)) = -\frac{\partial^2 \tilde{u}}{\partial \tilde{y}^2}$$

Defining the displacement thickness, the momentum thickness and the shape factor

$$\tilde{\delta}_1 = \int_0^{\infty}(1 - \frac{\tilde{u}}{\bar{u}_e})d\tilde{y}, \;\; \tilde{\delta}_2 = \int_0^{\infty}\frac{\tilde{u}}{\bar{u}_e}(1 - \frac{\tilde{u}}{\bar{u}_e})d\tilde{y} \;\text{ and }\; H = \frac{\tilde{\delta}_1}{\tilde{\delta}_2},$$

and defining a function f_2 linked to the skin friction as: $\frac{\partial \tilde{u}}{\partial \tilde{y}} = f_2\frac{H\bar{u}_e}{\delta_1}$ gives the following equation where the ideal fluid promotes the boundary layer:

$$\frac{d}{d\bar{x}}(\frac{\tilde{\delta}_1}{H}) + \frac{\tilde{\delta}_1}{\bar{u}_e}(1 + \frac{2}{H})\frac{d\bar{u}_e}{d\bar{x}} = \frac{f_2 H}{\tilde{\delta}_1 \bar{u}_e}, \qquad i.e. \;\; \tilde{\delta}_1 = F(\bar{u}_e), \tag{19}$$

Initial condition is for example $\tilde{\delta}_1(0) = 0$ (but the Hiemenz value may be a good first guess) and $\bar{u}_e(0) = 1$. In the classical approach, $\tilde{\delta}_1$ is obtained through the knowledge of $\bar{u}_e$, which we write formaly $\tilde{\delta}_1 = F(\bar{u}_e)$.

4.2 Pohlhausen closure

One needs the shape of the boundary layer and then compute the integrals and the shear. In the original methods, one needs a thickness, say δ_∞ (the effective δ_{99} is such that $u(\delta_{99}) = 0.99u_e$, here say $u(\delta_\infty) = u_e$. Hence, we construct a shape which is 1 for $y > \delta_\infty$ and varies from 0 to 1 for $0 < y < \delta_\infty$. Let us define $\eta = y/\delta_\infty$.

Trying a Polynomia closure is Pohlhausen idea, we already presented polynomials of order 1, 2, and 3 for the Blasius solution. We extend the method in the case of pressure gradients

$$u/u_e = a_0 + a_1\eta + a_2\eta^2 + a_3\eta^3 + a_4\eta^4 + ...$$

at order 4, we write the boundary conditions, $u(0) = 0$ $u(1) = 1$ $u'(1) = 1$, $0 = du_e/dx + \frac{u''}{\delta_\infty^2}$ so that the velocity is

$$u = (2\eta - 2\eta^3 + \eta^4) + \frac{1}{6}\Lambda(\eta - 3\eta^2 + 3\eta^3 - \eta^4)$$

or in a compact form

$$u = 1 - (1-\eta)^3(1 + (1 - \frac{1}{6}\Lambda)\eta)$$

where we have defined $\Lambda = \delta^2 du_e/dx$ (it introduced with the condition at the wall). Then, by integration:

$\delta_1/\delta_\infty = (36 - \Lambda)/120$

$\delta_2/\delta_\infty = 37/315 - \Lambda/945 - (\Lambda^2)/9072$,

$H = ((36 - \Lambda)/120)/(37/315 - \Lambda/945 - (\Lambda^2)/9072)$

$f_2 = (2 + \Lambda/6)(37/315 - \Lambda/945 - \Lambda^2/9072)$

With all those values, the profile is determined as a function of δ_∞ and u_e, or as function of δ_1 and u_e. The relation between δ_1 and u_e is found then with the Von Kármán equation. We plot on figure 4.3 in green, first left $H(\lambda_1)$ as a parametric plot of $\Lambda_1(\Lambda)$ and $H(\Lambda)$. We plot on figure 4.3 in green, second right $f_2(H)$ as a parametric plot of $f_2(\Lambda)$ and $H(\Lambda)$.

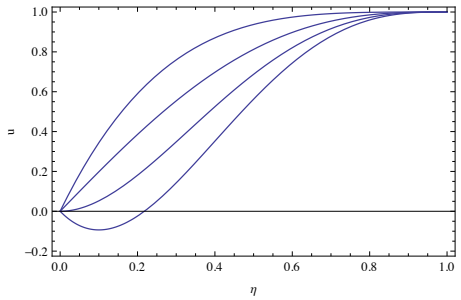

Figure 26: An example of closure Pohlhausen $\Lambda = 12, 0, -12, -24$.

Flat Plate case

In the case of zero pressure gradient $\Lambda = 0$, we first obtain the value of the coefficients $f_2 = 74/315 = 0.234921$ and $H(0) = 189/74 = 2.5540540$ (Blasius values are$H_B = 2.59$ the slope is 0.332 so $f_2 = 0.22 = 0.332 * 1.721/2.59$). and we put them in the Von Kármán equation with $u_e = 1$

$$\frac{d}{d\bar{x}}(\frac{\tilde{\delta}_1}{H}) = \frac{f_2 H}{\tilde{\delta}_1 \bar{u}_e},$$

the integration gives

$$\delta_1 = \sqrt{2f_2} H_0 x^{1/2}$$

hence $\sqrt{2f_2}\ H = 9\sqrt{7/185} = 1.75068$ (very close to the Blasius value). The shear at the wall is then evaluated, and is again close to the exact Blasius value $Hf_2/\delta_1 = (1/3)\sqrt{37/35}x^{-1/2} = 0.342725x^{-1/2}$

The "physical" Pohlhausen's thcickness $\delta = 120/36\delta_1 = 6\sqrt{35/37}x^{1/2} = 5.83559x^{1/2}$

4.3 Falkner Skan Closure

To solve this boundary layer equation, a closure relationship linking H and f_2 to the velocity and the displacement thickness is needed. This is of course a strong hypothesis. Defining $\Lambda_1 = \tilde{\delta}_1^2 \frac{d\bar{u}_e}{d\bar{x}}$, the system is closed from the resolution of the Falkner Skan system as done before. Remember the solution is $u_e = f'(\eta)\bar{x}^n$ with $\eta = (\sqrt{\frac{n+1}{2}})\frac{\tilde{y}}{\bar{x}^{(1-n)/2}}$ so that

$$\delta_1 = (\int (1 - f'(\eta))d\eta)/((\sqrt{\frac{n+1}{2}})\bar{x}^{(n-1)/2})$$

the "Pohlhausen" parameter Λ_1 is

$$\Lambda_1 = \delta_1^2 \frac{d\bar{u}_e}{d\bar{x}} = \frac{2n}{n+1}(\int (1 - f'(\eta))d\eta)^2 \bar{x}^{1-n+n-1}$$

then

$$\Lambda_1 = \beta(\int (1 - f'(\eta))d\eta)^2.$$

On figure (see figure 4.3):

$$H = \left\{ \begin{array}{ll} 2.5905e^{-0.37098\Lambda_1} & \text{if } \Lambda_1 < 0.6 \\ 2.074 & \text{if } \Lambda_1 > 0.6 \end{array} \right\}, \qquad f_2 = 1.05(-H^{-1} + 4H^{-2}).$$

It means that we suppose that each profile remains a Falkner Skan one in the boundary layer. We used this crude solution in exponential with the value of the sink $H = 2.074$ as a limiting value. We tested it to be enough good, other closures may be found in the literature. Some closures use the concept of entrainment. The closure may be done with other families of profiles, and Pohlhausen profiles are good candidates (the so-

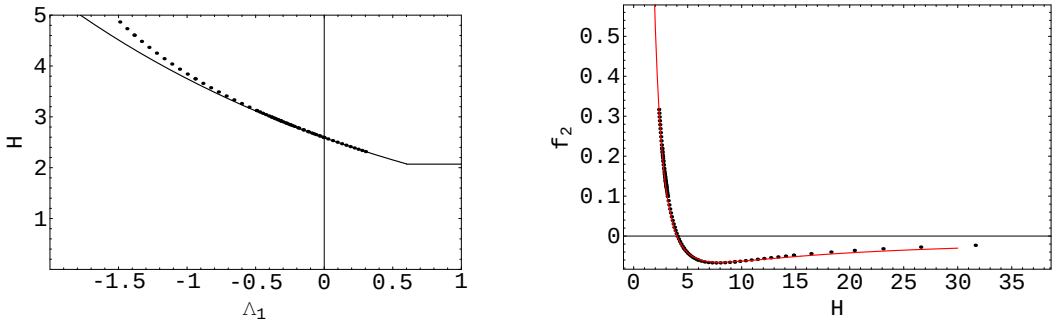

Figure 27: An example of closure of the integral relations. The dots are the Falkner Skan values and the line the proposed function. if $\Lambda_1 > 0.6$ in fact $H = 2.07$ is constant, for FS it means that $\beta \to 2$ (accelerated case). Note the very good agreement for f_2.

lution is part of a polynom). With those profiles the reverse flow is over estimated compared to Falkner Skan.

4.4 Remarks

In general, the Von Kármán equation is written with the momentum thickness $\tilde{\delta}_2$:

$$\frac{d}{d\bar{x}}(\tilde{\delta}_2 \bar{u}_e^2) + \tilde{\delta}_1 \bar{u}_e \frac{d\bar{u}_e}{d\bar{x}} = \frac{\partial \tilde{u}}{\partial \tilde{y}}|_{\tilde{y}=0} \tag{20}$$

(often the symbol $\tilde{\theta}$ is taken, and $\tilde{\delta}_1$ is written $\tilde{\delta}^*$), we prefer to write it with $\tilde{\delta}_1$ as we will see that this value has a real physical interpretation. The reason why mainly $\tilde{\delta}_2$ is used is that its derivative is clearly linked

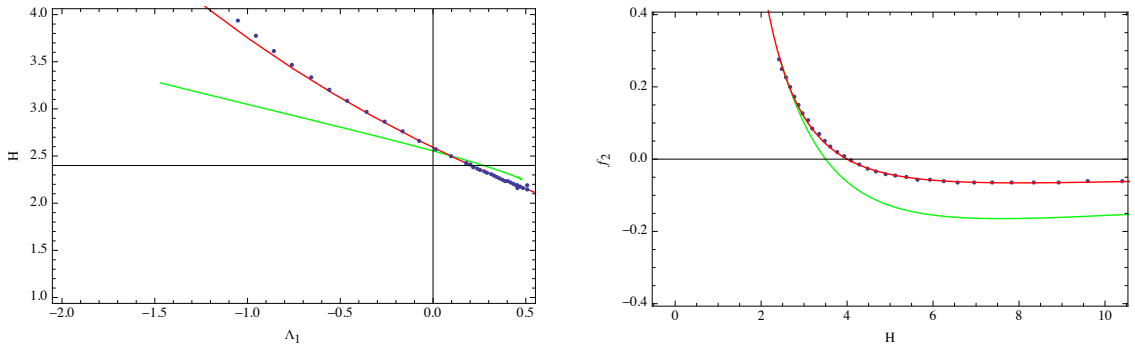

Figure 28: Left: we plot here with blue dots the result of Falkner Skan solution, H as a function of Λ_1 which is $\beta(\int(1-f'(\eta))d\eta)^2$. In red the approximation $2.5905e^{-0.37098\Lambda_1}$ if $\Lambda_1 < 0.6$. In green the plot of $H(\Lambda)$ as function of $\Lambda_1(\Lambda)$ from Pohlhausen. Right, blue dots Falkner Skan, red curve the fit $f_2 = 1.05(-H^{-1}+4H^{-2}$, green curve Pohlhausen for f_2 as function of H.

to the skin friction (this gives a technique to deduce the skin friction from even crude measurements of the boundary layer profile.

In general, another thickness is introduced, the "boundary layer thickness": $\tilde{\delta}_{99}$. The velocity is defined so that if $\tilde{y} > \tilde{\delta}_{99}$ we have $\tilde{u} = \bar{u}_e$. In the Falkner Skan description, this length does not exist as the velocity is attained only at infinity. That is why it is defined sometimes as position at which the velocity is $0.99\bar{u}_e$. We put this subscript not to confuse this "value" with the scale $\delta = L/\sqrt{Re} = L\tilde{\delta}$.
For instance, using this thickness, the Pohlhausen technique allows to approximate the Blasius profile by :

$$\tilde{u} = 1 - (1+\eta)(1-\eta)^3, \quad \tilde{\delta}_1 = .3\tilde{\delta}, \quad \tilde{\delta}_1/\tilde{\delta}_2 = 2.55$$

So, if we define nevertheless this thickness (it is common in turbulent flows, and it the original Pohlhausen approach as well). Starting from the incompressibility equation

$$\frac{\partial \tilde{v}}{\partial \tilde{y}} = -\frac{\partial \tilde{u}}{\partial \bar{x}}$$

we obtain, after adding and substracting $\frac{\partial \bar{u}_e}{\partial \bar{x}}$ and after integration (with $\tilde{v}(0) = 0$) up to a $\tilde{\delta}$ function of $\bar{x}$ that the velocity is:

$$\tilde{v}(\tilde{\delta}) = -\int_0^{\tilde{\delta}} \frac{\partial}{\partial \bar{x}} \tilde{u} d\tilde{y} = -\frac{\partial}{\partial \bar{x}} \int_0^{\tilde{\delta}} \tilde{u} d\tilde{y} + \bar{u}_e \frac{d\tilde{\delta}}{d\bar{x}}$$

so, as for $\tilde{y} > \tilde{\delta}$ by definition $\tilde{u} = \bar{u}_e$, then $\int_0^{\tilde{\delta}} \tilde{u} d\tilde{y} = \int_0^{\tilde{\delta}} \bar{u}_e d\tilde{y} - \int_0^{\tilde{\delta}} (\bar{u}_e - \tilde{u}) d\tilde{y}$ and we obtain the behaviour:

$$\frac{d\tilde{\delta}}{d\bar{x}} - \tilde{v}(\tilde{\delta}) = \frac{1}{\bar{u}_e} \frac{d}{d\bar{x}} (\bar{u}_e(\tilde{\delta} - \tilde{\delta}_1)).$$

This is the definition of the "entrainment coefficient" C_E. It represent the difference between the growth of the boundary layer and the velocity at the edge of the boundary layer. Closure relations may be written to model it. We will see that this concept is not so useful, we will write in a better way this same integral and we will do a proper matching to get rid with this non asymptotic concept of $\tilde{\delta}_{99}$

5 The problem of boundary layer separation

5.1 definition

Separation consists in the existence of a long vortex near the wall caused by a deceleration of the flow. Fluid is trapped in a "bubble" or a "bulb" which increases the apparent size of the body. From the point of vied of aerodynamics, it is not a good thing as it creates, dissipation, turbulence and decreases dramatically the lift of airplanes. The ideal fluid-boundary layer description is believed to fail due to boundary layer separation.

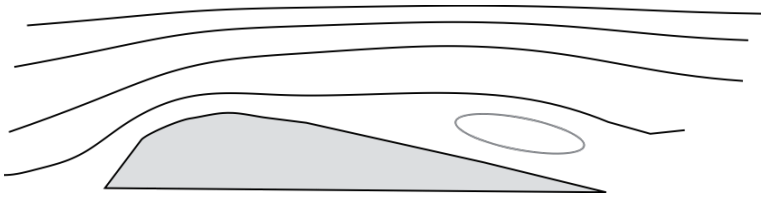

Figure 29: A sketch showing the body, the separated bulb, and the deflexion of stream lines.

Boundary layer separation occurs in the boundary layer. Due to the shape of the body, first the ideal fluid accelerates and then on the lee side decelerates. So does the slip velocity at the wall. When slip velocity is decreasing $u_e \frac{du_e}{dx} < 0$, It corresponds to a counter pressure: $\frac{dp}{dx} > 0$. The pressure is increasing, upstream to downstream. Note that the pressure does not depend on y. This correspond to the case of the ideal flow on a cylinder, this is a generic case: $\bar{u}_e = sin(\bar{x})$. Near the wall the influence of the adverse pressure gradient is larger and larger, as the velocity is smaller and smaller. So, near the wall, were the velocity is small, the velocity is more fragile. Hence, due to this adverse pressure gradient, a reverse flow may appear. This is boundary layer separation, it corresponds to the existence of a counter flow near the wall. A long vortex arises near the wall.

The point of separation is the point defined by $\frac{\partial \tilde{u}}{\partial \tilde{y}} = 0$ (definition is not so clear in unsteady flows). See an example of representation on figure 30 taken form Prandtl himself [18].

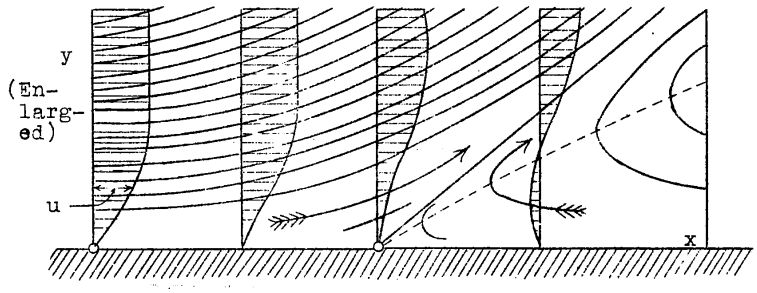

Figure 30: A sketch from Prandtl [18] of the flow near the point of vanishing shear stress.

Then when there is separated flow, near the wall, the dangerous terms in the BL are:

$$\tilde{u}\frac{\partial \tilde{u}}{\partial \bar{x}} + ... = ... + \frac{\partial^2 \tilde{u}}{\partial \tilde{y}^2}$$

with $\tilde{u} < 0$, and changing $\bar{x}$ in t, this is a kind of heat equation with a negative coefficient:

$$-\frac{\partial T}{\partial t} = \frac{\partial^2 T}{\partial y^2}$$

so it is unstable (ill posed). It is then impossible to cross the position of boundary layer separation. That is why, in most classical textbooks, the boundary layer separation is presented as the death of boundary layer. For example Kundu & Ira p368 of the fourth edition say: " The boundary layer equations are valid only as far downstream as the point of separation. Beyond it the boundary layer becomes so thick that the basic

underly- ing assumptions become invalid. Moreover, the parabolic character of the boundary layer equations requires that a numerical integration is possible only in the direc- tion of advection (along which information is propagated), which is upstream within the reversed flow region. A forward (downstream) integration of the boundary layer equations therefore breaks down after the separation point. Last, we can no longer apply potential theory to find the pressure distribution in the separated region, as the effective boundary of the irrotational flow is no longer the solid surface but some unknown shape encompassing part of the body plus the separated region." We will show that every thing is false, and even that the impossibilities presented are the clues to find the solution of the problem!

This problem of boundary layer separation is of course very important for flow around wings, as it creates "stall" (dramatic decrease of lift). It arise in most practical cases of flow and is responsible for dissipation of energy. Furthermore, it creates instability and turbulence. The boundary layer separation control is of high importance.

It is a real XXth century problem and victory of asymptotics. It has been introduced in 1904 by Prandt, then in the forties it was a dead end (Landau, Goldstein). In the fifties light hill had some intuition to understand it. In 1969 the framework was settled, it is known as "Triple Deck". In the 80' it was applied to a lot of configurations and was shown to be linked with instabilities.

5.2 Example of separation on a cylinder

In the classical framework it is not possible to trespass the separation point. This impossibility is known as Goldstein singularity (1948). On figure 31, is presented an example of boundary layer computation with an external flow $\bar{u}_e = sin(\bar{x})$ corresponding to the flow on a cylinder. A Integral resolution of the equations is compared with a complete boundary layer resolution showing how precise is the Von Kármán approach.

The flow is accelerated from $\bar{x} = 0$ to $\pi/2$, near $x = 0$ we have an Hiemenz linear flow. The flow is decelerated for $\bar{x} > \pi/2$, this deceleration promotes an increase of the boundary layer thickness and a decrease of the skin friction. At the point where $\frac{\partial \bar{u}}{\partial \bar{y}} = 0$, the boundary layer is singular, we can not compute numerically (here by finite difference) the boundary layer.
Using the Von Kármán equation gives the same behavior! It fails nearly at the same point (not exactly, but not so bad).

A simple way is to observe it is to look at the Von Kármán equation:

$$\frac{d}{d\bar{x}}(\frac{\tilde{\delta}_1}{H}) + \frac{\tilde{\delta}_1}{\bar{u}_e}(1 + \frac{2}{H})\frac{d\bar{u}_e}{d\bar{x}} = \frac{f_2 H}{\tilde{\delta}_1 \bar{u}_e},$$

in which the derivative of $\tilde{\delta}_1/H$ may be approximated by

$$\frac{d}{d\bar{x}}(\frac{\tilde{\delta}_1}{H}) = \frac{1}{H}(\frac{d}{d\bar{x}}\tilde{\delta}_1)(1 - \frac{\tilde{\delta}_1}{H}\frac{dH}{d\Lambda_1}\frac{d\Lambda_1}{d\tilde{\delta}_1})$$

so for a decelerating flow linearizing the velocity near the point of separation is say $\bar{u}_e = sin(\bar{x}_s) - a(\bar{x} - \bar{x}_s)$ with $a = cos(\bar{x}_s)$ and linearizing around small Λ_1 (which is not true but is a enough good approximation) $H = H_0 - H_p\Lambda_1$ where $H_0 = 2.59$ and $H_p \simeq -0.96$ this term is

$$\frac{d}{d\bar{x}}(\frac{\tilde{\delta}_1}{H}) \simeq (\frac{1}{H_0}\frac{d}{d\bar{x}}\tilde{\delta}_1)(1 - \frac{2H_p a\tilde{\delta}_1^2}{H_0})$$

and then the Kármán equation (with $f_2 = 0$, or not...)

$$(\frac{1}{H_0}\frac{d}{d\bar{x}}\tilde{\delta}_1) = \frac{-\frac{\tilde{\delta}_1}{\bar{u}_e}(1 + \frac{2}{H})(-a) + 0)}{(1 - \frac{2H_p a\tilde{\delta}_1^2}{H_0})}$$

then $\frac{d}{d\bar{x}}\tilde{\delta}_1$ is infinite, (with $\tilde{\delta}_1$ finite here) we can not march in $\bar{x}$ anymore. This crude estimation shows that the separation point is impossible to cross.

It is very disappointing as Falkner Skan profiles allow separation (Pohlhausen as well), but using this description it is not possible to cross the separation point. Direct numerical finite difference solution gives the same result (figure 31).

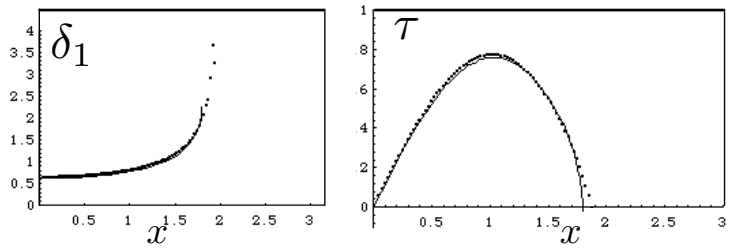

Figure 31: Boundary layer separation on a cylinder, the outer velocity is $\bar{u}_e = sin(\bar{x})$, points are numerical finite difference solution of the Boundary Layer equations, line is the integration of Von Kármán equation with the proposed closure. Separation occurs for an angle of 104^o.

5.3 Thwaites method 49.

Note that the more classical way to do that is tu use the Thwaites method which uses a simplification of the closure coefficients when integrating the Von Kármaán equation:

$$\tilde{\delta}_2^2 \bar{u}_e^6 = \tilde{\delta}_2(0)^2 \bar{u}_e(0)^6 + 0.45 \int_0^{\bar{x}} \bar{u}^5 d\bar{x}$$

5.4 Example of separation on a plate with a bump.

One may think that the cylinder case is to severe. A smoother plate is maybe less difficult to compute. It is of course not true, on figure 32 we show boundary layer computations examples for an outer flow $\bar{u_e} = 1 - \alpha e^{-6(\bar{x}-1.5)^2}$. For each case, velocity profiles displacement boundary layer thickness and skin friction are presented. Unfortunately again, even for such a smooth outer velocity, for $\alpha = 0.06$ there is the incipient separation. For greater α we can not go through the separation point, where $\frac{\partial \tilde{u}}{\partial \tilde{y}} = 0$, the boundary layer is singular.

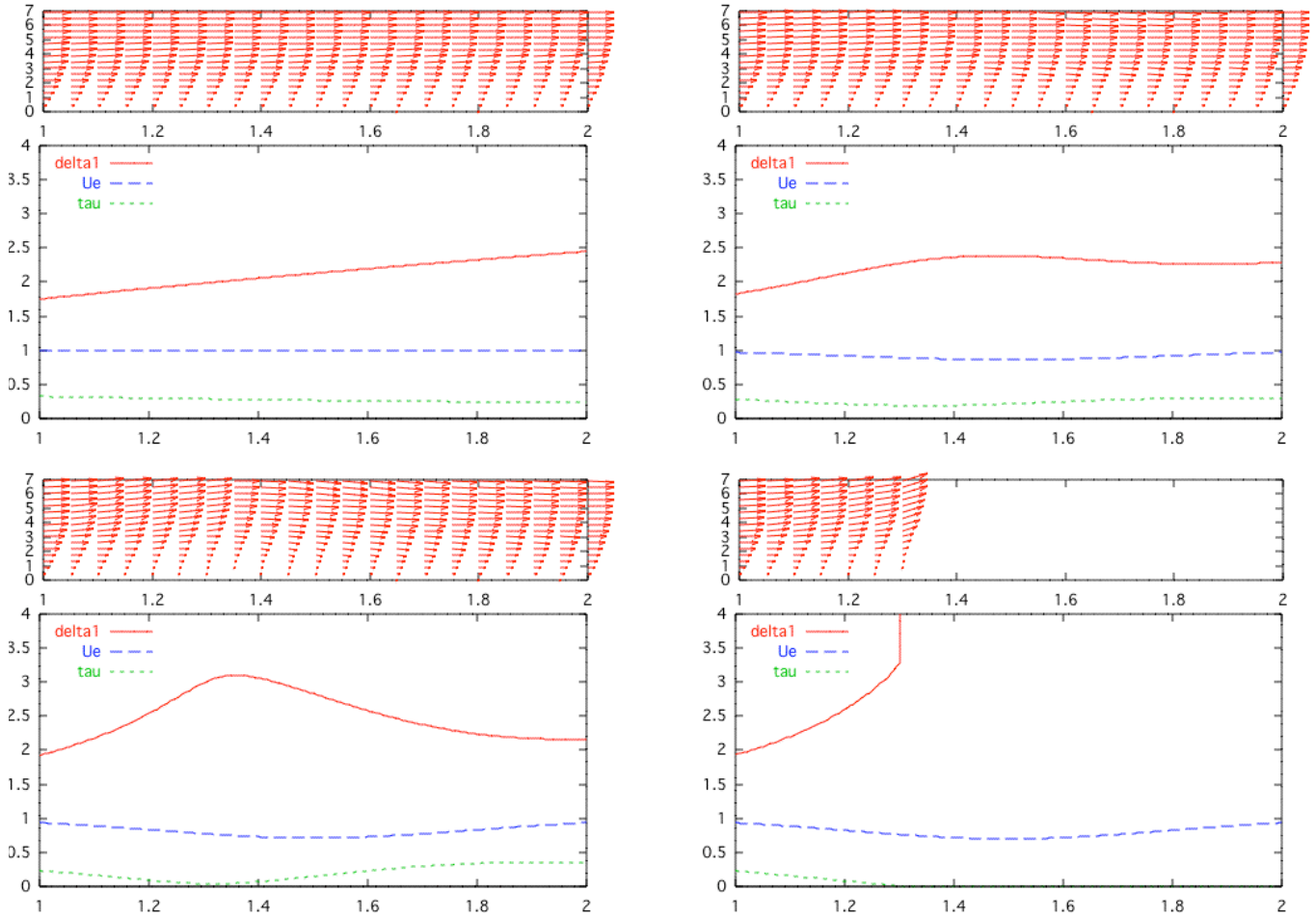

Figure 32: Examples of profiles of a boundary layer with an external given velocity $\bar{u}_e = 1 - \alpha e^{-6(\bar{x}-1.5)^2}$. For each case, velocity profiles, then from top to bottom $\tilde{\delta}_1 = 1.73\bar{x}^{1/2}$, $\bar{u_e}$, and skin friction. Top left , Blasius boundary layer ($\alpha = 0$, $\tilde{\delta}_1 = 1.73\bar{x}^{1/2}$, $\bar{u}_e = 1$, skin friction $0.33\bar{x}^{-1/2}$), top right $\alpha = 0.03$, the boundary layer thickness decreases, the skin friction increases when the velocity increases. For $\alpha = 0.06$ (bottom left) it is the incipient separation. For greater α we can not go through the separation point, where $\frac{\partial \bar{u}}{\partial \bar{y}} = 0$, the boundary layer is singular. [click to launch the movie, QuickTime Adobe/ Reader required]

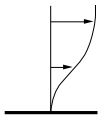

Figure 33: A typical velocity profile at separation is $u = (no\ terms\ in\ y) + \frac{1}{2}(\frac{dp}{dx})y^2 + (no\ terms\ in\ y^3) + a_4 y^4 + ...$

5.5 Attempts to understand the boundary layer separation

5.5.1 Landau

One of the first attempts may be found in the Landau Lifshitz book [14], §40. They notice that as in the boundary layer $v << u$, so the transverse velocity must increase a lot to be as large as the longitudinal one. it is apparently the case when the flow is separated (stream lines are ejected from the wall). In boundary layer variables they infer that $v = \infty$ and $\partial v/\partial y = \infty$ so that $\partial u/\partial x = -\infty$. The velocity is strongly decelerated near the point of separation x_s. So they propose to work with the inverse of the function $(\frac{\partial x}{\partial u})$ and propose a reciprocal expansion of x in u near x_s as:

$$x - x_s = \frac{\partial x}{\partial u}(u - u_s) + \frac{1}{2}\frac{\partial^2 x}{\partial u^2}(u - u_s)^2 = 0(u - u_s) + f(y)(u - u_s)^2 + ...$$

so that one may write the velocity u and by the continuity equation v as:

$$u = u_s(y) + 2\beta'(y)\sqrt{x_s - x} + ... \text{ and } v = \frac{\beta(y)}{\sqrt{x_s - x}} + ...$$

They inject it in the momentum equation in which they neglect the viscosity:

$$u\partial_x u + v\partial_y u = 0$$

but using incompressibility, $u\partial_x u + v\partial_y u = u^2(\partial_y(\frac{v}{u}))$. Hence

$$\partial_y(\frac{v}{u}) = 0$$

which means that v/u does not depend on y. The function β is just proportional to u. They then deduce an hint for the profile near separation as :

$$u = u_s(y) + \frac{\partial u_s}{\partial y}A(x) \quad v = -\frac{\partial A}{\partial x}u_s \quad A(x) = a\sqrt{x_s - x}.$$

unfortunately this description does not fit the good boundary conditions at the wall....

It is striking that the exercise in the Landau is exactly the one which allows to obtain the triple deck scaling.... see after.

5.5.2 Goldstein singularity 1948

The real serious attempt came from Goldstein, we present here an over simplified analysis of his paper. He wanted to look at the region of separation near the point where velocity may be written as

$$u = \Sigma_{r>1} a_r y^r$$

We put this development in the boundary layer equations (after manipulating the equations: derivating twice the boundary layer momentum equation in $y = 0$), we obtain:

$$u = \tau_p y + \frac{1}{2}(\frac{dp}{dx})y^2 + (no\ terms\ in\ y^3) + a_4 y^4 + ...$$

if we define $\tau_p = \partial u/\partial y|_{y=0}$ and if we note that $a_3 = 0$. Then after manipulation we can show that

$$\frac{\partial^4 u}{\partial y^4}|_{y=0} = 4! a_4 = \frac{1}{2}\frac{\partial}{\partial x}\tau_p^2.$$

* if a_4 is zero it is a special case (regular separation / marginal separation), but this case is not general.
* if a_4 is not zero:

$$\tau_p = \sqrt{48 a_4 (x_s - x))}.$$

so that $v = -\frac{1}{2}\frac{\partial}{\partial x}\tau_p^2$ behaves like $1/\sqrt{x_s - x}$. The paradox comes from the fact that $a_4 > 0$ before separation. But it would be negative after, so it is impossible. We can not go through the separation point, the stream lines have a vertical tangent. In fact Goldstein 48 analysis is far more complicated, it leads to developments in $y/(x_s - x)^{1/4}$, but the conclusion remains the same.

6 Unsteady boundary layer

6.1 Unsteady boundary layer flow over a semi infinite flat plate impulsively started

Reintroducing the time in the boundary layer equation seems a simple task, the convective time scale reintroduces $\partial/\partial t$. We show a first example which is simple (Stewartson 51 et 73, Smith 70 & 72 et Hall 69). At time $t = 0$ a semi infinite flat plate is impulsively put in motion. We are in the framework of the plate, so that the Ideal Fluid response is instantaneously $u_e = 1$ (the plate slips in the ideal fluid). One has only to introduce the time derivative in the boundary layer equations :

$$\begin{cases} \dfrac{\partial u}{\partial x} + \dfrac{\partial v}{\partial y} = 0, \\ \dfrac{\partial u}{\partial t} + u\dfrac{\partial u}{\partial x} + v\dfrac{\partial u}{\partial y} = \dfrac{\partial^2 u}{\partial y^2}, \\ u(x,0,t) = v(x,0,t) = 0, \\ u(x, y > 0, t = 0) = 1 \\ v(x, y > 0, t = 0) = 0 \\ \text{and } u(x,\infty,t > 0) = 1. \end{cases} \tag{21}$$

At a fixed position x we observe for short times the Rayleigh flow (or Stokes first problem, in fact as noted in Schlichting, this is the Stokes problem):

$$\partial_t u = \partial_y^2 u; \quad u(y > 0, t = 0) = 1, u(0,t) = 0, u(y \to \infty, t) = 1$$

The solution is with the terror function (self similar solution...)

$$u(x,y,t) = erf(\frac{y}{2\sqrt{t}})$$

we can compute the displacement thikness, the momentum thickness, the shape factor and the shear at the wall

$$\delta_1 = \frac{2t^{1/2}}{\sqrt{\pi}}, \;\; \delta_2 = \frac{2(\sqrt{2}-1)t^{1/2}}{\sqrt{\pi}}, \;\; H = 1+\sqrt{2}, \;\; \frac{\partial u}{\partial y}|_0 = \frac{1}{\sqrt{\pi t}}.$$

And we guess that for a long time, at a given x, the flow will finally be steady, $\partial u/\partial t = 0$, we will recover the Blasius flow. The good variable is $\tau = t/x$. Depending if it is small or large, we go from Rayleigh to Blasius. Transition occurs for $\tau = 1$, this time correspond to the time necessary so that information which travels at velocity 1 arrives at the considered point.

The solution is numerically computed on figure 34, we use simple finite difference technique.

For $1.5 < \tau < 4$, the difference between the two régimes is noticeable. We see it on the figure 34 (first obtained by Hall 69 with a specific method using similarity variables and valid for $\tau \geq 1$), we plot on this figure $\frac{\partial u(x,y=0,t)}{\partial y}\sqrt{x}$ so that

$$\tau >> 1 \quad \tau_w = .332/\sqrt{x}, \qquad \delta_1 = 1.732\sqrt{x}; \text{ and for } \quad \tau \leq 1 \quad \tau_w = 1/\sqrt{\pi t}, \qquad \delta_1 = 2\sqrt{\frac{1t}{\pi}}.$$

On the next figure we plot $2\sqrt{\frac{1}{\pi}} - \delta_1\sqrt{\frac{1}{t}}$, which is 0 for Rayleigh solution ($\tau \leq 1$) and which is function of τ in the Blasius case ($2\sqrt{\frac{1}{\pi}} - 1.732\sqrt{\frac{1}{\tau}}$, expression valid for $\tau >> 1$.

The analytic study of the problem of the transition between the two régimes is difficult. Stewartson had to do two papers (51 & 73) to solve it. The difficulty comes because there is an "essential singularity" in the developments around $\tau = 1$, it means that all the terms of the Taylor expansion are zero (just like e^{-x^2}, this function has no Taylor expansion in $x = 0$).

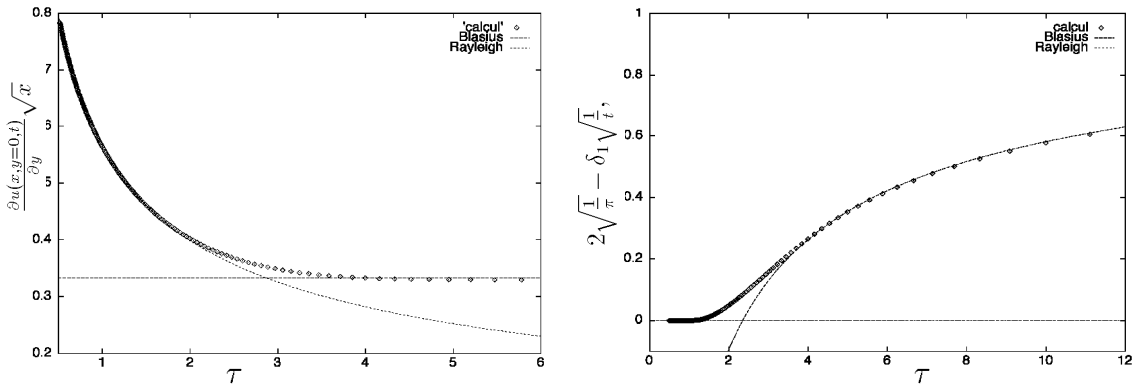

Figure 34: Unsteady numerical solution in finite differences of the unsteady boundary layer equation. We observe the transition from Rayleigh infinite flat plate impulsive solution to the Blasius steady solution. Left, shear times $\sqrt{x}$ at the wall, from Rayleigh, at small τ, to the constant Blasius value. Right, plot of $2\sqrt{\frac{1}{\pi}}-\delta_1\sqrt{\frac{1}{t}}$, (points) compared to the Balsius value $2\sqrt{\frac{1}{\pi}}-1.732\sqrt{\frac{1}{\tau}}$, line, as a function of τ

6.2 Unsteady boundary layer flow over a semi infinite flat plate impulsively started, integral point of view

The unsteady system may be written in integral form ($\partial_x u = -\partial_y v$),

$$\frac{\partial u}{\partial t}+u\frac{\partial u}{\partial x}+v\frac{\partial u}{\partial y}=\frac{\partial u}{\partial t}+\frac{\partial u^2}{\partial x}+\frac{\partial vu}{\partial y}=$$
$$\frac{\partial u}{\partial t}+\frac{\partial (u^2-u)}{\partial x}+\frac{\partial u}{\partial x}+\frac{\partial vu}{\partial y}=$$
$$\frac{\partial u}{\partial t}+\frac{\partial (u^2-u)}{\partial x}+\frac{\partial (v(u-1))}{\partial y}=-\frac{\partial^2 u}{\partial y^2},$$

were we have defined the displacement thickness, the momentum thickness and the shape factor

$$\delta_1=\int_0^\infty (1-u)dy,\ \ \delta_2=\int_0^\infty u(1-u)dy \ \text{ and } \ H=\frac{\delta_1}{\delta_2},$$

and defining a function f_2 linked to the skin friction as: $\frac{\partial u}{\partial y}=f_2\frac{H}{\delta_1}$. Then by integration, and by boundary condition in 0 and ∞

$$\frac{\partial}{\partial t}\delta_1+\frac{\partial}{\partial x}\frac{\delta_1}{H}=\frac{f_2 H}{\delta_1}$$

We see a convection equation $\partial_t\delta_1+H^{-1}\partial_x\delta_1$, of velocity $1/H$. This velocity is the velocity of propagation of the information of the existence of the leading edge of the semi infinite flat plate.

For small time, at a given position x from the nose, we are in the Rayleigh-Stokes problem: there is up to now no information that the plate is not infinite ∂_x is zero, we have only

$$\frac{\partial}{\partial t}\delta_1=\frac{f_2 H}{\delta_1}$$

which gives the square root behavior of δ_1 in time

$$\delta_1=\sqrt{2f_2 H}\sqrt{t}$$

using the closure, this gives $f_2=0.22$, $H=2.59$ and$\delta_1=1.06\sqrt{t}$ (Stokes value 1.12)

For long time, at a given position x from the nose, we are in the Blasius problem: there is no more the unsteady ∂_t term, we have only

$$\frac{\partial}{\partial x}\frac{\delta_1}{H} = \frac{f_2 H}{\delta_1}$$

which gives the square root behavior of δ_1 in space

$$\delta_1 = \sqrt{2f_2}H\sqrt{x}$$

using the closure, this gives $f_2 = 0.22$, $H = 2.59$ and $\delta_1 = 1.7\sqrt{x}$ (Blasius value 1.732)

Of course, we see that if $\tau = t/x$, then we go for small τ from $\delta_1 = \sqrt{2f_2 H}\sqrt{t}$ to $\delta_1 = \sqrt{2f_2}H\sqrt{x}$ at large τ. The propagation of the information of the existence of the leading edge of the plate is at velocity $1/H$. As $H \simeq 2.6$, we obtain the same estimate than previously on τ when solving the full problem.

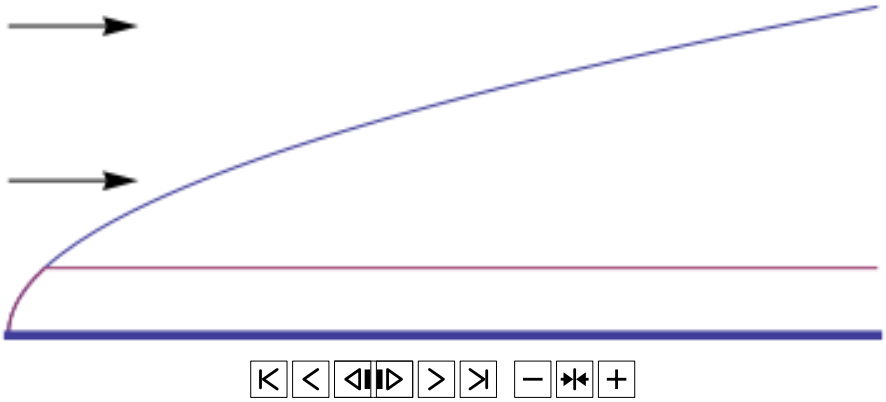

Figure (moovie): Boundary layer formation on an impulsively started semi infinite flat plate, the given external velocity is 1, solution obtained from equation $\frac{\partial}{\partial t}\delta_1 + \frac{\partial}{\partial x}\frac{\delta_1}{H} = \frac{f_2 H}{\delta_1}$ at small times the displacement thickness increases with $\sqrt{t}$ at large time it increases in $\sqrt{x}$ t from 0.1 to 2.5. [click to launch the movie, QuickTime Adobe/ Reader required].

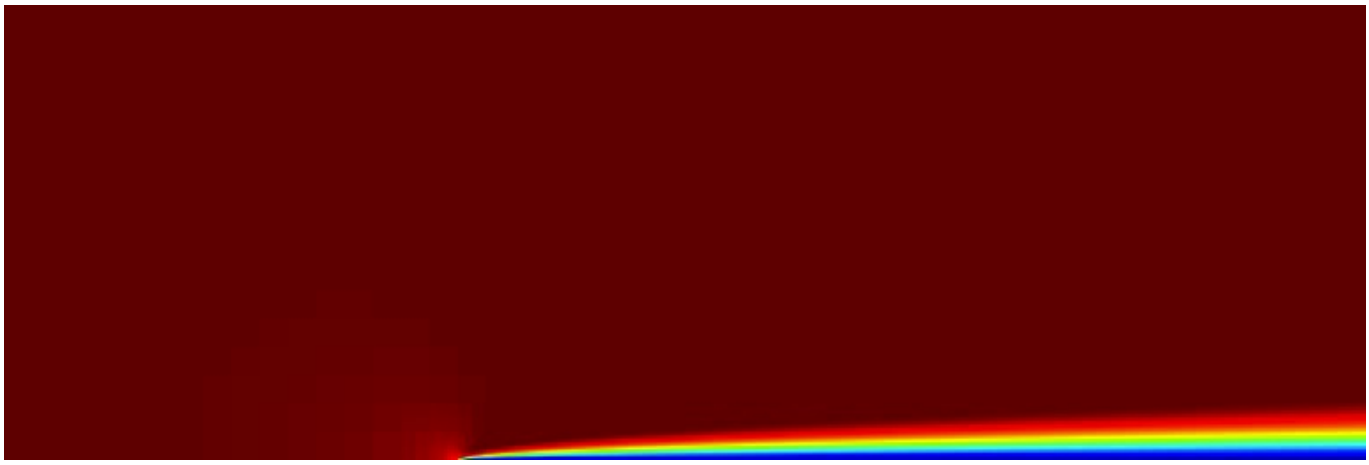

Figure 35: (moovie): Boundary layer formation on an impulsively started semi infinite flat plate, the given external velocity is 1, solution obtained from *Gerris* [click to launch the movie, QuickTime Adobe/ Reader required]..

6.3 Unsteady boundary layer flow over a cylinder impulsively started

An other fundamental example is the case of the flow round a impulsively started cylinder. We may expect no problem, as before. But here a terrible problem of singularity will appear. The equations are the same than previously, with a different matching, the velocity at time 0 is the Euler steady irrotational potential

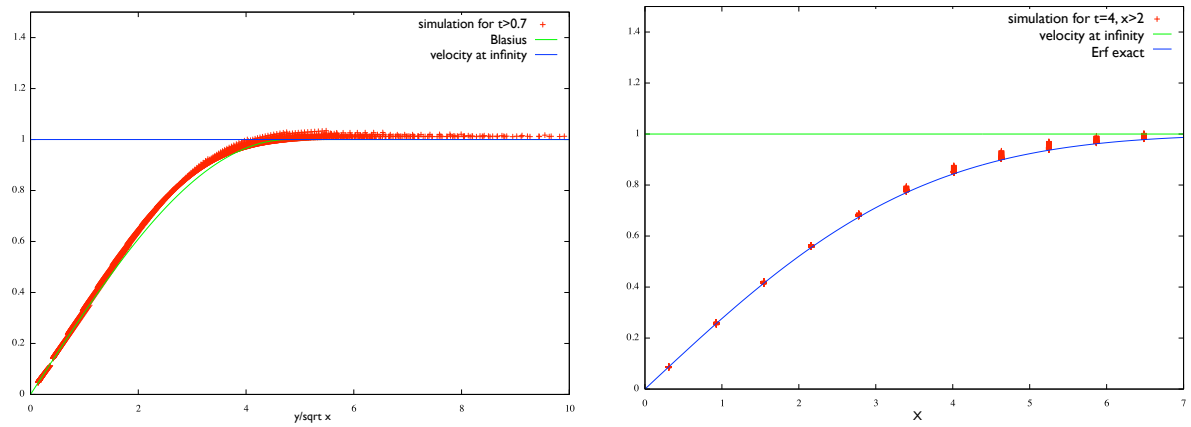

Figure 36: Navier Stokes computation by *Gerris* at $Re = 1000$, left we have the selfsimilar Blasius profile (superposition of several profiles plotted with $\bar{y}(Re/\bar{x})^{1/2}$). Right the erf solution.

flow. Velocity at the wall is $\sin(x)$ is x is the distance along the cylinder, so $x = 0$ is the leading edge and $x = \pi$ is the trailing edge.

$$\left\{\begin{array}{l} \dfrac{\partial u}{\partial x} + \dfrac{\partial v}{\partial y} = 0, \\ \dfrac{\partial u}{\partial t} + u\dfrac{\partial u}{\partial x} + v\dfrac{\partial u}{\partial y} = u_e\dfrac{du_e}{dx} + \dfrac{\partial^2 u}{\partial y^2}, \\ u(x,0,t) = v(x,0,t) = 0, \\ u(x, y>0, t=0) = u_e(x) \\ v(x, y>0, t=0) = 0 \\ \text{and } u(x,\infty,t>0) = u_e(x), \quad \text{with } \; u_e(x) = \sin(x). \end{array}\right. \tag{22}$$

This case is catastrophic.

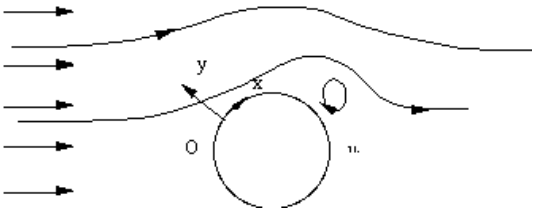

Figure 37: Unsteady separation on a cylinder $\bar{u}_e = \sin(\bar{x})$

Since Van Dommeln [25], it is known that an outer decelerated flow creates a nice separation bulb (which was not present in the steady case). But very soon there is a finite time singularity at time $t \simeq 3$. On figure 39 we see the development of the separation zone (left) and the singularity of the boundary layer displacement thickness (right). It has been shown by Smith that the time singularity behaves as

$$\delta_1 \simeq (t_s - t)^{-1/4}, \quad t_s \simeq 3.$$

Separation occurs for an angle of 115 degrees (angle of Goldstein). Notice that all the part computed before $x = 2.01$ is exactly the same than in the steady case. (see figure 31).

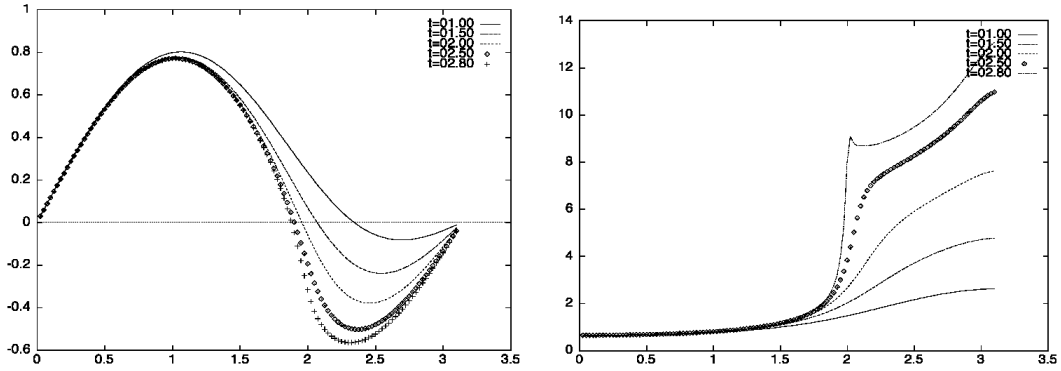

Figure 38: Unsteady separation on a cylinder $\bar{u}_e = \sin(\bar{x})$ at times $t = 1,\ 1.5,\ 2\ 2.5$ et 2.8 computed with finite differences. Left skin friction evolution, the separation occurs at time $t = 0.65$, it creates no Goldstein singularity. Nevertheless, for $t \simeq 3$, there is a time singularity. This time singularity is characterized by a pinching in the displacement thickness plotted on the right part for several time steps.

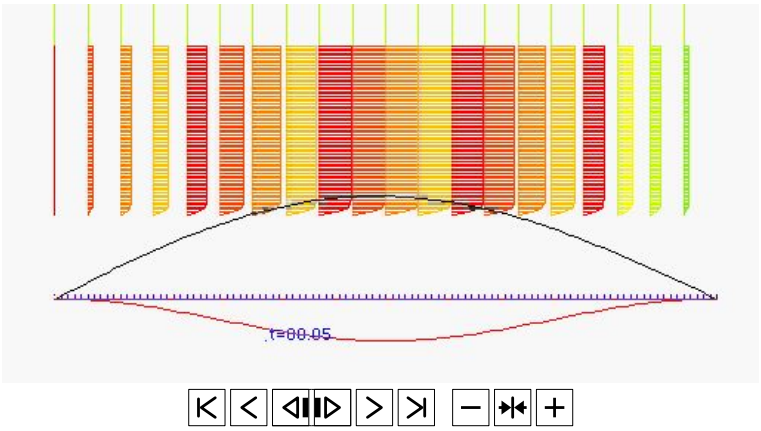

Figure- Boundary layer séparation on a cylinder, fields along θ [click to launch the movie, QuickTime Adobe/ Reader required].

7 Separation on a cylinder, Kirchhoff

7.1 Separation on a cylinder: free streamline

The boundary layer separation on a cylinder with external velocity $\bar{u}_e = \sin(\bar{x})$ gives a separation point at angle 1.9rad=108 degrees. In this point of view the external flow has been solved using the potential flow theory, and the sketch of the flow is on figure 39 (a) (from Stewartson).

The boundary layer is so thin that we do not see it, the boundary layer is singular at separation.

There is another point of view for separation on a cylinder using the inviscid theory of Kirchhoff. To model the separation in inviscid flow, we say that the separation bubble is infinite, it is a wake, it is at zero velocity and at constant pressure in the wake. This hypothesis has been proposed by Kirchhoff and by Rayleigh, this is based on the free-streamline theory of Helmholtz. There are contribution from Levi Cevita, Brillouin, Villat... the sketch of the flow is on figure 39 (b) (from Stewartson).

The classical resolution is :

$$\text{find } \psi \text{ so that } \vec{\nabla}^2\psi = 0, \text{ with } \psi = 0 \text{ on the symmetry line and } \psi = 0 \text{ on the body.}$$

This is solved with complex variables, $F(z) = \phi + i\psi$, and $z = x + iy$, the conjugate of the velocity $u - iv = dF/dz$, let us define q the modulus and θ the angle of the velocity. If one defines $\Omega = \ln(dz/dF)$, (some times people use $i\ln(dz/dF)$ see just after Imai analysis) as $dF/dz = qe^{-i\theta}$, then $\Omega = -\ln(q) + i\theta$. This $\Omega = L + i\theta$ is an analytic function of z, then of F, if we write $L = -\ln(q)$ we have always a laplacian

$$\frac{\partial^2}{\partial L^2}\psi + \frac{\partial^2}{\partial \theta^2}\psi = 0$$

in the Ω representation, the rigid walls are θ constant, and the free boundaries are L constant, on both ψ is constant as it is a stream line. The Kirchhoff-Helmoltz resolution is :

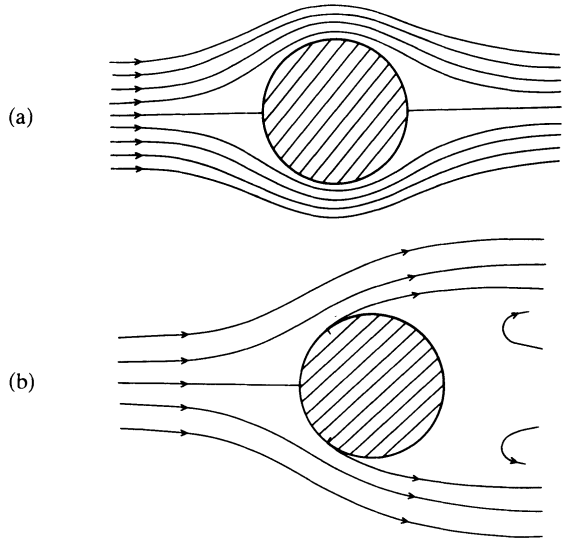

FIG. 1. *Two of the candidates for the steady solution of the Navier–Stokes equations for flow past a circular cylinder at* $\boldsymbol{R} \gg 1$. (a) *attached potential flow.* (b) *Kirchhoff free-streamline flow.*

Figure 39: Steady separation on a cylinder, upper Euler attached flow/ or external flow Lower half, the free stream line theory with a infinite wake, the angle of separation is $\simeq 55^o$, from Stewartson "d'Alembert Paradox", SIAM 81.

find ψ so that $\overrightarrow{\nabla}^2\psi = 0$, with $\psi = 0$ on the symmetry line and $\psi = 0$ on the body, find the pressure so that it is constant in the wake.

7.1.1 Separation on a cylinder, numerical resolution

As just said, the Kirchhoff-Helmoltz problem is :
find ψ so that $\overrightarrow{\nabla}^2\psi = 0$, with $\psi = 0$ on the symmetry line and $\psi = 0$ on the body, find the pressure so that it is constant in the wake.

This can be done with `FreeFem++`, it is a bit difficult as the wake must be adjusted to obtain the good value for pressure. In fact, we define the circle up to the fixed point of separation x_s. The part of the boundary which is after this position will change during the iterations. We move the mesh for $x > x_s$ depending on the value of the velocity on this boundary (see code in Annex 5).
Depending on the value of the pressure in the wake, there is a position of the point of separation. Or depending of the chosen point of separation, one has a pressure in the wake.

7.1.2 Separation on a cylinder, Imai analysis

Looking at the position where there is separation Imai 1953 introduced the classical complex potential $F(z)$, with $u - iv = F'$, he defines U velocity in the free streamline so that

$$\ln(dF(z)/dz/U) = \ln(q/U)e^{-i\theta}$$

then he writes $i\ln(dF(z)/dz) = i\ln(q) + \theta$. The function $i\ln(F')$ may be expressed as an expansion $kz^m + ...$ near $z = 0$ so in the streamline, $r > 0$, $q = U$ are such that $i\ln(F') = 0$. So that $\theta = kr^m$, hence k is real. Before the separation, on the wall, $z = re^{i\pi}$ then $i\ln q + \theta = kr^m e^{im\pi}$ taking the derivative along the surface with $ds = -dr$ so $\dfrac{d\theta}{ds} + i\dfrac{dq}{qds} = -kmr^{m-1}e^{im\pi}$ the real part $\dfrac{d\theta}{ds} = -kmr^{m-1}\cos(m\pi)$ hence $m = 1/2$ or $m \geq 1$ and

$$\frac{d\theta}{ds} + i\frac{dq}{qds} = -\frac{k}{2}ir^{-1/2} \text{ so that we have } i\ln(dF(z)/dz) = kz^{1/2}$$

So finally, the results from Imai are the two behaviors:
- $\dfrac{dq}{qds} = -\dfrac{k}{2}(-s)^{-1/2}$ and $\dfrac{d\theta}{ds}$ finite for $s < 0$
- $q = U$ and $\dfrac{d\theta}{ds} = \dfrac{k}{2}(s)^{-1/2}$ for $s > 0$.

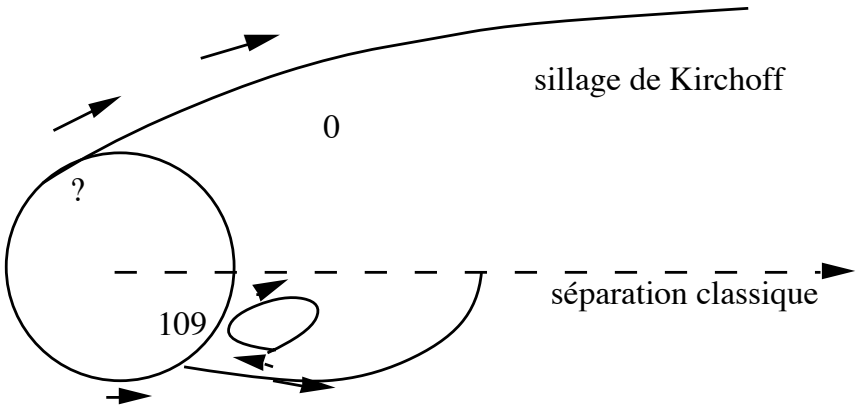

Figure 40: Steady separation on a cylinder, upper half, the Kirchhoff point of view (separation will maybe be around $\simeq 55^o$). In the inviscid theory one may construct a region of constant pressure (the separated wake). A stream line which is tangent to the body. Lower half, the boundary layer point of view, the angle of separation is $\simeq 108^o$, the separated bubble is a finite extent. The external ideal fluid is "attached" and as no wake

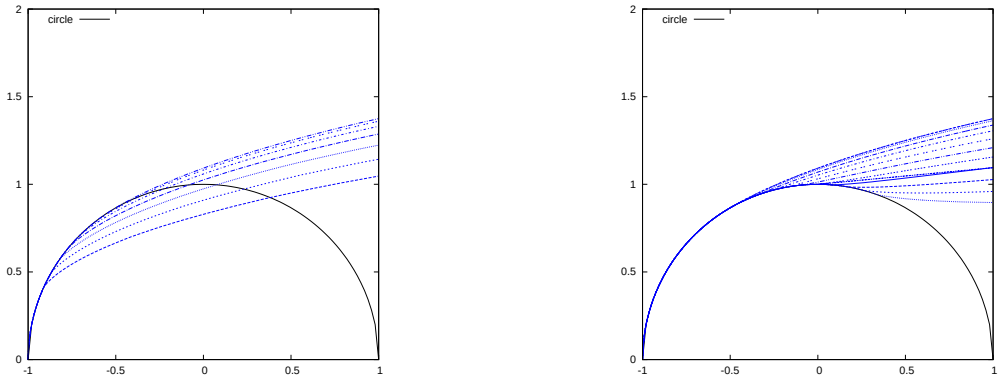

Figure 41: Steady separation on a cylinder Kirchhoff-Helmoltz problem solved with `FreeFem++`, with fixed $x_s = \cos(\pi - \alpha)$. Left, if the separation point is before $\alpha = 55^o$ (25, 30, 35, 40 45, 50 and 55) the curvature of the streamline is negative (which is unphysical). Right, if the separation point is after 55^o (55, 60, 65, 70, ..., 100, 105,110) the curvature of the free streamlines has an angle with the body. For an angle of about 55^o the stream line is tangent to the circle.

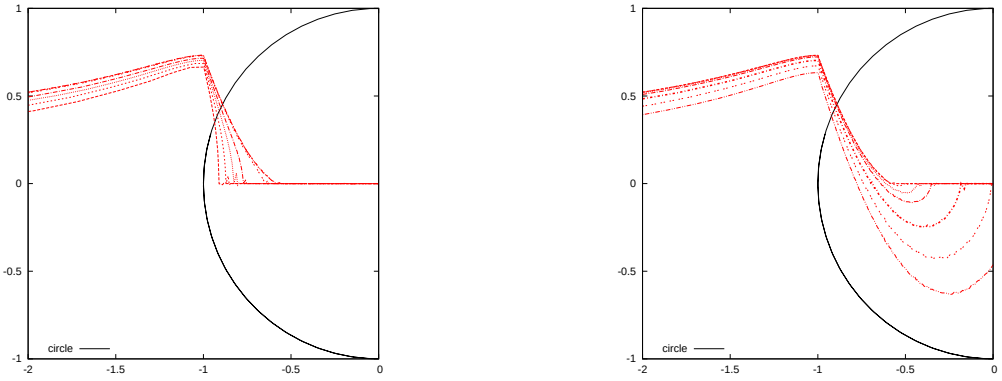

Figure 42: Steady separation on a cylinder Kirchhoff-Helmoltz problem solved with `FreeFem++`, with fixed $x_s = \cos(\pi - \alpha)$. Pressure along $y = 0$ and along the circle, pressure is taken to 0 in the wake. Left, if the separation point is before $\alpha = 55^o$ (25, 30 35 40 45,50 and 55) the pressure decreases from the stagnation point to the chosen x_s, with a square root behavior. For $\alpha = 55^o$, the pressure is tangent. Right, if the separation point is after 55^o (55, 60, 65, 70, 80, 90 100,)) the pressure decreases and re increases. This final counter pressure should move x_s

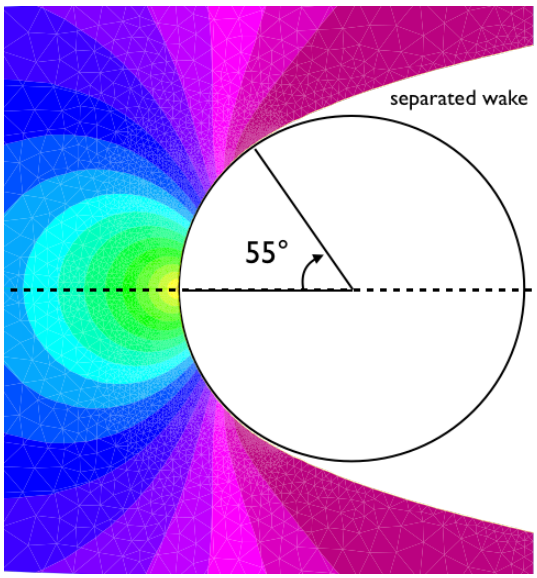

Figure 43: Steady separation on a cylinder with `FreeFem++`, the separation point is imposed to the value 55^o, Kirchhoff-Helmoltz wake of pressure constant.

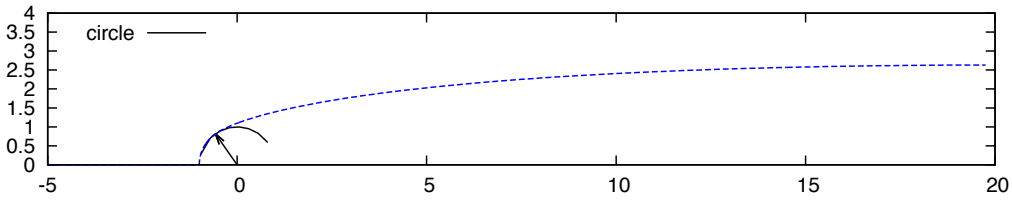

Figure 44: Steady separation on a cylinder with `FreeFem++`, the separation point is imposed to the value 55^o, Kirchhoff-Helmoltz wake of pressure constant. Iso $\sqrt{u^2+v^2}$ are ploted here

7.1.3 Separation on a cylinder, Sychev analysis

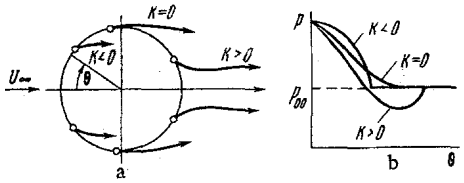

Fig. 1

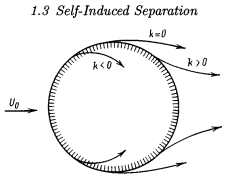

1.3 Self-Induced Separation 11

Fig. 1.4 The form of the free streamlines for Kirchhoff flows with various positions of the separation point.

решение, обладающее всеми необходимыми свойствами. Рассмотрим это более подробно.

Решение задачи обтекания гладкого препятствия, например кругового цилиндра по схеме Кирхгофа, вообще говоря, неоднозначно. Оно может быть построено при различных положениях точки отрыва нулевой линии тока от поверхности тела (рис. 1.4). Если начало криволинейной ортогональной системы координат Oxy поместить в точку отхода нулевой линии тока от поверхности тела, то кривизна свободной линии тока будет определяться выражением

$$\varkappa = -kx^{-1/2} + \varkappa_0 + O(x^{1/2}), \quad x \to +0 \qquad (3.1)$$

($\varkappa_0$ — безразмерная кривизна поверхности тела в точке отрыва, полагаемая конечной), а величина градиента давления на поверхности тела в окрестности этой точки будет равна

$$\frac{dp}{dx} = k(-x)^{-1/2} + \frac{16}{3}k^2 + O[(-x)^{1/2}], \quad x \to -0; \qquad (3.2)$$

$$\frac{dp}{dx} = 0, \quad x > 0.$$

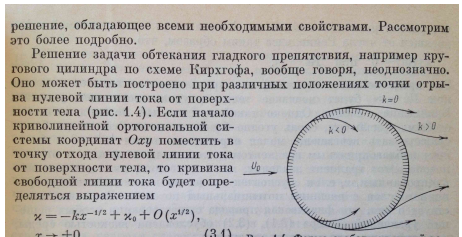

Рис. 1.4. Форма свободных линий тока в течении Кирхгофа при различных положениях точки отрыва

Figure 45: Steady separation on a cylinder, Brillouin Villat condition the curvature of the free streamlines is tangent to the body at the "separation point". Left from original 1972 Sychev's paper. Center from Vladimir V. Sychev, Anatoly I. Ruban, Victor V. Sychev, Georgi L. Korolev "Asymptotic Theory of Separated Flows". Left, from the initial edition Sychev Sychev, which is more clear.

In the freestreamline framework of 2D steady ideal fluids, we showed that the pressure on the body in a neighborhood of the separation point is (changing Imai notations, $x_s - x = -s$, $u\frac{du}{dx} = -\frac{dp}{dx}$) so that pressure gradient and pressure are:

$$\frac{dp}{dx} = \frac{k}{2\sqrt{x_s - x}} + ... \text{ before separation, and after } p = p_0.$$

$$p = p_0 - k\sqrt{x_s - x} + ... \text{ before separation, and after } p = p_0.$$

whereas the curvature $(\frac{d\theta}{ds})$ of the free stream line is $\frac{k}{2\sqrt{x-x_s}}$, where x_s is the point of separation. The streamline shape is $y_s(x) = \frac{3k}{2}(x - x_s)^{3/2}$ (Smith uses $-k$ in his 1977 paper).

It was noticed that this solution presents it self a paradox:
• If $k < 0$, pressure decreases to 0 (see figure 42 left), but stream lines enter in the obstacle (see figure 41 left). This is impossible.
• If $k > 0$, stream lines live the obstacle with an angle (see figure 41 right). The pressure decreases and increases just before x_s. So that its gradient will create a boundary layer separation before x_s, so before the "separation point" it self.... This is impossible.
• The sole solution is $k = 0$, this is the Brillouin-Villat condition: the curvature of the free streamlines is tangent to the body at the "separation point". This continuity of curvature was written by Brodetsky 1923 as well. But the flow is smooth, there is no counter pressure. So there is no separation. This is the "Brillouin-Villat" paradox.

This is discussed in Sychev Book and in Stewartson (d'Alembert's Paradox 1981). With complicated analysis Brillouin 11 Villat 14, Birkhoff 57. See Ruban [19] p201. We will see latter that the good idea comes from Sychev, a small positive counter pressure exists:

$$k(Re) \to 0 \text{ as } Re \to \infty,$$

it is vanishingly small with the Reynolds number.

7.1.4 Separation on a cylinder, Landau analysis

In the early 60's, Sychev had the idea that if a pressure gradient Δp can cause separation, the scales he proposed are exactly what is then used in the Triple Deck theory settled by Stewartson, Neiland and Messiter in 1969.

he considers that perturbations occurs near the wall in a layer of thickness δ_3 in the boundary layer of thickness δ. Near the wall, the velocity can be written

$$u \sim \frac{\delta_3}{\delta}$$

as very close to the wall the velocity is linear, with $\delta = Re^{-1/2}$ the boundary layer thickness and were δ_3 represents the order of magnitude of the transverse position. Then pressure inertia balance ($u\partial_x u \sim \partial_x p$) gives:

$$\Delta p \sim u^2.$$

This is the good order of magnitude to create a change in the sign of the longitudinal velocity. Then, the inertial pressure balance is after substitution

$$\Delta p \sim \frac{\delta_3^2}{\delta^2}$$

but the viscous inviscid equilibrium ($u\partial_x u \sim Re^{-1}\partial_y^2 u$) gives at a new small scale say x_3:

$$(\frac{\delta_3}{\delta})^2 \frac{1}{x_3} = Re^{-1}(\frac{\delta_3}{\delta})\frac{1}{\delta_3^2}$$

gives $\delta_3 = \Delta x^{1/3} Re^{-1}$, so that it gives the estimate between pressure and scale in x:

$$\Delta p \sim x_3^{2/3}.$$

Visiting Sychev institute (TsAGI), Landau reproduced this in his book as an "problem" end of §40 p 156 of reference [14]. We then deduce that the pressure gradient near the separation on a cylinder is $k/\sqrt{\Delta x}$ (due to the square root behavior of the pressure). Hence the previous estimate

$$\Delta p \sim k\sqrt{\Delta x} \sim \Delta x^{2/3}$$

gives that

$$k \sim \Delta x^{1/6}.$$

This is the first clue that the Brioullin Villat conditions holds: k is smaller and smaller as $Re \to \infty$ as $\Delta x \to 0$ for$Re \to \infty$

7.1.5 Separation on a cylinder, Sychev Triple Deck analysis

With a bit more estimates, we are close to the triple deck analysis that we will develop later, the displacement of the stream lines is then $Y/\Delta x$, the curvature of the flow is then $Y/\Delta x^2$ which is $Re^{-1}\Delta x^{-5/3}$ this is of same order of magnitude as the pressure gradient (by the potential flow theory). So $\partial p/\partial x \sim Re^{-1}\Delta x^{-5/3}$ but $\Delta p \sim \Delta x^{2/3}$ hence $\Delta x^{-1/3} \sim Re^{-1}\Delta x^{-5/3}$ which gives

$$\Delta x \sim Re^{-3/8} \text{ and } \; k \sim Re^{-1/16}$$

This is part of the resolution of the ∂'Alembert paradox with the ingredients of the Triple Deck that we will see more precisely in the next chapter. Before, we have to look at second order boundary layer theory.

8 Second order boundary layer

8.1 Sequence.

We may think that the second order of the boundary layer may fix the problems. But in fact not! Nevertheless, the scheme is as depicted on figure 46. The first order expansion of the ideal fluid creates a first order expansion of boundary layer. This first expansion disturbes the ideal fluid and creates a second order expansion. This perturbation creates a second order expansion in the boundary layer and so on.

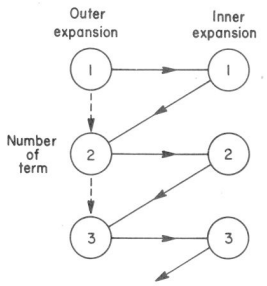

Fig. 5.6. Matching order for inner and outer expansions.

Figure 46: Classical sequence, image taken from Van Dyke's book.

8.2 Second Order

Let us look at the transverse velocity in the Boundary Layer, we up to now never match the transverse velocity. The reason was that is is of order $Re^{-1/2}$, which is negligible for the Ideal Fluid. We see that this velocity induces in the Ideal Fluid a perturbation.

Starting from the incompressibility equation and adding and substracting the same derivative of the velocity (in the spirit of Von Kármán integral equations):

$$\frac{\partial \tilde{v}}{\partial \tilde{y}} = (-\frac{\partial \tilde{u}}{\partial x} + \frac{\partial \bar{u}_e}{\partial \bar{x}}) - \frac{\partial \bar{u}_e}{\partial \bar{x}},$$

we obtain, after integration up to an $\tilde{y}$ ($\bar{x}$ and $\tilde{y}$ are independent variables) the velocity is:

$$\tilde{v}(\tilde{y}) - \tilde{v}(0) = -\frac{\partial}{\partial \bar{x}} \int_0^{\tilde{y}} (\tilde{u} - \bar{u}_e) d\tilde{y} - \tilde{y} \frac{\partial \bar{u}_e}{\partial \bar{x}}$$

so, if $\tilde{y}$ is large enough and as $\tilde{v}(0) = 0$ we obtain the behavior for large enough $\tilde{y}$:

$$\tilde{v}(\tilde{y}) \simeq \frac{\partial}{\partial \bar{x}} (\bar{u}_e \tilde{\delta}_1) - \tilde{y} \frac{\partial \bar{u}_e}{\partial \bar{x}}$$

This velocity must be multiplied by $Re^{-1/2}$; and $\bar{y} = Re^{-1/2}\tilde{y}$. Now, we write the velocity in the ideal fluid as a Taylor expansion near the wall for small $\bar{y}$:

$$\bar{v} = \bar{v}(\bar{x}, 0) + \bar{y} \frac{\partial \bar{v}}{\partial \bar{y}} + ... = \bar{v}(\bar{x}, 0) - \bar{y} \frac{\partial \bar{u}_e}{\partial \bar{x}} + ...$$

matching this velocity and the boundary layer velocity show that:

$$\bar{v}(\bar{x}, 0) = Re^{-1/2} \frac{\partial}{\partial \bar{x}} (\bar{u}_e \tilde{\delta}_1)$$

So that the boundary layer disturbates the ideal fluid at order $Re^{-1/2}$. It is called the "blowing velocity". So the velocity in the ideal fluid (called transpiration boundary condition as well):

$$\bar{u} = \bar{u}_1 + Re^{-1/2}\bar{u}_2, \;\; \bar{v} = \bar{v}_1 + Re^{-1/2}\bar{v}_2 \; \bar{p} = \bar{p}_1 + Re^{-1/2}\bar{p}_2....$$

with $\bar{u}_1(x,0) = \bar{u}_e(x)$.

Note that we have always slip boundary condition for u_2.

8.3 Flat plane case

We substitute this in Euler equation and have to find what is the flow created by a flat plate with a given blowing velocity which is in $\beta\sqrt{\bar{x}}/2$ with $\beta = 1.7$.

$$\begin{cases} \dfrac{\partial \bar{u}_2}{\partial \bar{y}} - \dfrac{\partial \bar{v}_2}{\partial \bar{x}} = 0, \\ \dfrac{\partial \bar{u}_2}{\partial \bar{x}} + \dfrac{\partial \bar{v}_2}{\partial \bar{y}} = 0. \end{cases} \tag{23}$$

We easily see that an irrotationnal solution in cylindrical variables $\bar{r}, \theta$ like $\bar{\psi} = -\beta\sqrt{\bar{r}}\cos(\frac{\theta}{2})$:

$$\bar{u}_2 = -\frac{\beta}{2\sqrt{\bar{r}}}\sin(\frac{\theta}{2}), \quad \bar{v}_2 = \frac{\beta}{2\sqrt{\bar{r}}}\cos(\frac{\theta}{2}),$$

as a result we have a solution with $\bar{u}_2 = 0$ at the wall allows to fit the boundary conditions, the two velocity are plotted on figure 47. We observe that the ideal fluid longitudinal velocity is zero at the wall, so it has no effect at the next order on the boundary layer. The Blasius solution is valid up to the order 2 for a flat plate in an external constant flow!

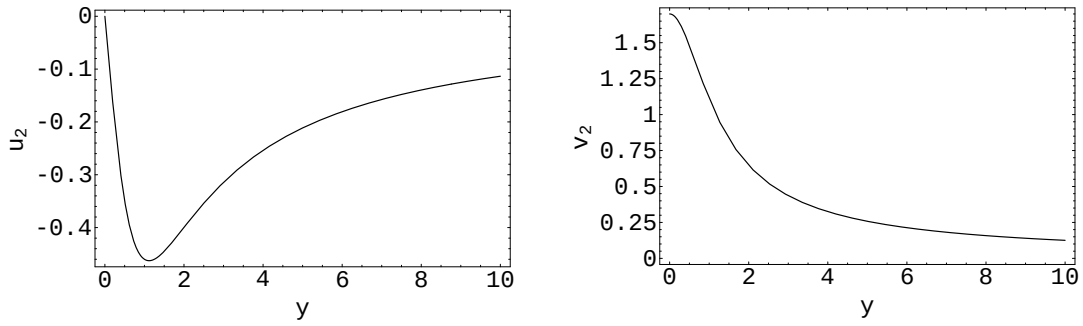

Figure 47: Second order velocity field $\bar{u}_2$ and $\bar{v}_2$ induced by the blowing of the displacement thickness at $\bar{x} = 1$ for $\bar{y}$ increasing.

On figure 48 we plot the iso $\bar{\psi}$ over a flat plate. On the middle figure, we plot the solution of the linear system $\partial^2_{\bar{x}}\bar{\psi} + \partial^2_{\bar{y}}\bar{\psi} = 0$ with naive boundary conditions $\bar{x} < 0$ and $\bar{y} = 0$ $\bar{\psi} = \bar{y}$ (like an incoming constant flow), $\bar{x} > 0$ and $\bar{y} = 0$ $\bar{\psi} = -\beta\bar{x}^{1/4}$. $\bar{x} = 0$, $\bar{\psi} = \bar{y}$ on $\bar{y} = \bar{y}_{max}$ $\bar{\psi} = \bar{y}_{max}$ (as if there is no more perturbation far from the plate) and on $\bar{x} = \bar{x}_{max}$, $\frac{\partial\bar{\psi}}{\partial\bar{x}} = 0$ (a Neuman condition).

So we clearly see that the influence of the blowing is not negligible ($Re = 500$) and that it as an influence on the incoming profile. One should then be very careful to compute the Navier Stokes flow with a numerical solver.

8.4 Curvature effects

Nevertheless it is not so simple in the other cases. We examine now the case of non flat plates. Starting from Navier Stokes equations (see all the Van Dykes articles [26] [27]) written in curvilinear coordinates: s

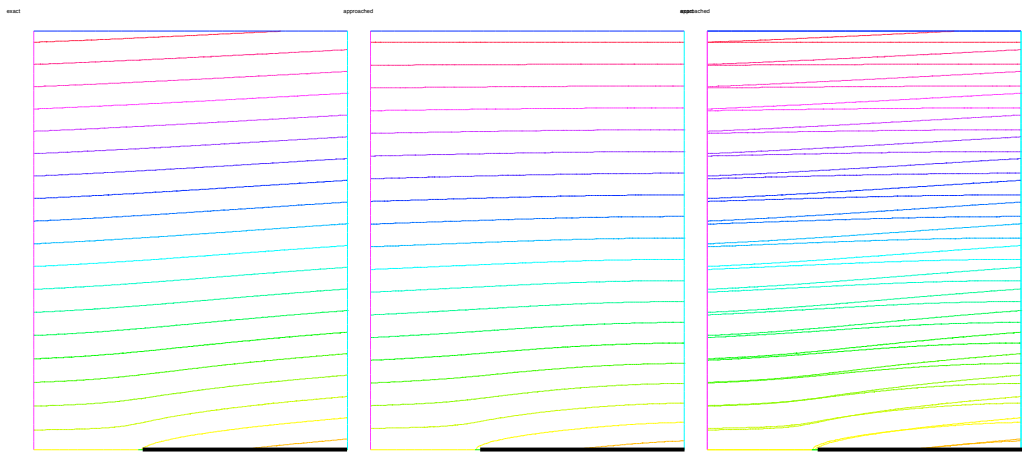

Figure 48: Inviscid first + second order iso ψ field induced by the blowing of the displacement thickness. Left the exact solution $rsin(\theta) - \beta Re^{-1/2}\sqrt{r}cos(\frac{\theta}{2})$, center solution of Laplacian, right superposition of both.

measured along and n normal to the surface, with $h = 1 + \kappa(s)n$, where the curvature κ is positive on a convex surface.

$$\begin{cases} \dfrac{\partial u}{\partial s} + \dfrac{\partial (hv)}{\partial n} = 0, \\ u\dfrac{\partial u}{\partial s} + v\dfrac{\partial (hu)}{\partial n} = -\dfrac{\partial p}{\partial s} + h\dfrac{\partial}{\partial n}\big(h^{-1}(\dfrac{\partial (hu)}{\partial n})\big), \\ -\kappa u^2 = -h\dfrac{\partial p}{\partial n}. \end{cases} \tag{24}$$

Expanding in the boundary layer variables in powers of Reynolds number:

$$u = u_1 + Re^{-1/2}u_2 + ...$$

gives at first order the classical equations the second order is then

$$\begin{cases} \dfrac{\partial u_2}{\partial s} + \dfrac{\partial v_2}{\partial n} = -\kappa\dfrac{\partial (nv_1)}{\partial n} \\ u_1\dfrac{\partial u_2}{\partial s} + v_1\dfrac{\partial u_2}{\partial n} + u_2\dfrac{\partial u_1}{\partial s} + v_2\dfrac{\partial u_1}{\partial n} = -\dfrac{\partial p_1}{\partial s} + \dfrac{\partial}{\partial n}\dfrac{\partial u_2}{\partial n} - \kappa[\dfrac{\partial}{\partial n}(n\dfrac{\partial}{\partial n}u_1) - v_1\dfrac{\partial}{\partial n}(nu_1)], \\ -\kappa u_1^2 = -\dfrac{\partial p_2}{\partial n}. \end{cases} \tag{25}$$

so all the effect of curvature appear as a linear contribution to the non-curvature case. Again the pressure is constant in y if there is no curvature effects.

In $n = 0$ $u_2 = v_2 = 0$, the matching at infinity is

$$u_2(x, \infty) = u_2(x, 0) - \kappa u_1(x, 0)n$$

and for large n the matching in pressure requires

$$p_2(x, n \to \infty) = p_2(x, 0) - \kappa u_1(x, 0)^2 n.$$

8.5 Rotational effect

Ideal incompressible fluids are rarely rotational. Compressible fluids are mainly rotational due to shock waves. Nevertheless we may imagine a rotational flow at first order $u_1 = 1 + \omega y, v_1 = 0$ (first done by Murray [16] before than a clear definition of second order equations had been settled by Van Dyke the next year, see Brazier [3]).

At first order, we have the standard boundary layer equations; again the velocity at infinity creates the second order of Ideal Fluid, again the solution at order two is the solution on a paraboloïd $\psi = -\beta\sqrt{r}cos(\frac{\theta}{2})$. Even u_2 is always zero at the wall, now there is pressure gradient due to the vorticity:

$$-\frac{\partial p_2}{\partial x} = v_2(x,0) - \frac{\partial u_1(x,0)}{\partial y} = \frac{\beta}{2\sqrt{x}}\omega.$$

In the boundary layer:

$$\begin{cases} \dfrac{\partial u_2}{\partial x} + \dfrac{\partial v_2}{\partial y} = 0 \\ u_1\dfrac{\partial u_2}{\partial x} + v_1\dfrac{\partial u_2}{\partial y} + u_2\dfrac{\partial u_1}{\partial x} + v_2\dfrac{\partial u_1}{\partial y} = -\dfrac{\partial p_1}{\partial x} + \dfrac{\partial}{\partial y}\dfrac{\partial u_2}{\partial y}, \\ 0 = -\dfrac{\partial p_2}{\partial n}. \end{cases} \tag{26}$$

in $y = 0, u_2 = v_2 = 0$ and then in ∞ $u_2 \to u_2(x,0) + y\frac{\partial u_1(x,0)}{\partial y} = \omega y$ so we search u_2 as $u_2 = \omega\sqrt{x}g'(\eta)$ after substitution:

$$2g''' + fg" - f'g' + 2f''g = -\beta$$

After computation we find the correction to the skin friction which is

$$\frac{C_f}{2} = \frac{0.332}{\sqrt{xRe}} + 3.12\frac{\omega}{Re}$$

8.6 finite flat plate

We just remark that there is a far wake solution in exponential which describes the finite flat plate problem. But the trailing edge problem is not simple, it requires a new development. Kuo in 1953 supposed that teh displacement thickness remains constant at the trailing edge and presented a kind of second order problem for $x > L$ where $v_2 = 0$ in $y = 0$ (instead of $1/\sqrt{x}$). After difficult computations he obtained the global drag coefficient:

$$\frac{C_D}{2} = \frac{1.33}{\sqrt{Re}} + 4.12\frac{1}{Re}$$

But the triple deck theory that we will see soon shows that there is an extra term which is larger than the second order one.

8.7 The Lock-Ting Wake problem

9 Annex 1: An example of NS computation on a flat plate

For sake of illustration we use `FreeFem++` to compute the flow over a flat plate at $Re = 500$ (figure 49 left). If we plot several velocity profiles with the self similar variable $\bar{y}(Re/\bar{x})^{1/2}$ all the profiles are the same (figure 50 left for $\bar{y}(Re/\bar{x})^{1/2} < 7$). If we go further, for values of $\bar{y}(Re/\bar{x})^{1/2}$ larger than 7; we see an overshoot of velocity. This is a second order effect.

But this is a spurious effect do to the boundary conditions. In fact, to compute it, we imposed naive boundary conditions. On the entrance: $\bar{u} = 1, \bar{v} = 0$. On the top $\partial_{\bar{y}}\bar{u} = \partial_{\bar{y}}\bar{v} = \partial_{\bar{y}}\bar{p} = 0$. At the output $\bar{p} = 0$ and $\partial_{\bar{x}}u = \partial_{\bar{x}}\bar{v} = 0$.
The boundary condition at the top of the domain produces a kind of channel effect. To confirm this, we compute the solution of the linear system of Ideal Fluid $\partial^2_{\bar{x}}\bar{\psi} + \partial^2_{\bar{y}}\bar{\psi} = 0$ with naive boundary conditions $\bar{x} < 0$ and $\bar{y} = 0$ $\bar{\psi} = \bar{y}$ (like an incoming constant flow), $\bar{x} > 0$ and $\bar{y} = \beta\sqrt{\bar{x}/Re}$ $\bar{\psi} = 0$. $\bar{x} = 0$, $\bar{\psi} = \bar{y}$ on $\bar{y} = \bar{y}_{max}$ $\bar{\psi} = \bar{y}_{max}$ (as if there is no more perturbation far from the plate) and on $\bar{x} = \bar{x}_{max}$ $\frac{\partial\bar{\psi}}{\partial\bar{x}} = 0$ (a Neuman condition). The streeam line are on figure 49 right and are similar to the Navier Stokes ones on figure 49 left. The ideal fluid velocity is larger at the wall $1.7(Re)^{-1/2}\bar{x}^{1/2}$. This extremum is visible on figure 50 right and correspond to the overshoot of the Navier Stokes solution of figure 50 middle.

So we clearly see that the influence of the blowing is not negligible ($Re = 500$) and that it as an influence on the incoming profile. One should then be very careful to compute the Navier Stokes flow with a numerical solver.

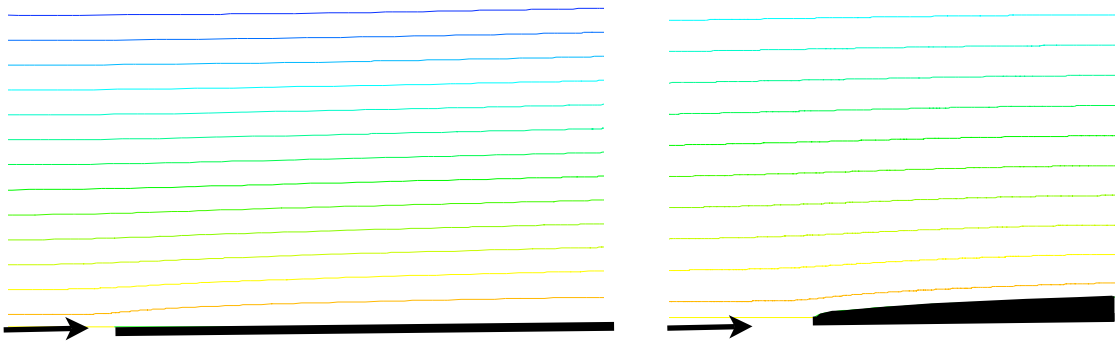

Figure 49: Left Navier Stokes solution by FreeFem++ at $Re = 500$, stream lines. Right, Ideal Fluid solution by FreeFem++ over a body $1.7(Re)^{-1/2}\bar{x}^{1/2}$, stream lines are nearly the same and one see the displacement effect induced by the boundary layer..

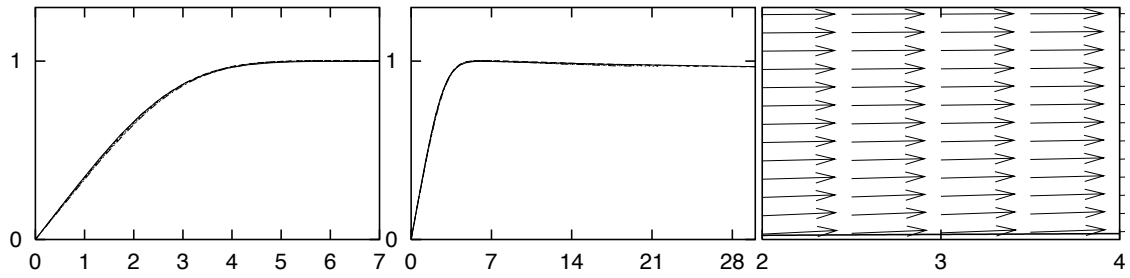

Figure 50: Navier Stokes computation by FreeFem++ at $Re = 500$, left we have the selsimilar Blasius profile (superposition of several profils tracés plotted with $\bar{y}(Re/\bar{x})^{1/2}$). Middle, the same profiles but up to a larger value of $\bar{y}(Re/\bar{x})^{1/2}$, we see the decrease of the velocity. Right Ideal Flow over a body in $1.7(Re)^{-1/2}\bar{x}^{/2}$, the velocity decreases from the body to the top of the domain. This overshoot of velocity is a spurious second order effect of displacement of the stream lines.

10 Annex 2: Hypersonic Strong interaction

The strong interaction ($p = M^2\theta^2$) and the $x^{3/4}$ shock and boundary layer.
the Weak intearction ($p = 1 + M\theta$) (see Hayes en Probstein [12])

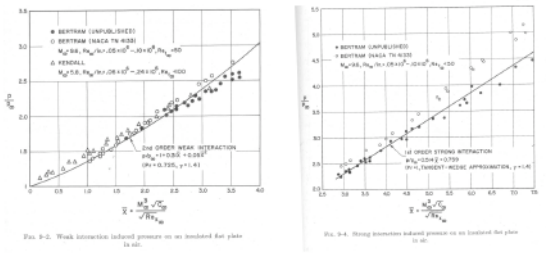

Figure 51: Weak and strong interaction

11 Annex 3: Von Kármán equation axi and plane

Let us look again Von Kármán equation, we write the total derivative:

$$u\frac{\partial u}{\partial r} + w\frac{\partial u}{\partial z}$$

in conservative form

$$\frac{1}{r^\alpha}\frac{\partial r^\alpha u^2}{\partial r} + \frac{\partial uw}{\partial z} = [\frac{u}{r^\alpha}\frac{\partial r^\alpha u}{\partial r} + u\frac{\partial w}{\partial z}] + u\frac{\partial u}{\partial r} + w\frac{\partial u}{\partial z}$$

because ($\alpha = 1, 0$ in axi or 2D)

$$\frac{1}{r^\alpha}\frac{\partial r^\alpha u}{\partial r} + \frac{\partial w}{\partial z} = 0$$

as

$$r^{-\alpha}\partial_r(r^\alpha u u_e) = u_e r^{-\alpha}\partial_r(r^\alpha u) + u\partial_r(u_e)$$

again using incompressiblilty and as u_e does not depend on z, we have $u_e\partial_z w = \partial_z(wu_e)$ so that

$$r^{-\alpha}\partial_r(r^\alpha u u_e) = u\partial_r(u_e) - \partial_z(wu_e)$$

we substract the momentum equation

$$r^{-\alpha}\partial_r(r^\alpha u u_e) - \frac{1}{r^\alpha}\frac{\partial r^\alpha u^2}{\partial r} + (u_e - u)\partial_r(u_e) + \partial_z(w(u_e - u)) = -\frac{\partial^2 u}{\partial z^2}$$

allows to write the momentum equation as:

$$\frac{1}{r^\alpha}\frac{\partial r^\alpha(u(u_e - u))}{\partial r} + (u_e - u)\frac{\partial}{\partial r}(u_e) + \frac{\partial}{\partial z}(w(u_e - u)) = -\frac{\partial^2 u}{\partial z^2}$$

remember the 2D expression:

$$\frac{\partial}{\partial \bar{x}}(\tilde{u}\bar{u}_e - \tilde{u}^2) + (\bar{u}_e - \tilde{u})\frac{\partial \bar{u}_e}{\partial \bar{x}} - \frac{\partial}{\partial \tilde{y}}(\tilde{v}(\tilde{u} - \bar{u}_e)) = -\frac{\partial^2 \tilde{u}}{\partial \tilde{y}^2}$$

Defining the displacement thickness, the momentum thickness and the shape factor

$$\tilde{\delta}_1 = \int_0^\infty (1 - \frac{\tilde{u}}{\bar{u}_e})d\tilde{y}, \quad \tilde{\delta}_2 = \int_0^\infty \frac{\tilde{u}}{\bar{u}_e}(1 - \frac{\tilde{u}}{\bar{u}_e})d\tilde{y} \text{ and } H = \frac{\tilde{\delta}_1}{\tilde{\delta}_2},$$

and defining a function f_2 linked to the skin friction as: $\frac{\partial \bar{u}}{\partial \bar{y}} = f_2 \frac{H\bar{u}_e}{\delta_1}$ gives the following equation where the ideal fluid promotes the boundary layer:

$$\frac{1}{r^\alpha}\frac{\partial r^\alpha (u_e^2 \delta_2)}{\partial r} + \delta_1 u_e \frac{\partial}{\partial r}(u_e) = \frac{\partial u}{\partial z}|_0$$

or

$$u_e^2 \frac{1}{r^\alpha}\frac{\partial r^\alpha (\delta_2)}{\partial r} + \delta_2 \frac{\partial u_e^2}{\partial r} + \delta_1 u_e \frac{\partial}{\partial r}(u_e) = \frac{\partial u}{\partial z}|_0$$

developing the derivative

$$u_e^2 \frac{1}{r^\alpha}\frac{\partial}{\partial r}(r^\alpha \frac{\delta_1}{H}) + (1+\frac{2}{H})\delta_1 u_e \frac{\partial}{\partial r} u_e = \frac{\partial u}{\partial z}|_0$$

with $\alpha = 0$ we have again:

$$\frac{d}{d\bar{x}}(\frac{\tilde{\delta}_1}{H}) + \frac{\tilde{\delta}_1}{\bar{u}_e}(1+\frac{2}{H})\frac{d\bar{u}_e}{d\bar{x}} = \frac{f_2 H}{\tilde{\delta}_1 \bar{u}_e}, \qquad i.e.\ \ \tilde{\delta}_1 = F(\bar{u}_e), \tag{27}$$

Initial condition is for example $\tilde{\delta}_1(0) = 0$ (but the Hiemenz value may be a good first guess) and $\bar{u}_e(0) = 1$. In the classical approach, $\tilde{\delta}_1$ is obtained through the knowledge of $\bar{u}_e$, which we write formaly $\tilde{\delta}_1 = F(\bar{u}_e)$.

12 Annex 4 Pohlhausen closure for Hiemenz flow

We use the polynomial closure at order 4, so that

$$\frac{u(\eta)}{\bar{u}_e} = (2\eta - 2\eta^3 + \eta^4) + \frac{1}{6}\Lambda(\eta - 3\eta^2 + 3\eta^3 - \eta^4)$$

with $\Lambda = \delta^2 d\bar{u}_e/d\bar{x}$ in the Hiemenz case $\bar{u}_e = \bar{x}$ then $\Lambda = \delta^2$, The Von Kármanán equation

$$\frac{d}{d\bar{x}}(\bar{u}_e^2 \tilde{\delta}_2) + \tilde{\delta}_1 \bar{u}_e \frac{d\bar{u}_e}{d\bar{x}} = \frac{u'(0)}{\tilde{\delta}}\bar{u}_e,$$

reads

$$2\tilde{\delta}_2 + \tilde{\delta}_1 = \frac{u'(0)}{\tilde{\delta}},$$

which is an equation were $\delta_1/\delta = (36-\Lambda)/120$ and $\delta_2/\delta = 37/315 - \Lambda/945 - (\Lambda^2)/9072$, and $u'(0) = 2 + \Lambda/6)$ and remember that $\Lambda = \delta^2$, we then substitute in VK:

$$\delta\left(\frac{3}{10} - \frac{\delta^2}{120}\right) - \frac{\frac{\delta^2}{6}+2}{\delta} + 2\delta\left(-\frac{\delta^4}{9072} - \frac{\delta^2}{945} + \frac{37}{315}\right) = 0$$

we solve and find numericaly $\delta = 2.65562$ this gives $\Lambda = 7.05$ and $\delta_1 = 0.640617$, and $H = 2.30809$ and $\tau = \frac{u'(0)}{\tilde{\delta}} = 1.1957$

The real Hiemenz flow $f''' + ff'' + (1 - f'^2) = 0$ as solution $f''(0) = 1.2325$ (compare to 1.1957 for Pohlhausen4), the displacement thickness is $\int (1 - f')d\eta = 0.6479$ (compare to 0.640617 for Pohlhausen4).

Note that the axi Hiemenz flow $f''' + 2ff'' + (1 - f'^2) = 0$ as solution $f''(0) = 1.31194$ (in 2D 1.2325), the displacement thickness is $\int (1 - f')d\eta = 0.568902$ (compare to 0.6479 in 2D).

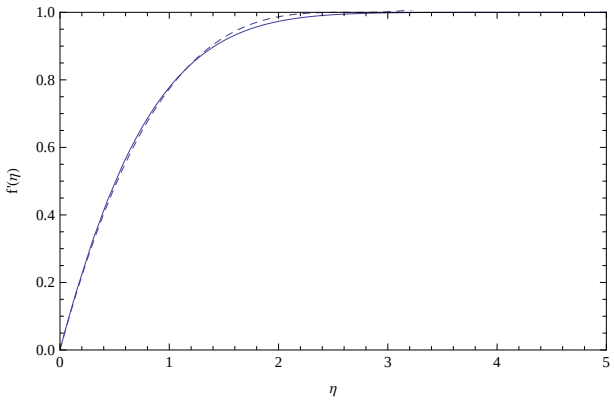

Figure 52: Pohlhausen (dashed) compared to Hiemenz (line)

13 Annex 5 : Falkner Skan with Mathematica

```
(** Falkner Skan Equation **)

eqf = f'''[y] +  f[y] f''[y] + b (1 - f'[y]*f'[y]);

fs[fpp_?NumberQ, beta_?NumberQ, etamx_?NumberQ] := Block[{fpinf, dinf},b = beta;
           sol = NDSolve[{
              (eqf  ) == 0,
              f[0] == 0, f'[0] == 0, f''[0] == fpp  }, {f }, {y, 0, etamx}];

           fpinf = f'[etamx] /. sol[[1, 1]];
           dinf = etamx - f[etamx] /. sol[[1, 1]];
         (*   Print[ "1=",fpinf," ",dinf]; *)
           Return[{fpinf,dinf}]]

fs1[fpp_?NumberQ, beta_?NumberQ, etamx_?NumberQ] := Block[{fpinf, dinf},b = beta;
           sol = NDSolve[{
              (eqf  ) == 0,
              f[0] == 0, f'[0] == 0, f''[0] == fpp  }, {f }, {y, 0, etamx}];

           fpinf = f'[etamx] /. sol[[1, 1]];
           dinf = etamx - f[etamx] /. sol[[1, 1]];
         (*   Print[ "1=",fpinf," ",dinf]; *)
           Return[{ fpinf}]]

FindRoot[fs1[xx, 0, 4] == {1}, {xx, .44, .48}, MaxIterations -> 20]

p1p21 = Plot[{Evaluate[f'[y] /. sol[[1, 1]]] , 2*(2*y/3 - (y/3)^2)/2}, {y,
   0.01, 7}, PlotRange -> {{0, 7}, {-1, 1}}]
```

14 Annex 4: Navier Stokes

Navier Stokes computation with *Gerris*

```
#########################################################################
# Blasius par PYL, sauver dans "blasius.gfs"
# lancer avec
# gerris2D -DRe=1000. blasius.gfs | gfsview2D v.gfv
# 29/09/10
# valeur du Reynolds
#Define Re 100000.
# definition de 3 boites avec 2 connections
3 2 GfsSimulation GfsBox GfsGEdge{
# met le coin gauche decalle - > paque 2 est en 0,0
    x = -0.5 y = 0.5  } {
  SourceViscosity {} 1./Re
  PhysicalParams { L = 2 }
#   precision 2**(-4.) = 1/16=0.06   5-> 32  0.03  6 ->  0.015625 2**(-8.) = 0.00390625   pr 2**(-8
   Refine 6
# temps initial 0
```

```
  Init {} { U = 1
            V = 0 }
  Init {istep = 1}{
    dyU = dy("U"); }
   AdaptVorticity { istep = 1 } { maxlevel = 8 minlevel = 4 cmax = 1e-2 }
# sortie tous les 20 pas de calculs du temps en cours
  OutputTime { istep = 20 } stderr
# valeurs qui vont sortir pour entrer dans gfsview
# tous les 30 pas de calcul
  OutputSimulation { istep = 30 } stdout
  OutputLocation { step = 0.1 } vals.data  cut.dat
  OutputSimulation { step = 0.25 } SIM/sim-%g.txt { format = text }
  EventScript { step = 0.25 } { cp SIM/sim-$GfsTime.txt sim.data}
  OutputPPM { step= 0.05 } { ppm2mpeg > blastok.mpg } { min = 0 max = 1 v = Velocity }
# p[0:10][0:1.5]"< awk '{if($1>.7){print $0}}' sim.data" u ($2/sqrt($1/1000)):6,sin(pi*x/2/4.79)*1.
# p[0:10][0:1.5]"< awk '{if($1>.9){print $0}}' sim.data" u ($2/sqrt($1/1000)):6,sin(pi*x/2/4.79)*1.
# p[0:5][0:1.5]"< awk '{if($1>0){print $0}}' SIM/sim-3.txt" u ($2*sqrt(1000)):6,1,erf(x/2/sqrt(3))
#p[][:] "< awk '{if($2<0.01){print $0}}' sim.data" u ($1):($9),.33/sqrt(x/1000)
# arret lorsque la variation de U devient "petite"
  EventStop { istep = 10 } U 1.e-4 DU}
#conditions aux limites
# first box free stream
GfsBox {
left = Boundary {
            BcDirichlet U 1
            BcDirichlet V 0 }
    bottom = Boundary {
            BcNeumann U 0
            BcDirichlet V 0 }
     top = Boundary {
            BcNeumann U 0
            BcNeumann V 0 }
        }
 GfsBox {
# en bas vitesse nulle
# second box the flat plate
        bottom = Boundary {
            BcDirichlet U 0
            BcDirichlet V 0 }
          top = Boundary {
            BcNeumann U 0
            BcNeumann V 0}
         }
 GfsBox {
# thrid box
  bottom = Boundary {
          # BcNeumann U 0
          #the trailing  edge
          BcDirichlet U 0
          # or the plate
           BcDirichlet V 0 }
```

```
      top = Boundary {
            BcNeumann U 0
            BcNeumann V 0}

    right = Boundary {
            BcDirichlet P 0
            BcNeumann U 0 }
 }
1 2 right
2 3 right
##########################################################################
```

15 Annex 5: Massive separation

Separation with FreeFem++

```
exec("echo \"Kirchhoff\"");
/* Lausanne fev 2013 */
/* OK 2018 */

verbosity=-1;
real s0=clock();
real t=0;

// solution de Kirchhof-Helmoltz
real h0=17;   //hauteur domaine
real L1=15;    //longueur gauche
real L2=20;   //longueur droite
real hb=1;    //hauteur free init
real R=1;     // rayon
real ts,xs,ys,alpha;   //  freestream droite
real hm=0.01;  //0.01
real hM=.25;    //.5
int n=8; //nbre de points
int i=0;

real coef=1;
real U0=1.1,Uf=0,UfmU0=1;
real psi0=h0;

  ofstream ff("U0.txt");
  for (int ia=0;ia<27;ia++)
{
alpha=10+ia*5;
UfmU0=1;
coef=1;
i=0;
t=0;
        hb=0;

ts= cos((180-alpha)/180.*pi);
```

```
xs=R*ts;
ys=sqrt(R*R-xs*xs);

// definition des cotes Maillage
border bas1(t=-1,0) { x= t*(L1-2*R)-2*R;     y = 0   ; label = 2; };
border bas2(t=-2,-1){ x= R*t;                y = 0   ; label = 2; };
border bas3(t=-1,ts){ x= R*t;                y = sqrt(R*R-x*x); label = 1; };
border bas4(t=ts,1) { x= R*t;                y = ys; label = 799; };
border free(t=0,1)  { x= t*(L2-R)+R;         y = ys; label = 799; };
border droit(t=0,1) { x= L2;                 y = ys+(h0-ys)*t; };
border haut(t=1,0)  { x= L2*(t) - (1-t)*L1;  y = h0; label = 33;};
border gauch(t=1,0) { x= -L1;                y = h0 * t ; };
border c1(t=0,1)    { x= R;                  y = (R*1.5-ys)*t+ys; }
border c2(t=1,-2)   { x= R*t;                y = 1.5*R; }
border c3(t=1,0)    { x= -2*R ;              y = 1.5*R*t; }


mesh Zoom = buildmesh(bas2(30)+bas3(30)+bas4(30)+c1(30)+c2(30)+c3(30));
mesh Th= buildmesh(bas1(n*L1)+bas2(10)+bas3(100)+bas4(100)+free(L2*n)+droit(n*(h0-ys)/4)+haut(n*L1/4
plot(Th,wait=0);

//espace EF
fespace Vh2(Th,P2);
Vh2 psi,psiT;
Vh2 phi,phiT;
Vh2 w,wT;
fespace Vh1(Th,P1);
Vh1 u,v,U;
fespace Vhz1(Zoom,P1);
Vhz1 Uz,wz;

// visu
real [int] visopsi=[ 0,0.5,1,1.5,2,2.5,3,4,6];
real [int] visophi=[-5,-3,-2, -1.5, -1, -0.5,  0,0.5,1,1.5,2,2.5,3,3.5,4,5,7];
real[int] viso(61);
for (int i=0;i<viso.n;i++) viso[i]=i*h0/60.;

/** problemes */
problem freeb(w,wT,solver=CG) =
     int2d(Th)(
     dx(w)*dx(wT)+dy(w)*dy(wT))
     + on (gauch,w=0)
     + on (33, w=0)
     + on (bas1,bas2,bas3, w=0)
     + int1d(Th,799)(-wT*(U0 - U));


problem Lappsi (psi,psiT) =
    int2d(Th)(
              (dx(psi)*dx(psiT) + dy(psi)*dy(psiT))  )
 //   + on(gauch,psi=y)
```

```
    + on(2,psi=0)
    + on(1,psi=0)
    + on(799,psi=0)
    + on(33,psi=psi0) ;
//


problem Lapphi (phi,phiT) =
    int2d(Th)(
              (dx(phi)*dx(phiT) + dy(phi)*dy(phiT))  )
    + on(gauch,phi=-L1)
    + on(droit,phi=L2); ;

    while((abs((UfmU0))>.00001))
    {
    if (i>1666) break ;
    i++;
    Lappsi;
    u= dy(psi);
    v=-dx(psi);
    U=sqrt(u*u+v*v);
    Uz=U;
    plot(Uz,fill=1);

     if(i%50==1) plot(Th,cmm="psi=",psi, viso=viso,fill=0,wait=0);

     freeb;

//    xs=R*ts-2*hm;
//    xs=R*ts;
//    ys=sqrt(R*R-xs*xs);
// dernier point
      real xm=-10000,ym=0;
      for (int i=0;i<Th.nt;i++)
     {  for (int j=0; j <3; j++){
        if(Th[i][j].label==1){
         if( Th[i][j].x >=xm)
         { xm = Th[i][j].x;
           ym = Th[i][j].y;}
      }
       }
     }

     xs=xm;
     ys=ym;

     Uf=U(xs,ys);
     UfmU0=Uf-U0;
    if((i>1) ) { U0=U0+.005*(UfmU0);}   // relaxation

     if(i%15==1)
```

```
   {
     ofstream ff2("free.txt");
     for (int i=0;i<Th.nt;i++)
     {  for (int j=0; j <3; j++){
        if((Th[i][j].label==799)||(Th[i][j].label==1)||(Th[i][j].label==2)){
         ff2<<Th[i][j].x << " "<< Th[i][j].y << " "<< U[][Vh1(i,j)] << " " << U0 << endl;
        }
      }
     }
    }
  //


 cout <<"    "<< t <<"  w max="<< abs(w[].max)+abs(w[].min)<<"  +++++++++++++++++  +++++++ +++  U0=

  real minT0= checkmovemesh(Th,[x,y]); // the min triangle area
   while(1) // find a correct move mesh
 {
 real minT=checkmovemesh(Th,[x,y+coef*w]);  // the min triangle area
  if (minT > minT0/5) break ;
     coef=coef/1.5;
// if big enough
}
  Th=movemesh(Th,[x ,y+coef*w]);
  wz=w;
  Zoom=movemesh(Zoom,[x ,y+coef*wz]);

 if((i%15==1)&&(i<100))Th = adaptmesh(Th,dx(u),dx(v),w,hmax=hM,hmin=hm,iso=true,ratio=1);
 if((i%15==1)&&(i<100))Zoom = adaptmesh(Zoom,dx(Uz),wz,hmax=hM,hmin=hm,iso=true,ratio=1);


 if(i%10==6)  plot(Th, U,fill=1,wait=0);
   t=t+coef;
   coef=.1;
    }

   Lappsi;
   Lapphi;
   cout << "  " << t << "  w max=" <<  abs(w[].max)+abs(w[].min) <<  " aa== " << alpha << "   +++  
   plot(Uz,fill=1,ps="uz.eps");
   plot(phi,psi,U,fill=0,wait=0);
   ff << alpha << " "  << U0 << endl;
   exec("  sort -n -k 1 free.txt > tfree"+alpha+".txt");
   exec("  cp uz.eps uz"+alpha+".eps");

}

 cout << "CPU " << clock()-s0 << "s " << endl;
 exec(" gnuplot kirchoff.gnu");
```

16 Annex 6 : Speed of sound

Acoustics corresponds to perturbation of steady state, there is no free stream velocity U_0, but there may be a characteristic velocity constructed with p_0 and ρ_0 which is $U_0 = \sqrt{(p_0/\rho_0)}$ say that $\varepsilon\sqrt{(p_0/\rho_0)}$ is the velocity of the sound source of pulsation ω so that the scale of length will be $L = U_0/\omega$, then

$$u = U_0(\varepsilon u_1 + ...), \;\; u = U_0(\varepsilon \bar{v}_1 + ...), \;\; p = p_0(1 + \varepsilon p_1 + ...)$$

and $t = \bar{t}/\omega$ and $x = L\bar{x}$.... the first order equations of perturbation are:

$$\begin{cases} \dfrac{\partial \bar{\rho}_1}{\partial \bar{t}} + \dfrac{\partial \bar{u}_1}{\partial \bar{x}} + \dfrac{\partial \bar{v}_1}{\partial \bar{y}} = 0, \\ \dfrac{\partial \bar{u}_1}{\partial \bar{t}} = -\dfrac{\partial \bar{p}_1}{\partial \bar{x}}, \\ \dfrac{\partial \bar{v}_1}{\partial \bar{t}} = -\dfrac{\partial \bar{p}_1}{\partial \bar{y}}. \end{cases} \tag{28}$$

Eliminating the velocity gives :

$$\frac{\partial^2 \bar{\rho}_1}{\partial \bar{t}^2} - \frac{\partial^2 \bar{p}_1}{\partial \bar{x}^2} - \frac{\partial^2 \bar{p}_1}{\partial \bar{y}^2} = 0.$$

We need a final relation, the one coming from entropy or from any equation of state like $p = P(\rho)$, the isentropic cas gives $p/p_0 = (\rho/\rho_0)^\gamma$ so that $\bar{p}_1 = \gamma \bar{\rho}_1$ and

$$(\frac{\partial^2 \bar{p}_1}{\partial \bar{x}^2} + \frac{\partial^2 \bar{p}_1}{\partial \bar{y}^2}) - \frac{1}{\gamma}\frac{\partial^2 \bar{p}_1}{\partial \bar{t}^2} = 0.$$

This is the ∂'Alembert equation with wave velocity γ. Coming back to dimensions

$$(\frac{\partial^2 p_1}{\partial x^2} + \frac{\partial^2 p_1}{\partial y^2}) - \frac{1}{c_0^2}\frac{\partial^2 p_1}{\partial t^2} = 0,$$

with $c_0^2 = \gamma p_0/\rho_0$ the speed of sound. This is the usual equation for linear acoustics.

Note that if $p = P(\rho)$ (any given relation) then $c_0^2 = \frac{dP(\rho)}{d\rho}$.

References

[1] Jean Le Rond d'Alembert (1752): "Essai d'une nouvelle théorie de la résistance des fluides"

[2] Ashley, H. & Landhal, M. 1965 Aerodynamics of wings and bodies , pp. 88-98. Addison-Wesley.

[3] Brazier J.-P. "Étude asymptotique des équations de couche limite en formulation déficitaire" PhD Thesis ENSAE 1990

[4] Chernyi (1961): "Introduction to hypersonic flow" , Academic Press

[5] J. Cousteix : Couche limite laminaire, ed. Cepadues (1988)

[6] Cebeci T. & Cousteix J. (1999): "Modeling and computation of boundary layer flows", Springer Verlag.

[7] Cousteix J., & Mauss J. (2006): "Analyse asymptotique et couche limite", Mathématiques et Applications, Vol. 56 2006, XII, 396 p.

[8] Cousteix J., & Mauss J. (200X): "Asymptotique Analysis and Boundary Layers ", Mathématiques et Applications, Vol. X 200X, XII, 396 p.

[9] Darrozès J.S. et François C. "Mécanique des fluides incompressibles". Berlin : Springer Verlag, 1982. 461 p. Lecture notes in Physics 163. ISBN 3-540-11578-1

[10] Paul Germain (1986) "Mécanique, Volume 1 et Volume 2", Ellipses, 1986 Germain's life.

[11] Gersten, K. and Hervig, H. (1992): "Strömungsmechanik : Grundlagen der Impuls-Wärme-und Stoffübertragung aus asymptotischer Sicht", Vieweg, Wiesbaden.

[12] Hayes & Probstein (1959):"Hypersonic flow theory" Academic Press .

[13] J. Kevorkian & J.D. Cole, Perturbation Methods in Applied Mathematics, Springer AMS 34 (1981)

[14] Landau L. Lifshitz E. (1997) "Fluid Mechanics" Butterworth-Heinemann, 539 pages

[15] L. Landau & E. Lifshitz (1989) "Mécanique des fluides" ed MIR.

[16] Murray J.D. (1961) "the boundary layer on a flat plate in a stream with uniform shear" JFM vol 11 pp. 309-316.

[17] H. Schlichting (1987): "Boundary layer theory" , 7th ed Mc Graw Hill.

[18] Prandtl L. (1928) "Motion of fluids with little viscosity/ Vier Abhandlungen zur Hydrodynamik und Aerodynamik Göttingen 1927", NACA report 452.

[19] Anatoly I. Ruban (2017) "Fluid Dynamics, Part 3 Boundary Layers" ISBN: 9780199681754 `https://books.google.fr/books?id=X_pADwAAQBAJ&printsec=frontcover&dq=Anatoly+I.+Ruban+(2017)+%22Fluid+Dynamics,+Part+3+Boundary+Layers%22+ISBN:+9780199681754&hl=en&sa=X&ved=0ahUKEwje9Jqk-5feAhVBxYUKHUBeDRwQ6AEILTAB#v=onepage&q&f=false`

[20] Stewartson K. "The theory of laminar compressible boundary layer in compressible fluids", Oxford University Press 1964.

[21] H. Schlichting (1987): "Boundary Layer Theory", 7th edition Mac Graw Hill.

[22] H. Schlichting K. Gersten (2000): "Boundary Layer Theory", 8th edition Springer.

[23] I.J. Sobey (2000): "Introduction to interactive boundary layer theory", Oxford applied and engineering mathematics, 256 p.

[24] Sychev V. V. , Ruban A. I. , Sychev V. V. & Korolev G. L. (1998): "Asymptotic theory of separated flows", Cambridge University Press.

[25] Van Dommeln L. & Shen S.F. (1980): "The spontaneous generation of the singularity in a separating boundary layer", J. Comp. Phys. , vol 38, pp. 125-140.

[26] Van Dyke M. (1975): "Perturbation Methods in Fluid Mechanics" Parabolic Press.

[27] Van Dyke M. (1962): 'Higher approximations in boundary layer theory", JFM 14, pp 161-177.

Rapports

[28] P.-Y. Lagrée (1992): "Structures interactives Fluide Parfait/ Couche limite en hypersonique, Variations autour du thème de la triple couche", Thèse de l'Université Paris VI, janvier 92, Contrat BDI Aérospatiale.

[29] P.-Y. Lagrée (1997): "Résolution des équations de couche limite interactive instationnaire et applications", rapport DSPT 8, fév 97. Chapitre 2, "couche limite instationnaire" (Rapport de Contrat)

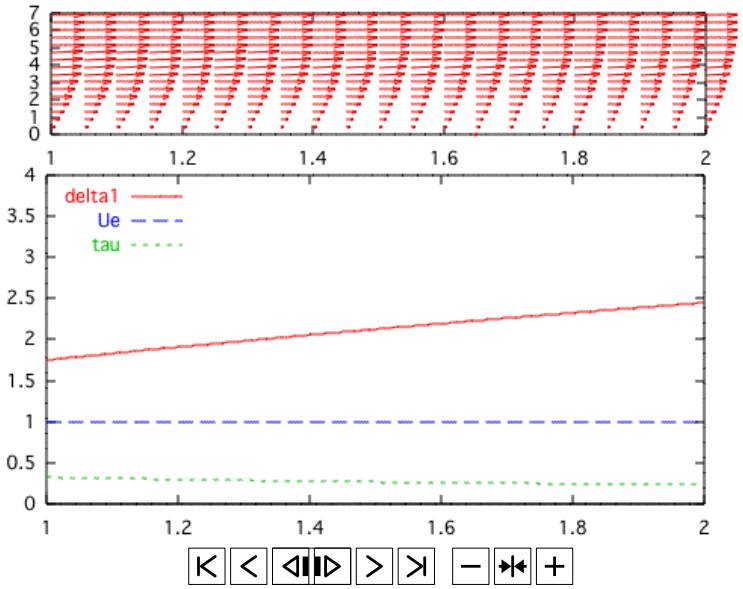

Boundary layer separation in a given external velocity U_e, [click to launch the movie, QuickTime Adobe/ Reader required].

The web page of this text is:
`http://www.lmm.jussieu.fr/~lagree/COURS/CISM/`

The last version of this file is on:
`http://www.lmm.jussieu.fr/~lagree/COURS/CISM/blasius_CISM.pdf`
This course is a part of a larger set of files devoted on perturbations methods, asymptotic methods (Matched Asymptotic Expansions, Multiple Scales) and boundary layers (triple deck) by $\mathscr{P}$.-$\mathscr{Y}$. $\mathscr{L}$agrée .
The web page of these files is `http://www.lmm.jussieu.fr/~lagree/COURS/M2MHP`.